Transcription regulation in time and space: Engineered cell systems to modulate the epigenetic chromatin structure: The role of Methyl-CpG-binding protein 2

Piebes, D.G.E.

Publication date
2016

Document Version
Final published version

Transcription regulation in time and space

Engineered cell systems to modulate the epigenetic chromatin structure: The role of Metyl-CpG binding protein 2

Diewertje Piebes

Transcription regulation in time and space

Engineered cell systems to modulate the epigenetic chromatin structure:
The role of Methyl-CpG-binding protein 2

ACADEMISCH PROEFSCHRIFT

ter verkrijging van de graad van doctor

aan de Universiteit van Amsterdam

op gezag van de Rector Magnificus

prof. dr. ir. K.I.J. Maex

ten overstaan van een door het College voor Promoties ingestelde commissie,

in het openbaar te verdedigen in de Agnietenkapel

op dinsdag 15 november 2016, te 14.00 uur

door

Diewertje Gerardine Eveline Piebes

geboren te Naarden

Promotiecommissie

Promotor:	dhr. prof. dr. H.V. Westerhoff
Copromotor:	mw. dr. P.J. Verschure
Overige leden:	mw. prof. dr. E.M. Hol, Universiteit van Amsterdam
	dhr. prof. dr. J.H. van Maarseveen, Universiteit van Amsterdam
	dhr. dr. E.M.M Manders, Universiteit van Amsterdam
	dhr. prof. dr. A.B. Houtsmuller, Erasmus Medisch Centrum
	mw. prof. dr. M.G. Rots, Universitair Medisch Centrum Groningen
	mw. prof. dr. M.J. Smit, Vrije Universiteit Amsterdam

Faculteit der Natuurwetenschappen, Wiskunde en Informatica,
Universiteit van Amsterdam

Het onderzoek in dit proefschrift is gefinancierd door:

Netherlands Organization of Scientific Research NWO ALW-ZonMW-Meervoud

NISB Glue project NWO grant

Contents

INTRODUCTION - 9 -

SCOPE OF THE THESIS - 17 -

CHAPTER 1 - 21 -

MECP2 ACCELERATES THE TRANSITION RATE OF TRANSCRIPTION REPRESSION DYNAMICS MEASURED AT A DEFINED CHROMATIN LOCUS IN SINGLE CELLS

CHAPTER 2 - 45 -

GENERATING CELL CLONES TO MEASURE TRANSCRIPTION DYNAMICS IN AN INDUCED VARIABLE EPIGENETIC CHROMATIN STATE

CHAPTER 3 - 63 -

THE BALANCING ACT OF MECP2: A MULTI-TASKING PROTEIN

CHAPTER 4 - 87 -

A ROLE FOR MECP2 IN SWITCHING GENE ACTIVITY VIA CHROMATIN UNFOLDING AND HP1γ DISPLACEMENT

BIBLIOGRAPHY - 115 -

SUMMARY - 137 -

SAMENVATTING - 143 -

DANKWOORD - 149 -

Introduction

D.G.E Piebes, P.J. Verschure

The simplest paradigm of transcription regulation dictates that at the end of a signalling cascade towards the nucleus single molecules bind to regulatory proteins which alter their affinity for the DNA. The interaction of the DNA-protein complex with RNA polymerase thereby triggers transcription. Transcription changes instantaneously upon fluctuations in the concentration of regulatory molecules. In differentiated cell types of multicellular organisms the intricate task of gene regulation is achieved by combined actions of multiple different transcription regulatory proteins including proteins that affect DNA and chromatin structure.

Several components of gene expression regulation including transcription factors, epigenetic enzymes and chromatin binding proteins are well known, however insight on dynamic and subsequent interactions of such proteins with DNA and chromatin is still unresolved. The epigenetic composition exhibits a regulatory layer that establishes heritable changes in gene activity that are not encoded in the DNA sequence. Alterations in the epigenetic state can be obtained via changes in chemical modifications of the DNA and chromatin and via conformational changes of the chromatin. Transcription patterns illustrating which genes are transcribed and to what extent, differ from cell to cell and they can change throughout the life span of an organism. Cell type specific gene expression patterns in higher eukaryotes confer stability of cellular phenotypes, while allowing changes in expression in response to environmental or developmental cues. Derangements in gene regulation have severe effects on cell behaviour and contribute to development of a diseased state.

Below a highlight is given of the actors and molecular events of gene expression regulation. In this thesis the intricate composition of chromatin including the role of core and variant histone proteins, posttranslational histone modifications and the nucleosomal and chromosomal structure are discussed. Moreover, the sequence of events when a gene is transcribed or repressed is discussed and we highlight some involved proteins, specifically focusing on the epigenetic regulatory protein methyl-CpG binding protein 2 (MeCP2). Finally we discuss the use of reporter gene cassette containing cells to perform systematic and quantitative, spatial and time resolved, single cell and single gene

transcription measurements and to determine the role of targeted alterations in the epigenetic chromatin state.

Chromatin

Chromatin consists of DNA, enzymes and proteins together exhibiting a very dynamic interplay in the confined space of the cell nucleus. To enable the folding of the DNA in the cell nucleus, DNA is wrapped around nucleosomes consisting of 2 of each H2A, H2B, H3 and H4 core histone proteins and linker histone H1 connector proteins. Besides these canonical histones which are incorporated into chromatin during replication of the genome, there are several variants of each histone, which are built into nucleosomes allowing defined activities. There are several histone variants known to be associated with transcription and to facilitate or prevent transcription regulatory proteins to bind at promoter regions. Some histone variants are more associated with the structure of the chromatin. For instance H3CENPA occurs only at centromeres, H3.3, H2AZ and H2ABdb are associated with transcriptionally active chromatin and macroH2A is found at inactive chromatin being abundantly present at the inactive X chromosome. The presence of conventional or variant histones in the nucleosome represents a layer of information controlling transcriptional gene activity (Gurard-Levin and Almouzni, 2014; Li et al., 2007).

Histone proteins consist of N-terminal tails that stick out of the nucleosomal structure. The amino acids at these histone tails can be modified by enzymes that act either as ‘writer’ or ‘eraser’ enzymes inducing the addition or removal of small chemical groups such as acetyl, methyl, phospho and more (Kouzarides, 2007a). The posttranslational histone modification state also provides binding sites for so-called epigenetic ‘reader’ proteins and enzymes that attract additional regulatory proteins. The specific amino acid as well as its position at the N-terminal tail or globular domain that is chemically modified largely determines the outcome of posttranslational histone modifications. Also the addition of one, two or three methyl groups can have an opposite effect. For example histone H3 lysine 4 monomethylation involves transcriptional activation whereas histone H3 lysine 9 trimethylation gene repression. These posttranslational histone modifications,

together with chemical modification of the DNA, e.g. DNA methylation or hydroxymethylation, form an important regulatory layer known as the epigenome that guides processes in the nucleus, i.e. the folding of the chromatin and hence gene expression patterning (Cutter and Hayes, 2015; Li and Zhu, 2015; Li et al., 2007; Luger and Hansen, 2005).

Posttranslational histone modifications create binding sites for transcription regulatory proteins allowing the establishment of protein complexes at defined genomic loci thereby altering the folding of the chromatin structure. Moreover, histone acetylation is able to directly alter the compaction of the chromatin structure since it neutralizes the positive charge of histones thereby decreasing the interaction of the histone N-terminal tail with negatively charged phosphate groups of DNA (Iizuka and Smith, 2003; Kouzarides, 2007b).

The folding of DNA into nucleosomal chromatin structures provides chromatin a dynamic behavior, allowing the chromatin to 'loop' and nucleosomes to 'breath'. Another advantage of nucleosomal chromatin packaging is that genes or regulatory sequences can be transcribed from the chromatin structure via local chromatin unwinding preventing the need to unwind the entire genome (Luger and Hansen, 2005). In principle genes with high nucleosomal density are less accessible for the transcription machinery, whereas a low nucleosomal density has a more open and accessible composition (Li et al., 2007). Although detailed information of the nucleosomal structure and the positioning of nucleosomes exist, knowledge of higher levels of chromatin structure remains incomplete. High-resolution transmission electron microscopy studies revealed that the fraction of the nuclear volume that is occupied with chromosomal material is small and that the majority of the genome is packed into large-scale chromatin structures. Several observations relating transcriptional regulation to interphase chromosomal folding have emerged, (1) interphase chromosomes occupy chromosome territories, (2) gene-rich chromosomes are spatially segregated from gene-poor chromosomes and show an increased chromosomal decondensation and a more nuclear internal position compared to gene-poor chromosome territories, (3) megabase-sized gene loci are able to loop outside of chromosome territories upon transcriptional activation of such loci, (4)

transcriptionally active or silent gene loci preferentially position at defined nuclear structures including 'nuclear bodies', (5) the association of cis and trans chromosomal regions is likely mediated by the association with nuclear domains. (Hemmerich et al., 2011; van Steensel, 2011; Verschure et al., 1999; Zhao et al., 2009)The use of engineered chromosome regions using bacterial lac operator/lac repressor or tet operator/tet repressor systems allowing targeted protein-DNA biding has a large impact on exploring the functional large-scale chromatin organization. Genome folding plays an important role in gene regulation. The causal relationship between gene folding and gene expression representing various hierarchical levels of transcription regulation is still largely unresolved.

Transcription

Gene expression is accomplished by the activity of RNA polymerase. Polymerization of the RNA polymerase enzyme requires other proteins to make the DNA accessible for RNA polymerase and to direct the enzyme to the site of transcription. RNA polymerase II is one of the proteins of the transcription machinery. RNA polymerase II transcribes a large set of genes, which is largely determined by the epigenetic composition of the chromatin. RNA polymerase forms a complex with proteins that guide the polymerase to correct genomic sites, whereas RNA polymerase II itself performs polymerisation of the mRNA based upon an intact DNA sequence. Polymerization has a certain reaction rate and seems to either take place or not following a large chain of events. The reaction rate of the synthesis of an entire mRNA can be regulated by the stalling of subsequent events of polymerisation. mRNA synthesis can also be regulated by the number of RNA polymerases that are progressing over a genomic sequence and transcribing the respective gene. The reaction rate of polymerizing the entire mRNA is determined by the epigenetic chromatin state including the functioning of DNA regulatory elements such as enhancer looping, the CpG content of the promoter and insulator elements (Svejstrup, 2004; Zhou et al., 2012).The initiation and elongation of RNA polymerase II producing a few transcripts is a rather inefficient process. In an active chromatin context only 10% of the RNA polymerases that are attracted to the transcription site will initiate and of these

initiated RNA polymerases, only 10% will successfully elongate and produce a mRNA molecule (Darzacq et al., 2007). Upon RNA polymerase initiation, proteins involved in RNA capping are required to ensure the creation of mature mRNA. RNA polymerase II progression is driven by posttranslational modifications such as phospho groups on RNA polymerase subunits, i.e. phosphorylation of serine 2 or serine 5 of the C-terminal domain. It is speculated that phosphorylation of RNA polymerase II functions as a checkpoint to prevent mRNA malformation by attracting the capping machinery before RNA polymerase II starts the elongation phase (Svejstrup, 2004). Of interest histone acetylation indirectly drives RNA polymerase from pausing to elongating. For instance, acetyl groups attract bromodomain reader proteins such as bromodomain-containing protein 4 (BRD4), which attracts positive elongation factor b (P-tefb) a cyclin dependent kinase which phosphorylates proteins that induce RNA polymerase pausing, as well as proteins that induce RNA polymerase elongation (Zhou et al., 2012).

Gene repression

Similar as transcriptional activation, transcription repression involves an intricate regulation of a variety of regulatory proteins and involves changes in the chromatin structure. Several transcription repression regulatory proteins are involved in recruiting enzymes that act as histone posttranslational ‘eraser’ enzymes, e.g. a histone deacetylases or histone demethylases.

Transcription repression involves DNA methylation. Genes with a high CpG content in their DNA sequence upstream of their transcription start site and promoter, i.e. CpG islands, generally exhibit a low amount of cytosine methylation and exhibit a transcriptionally active default state, whereas genes with low CpG content promoter regions generally consist of cytosine methylated sites and exhibit a transcriptional ‘off’ state. When a CpG island in the promoter region of a gene becomes methylated its expression is repressed. The addition of methyl groups is carried out by DNA methyltransferase enzymes that are responsible for the maintenance of established DNA

methylation or new or de novo methylation patterns.(Bodnar and Spector, 2013; Nan et al., 1998a)

Methyl CpG binding proteins play an important role as biological mediator of DNA methylation. Methyl CpG binding Protein 2 (MeCP2) contains both a methylated DNA and a transcription repression binding domain and exhibits chromatin remodeling activities. Depending on its protein folding MeCP2 attracts other proteins that are able to trigger a variety of functions in the nucleus. Transcription repression involving the presence of MeCP2 is often accompanied by the Heterochromatin Protein 1 (HP1) α, β and γ isoforms. HP1 is a chromatin-binding protein that binds with its chromo- and chromoshadow domain to H3K9-methylated histones and to proteins having histone modifying activities thereby advancing the 'spreading' of heterochromatin in cis (Verschure et al., 2005). HP1 proteins are involved in a wide variety of chromatin regulatory processes.

MeCP2 and MeCP2-related diseases

Each cell type exhibits a unique epigenetic chromatin make-up allowing it to maintain its cell type-specific gene expression pattern and hence cell identity. MeCP2 is a chromatin regulatory protein that is expressed in every cell type, but most abundantly in neuronal cells (Song et al., 2014). MeCP2 does not have a catalytic domain but it exists of domains that enable to trigger a variety of functions (Nan et al., 1993, 1998b). MeCP2 is able to attract transcription regulatory proteins and to direct them to a target gene increasing the probability to bind distinct sites (Hager et al., 2009).

MeCP2 mutations, deletion or amplification of the MeCP2 protein are the cause of two progressive neurodevelopmental disorders, i.e. Rett syndrome and Xq28 duplication syndrome. Rett syndrome typically affects the binding properties of MeCP2 whereas Xq28 duplication syndrome affects the concentration of MeCP2 in the nucleus. Both MeCP2-related disorders involve an altered chromatin structure thereby distorting genomic transcription patterns and neuronal behavior (Amir et al., 1999; Ramocki et al., 2010).

Reporter gene cassette containing cells

The composition of the epigenome has in many instances been mapped genome-wide and is actively pursued in large consortia. These efforts have resulted in impressive databases of epigenetic information. However, the rules that dictate how the structural, mechanistic and kinetic aspects of epigenetic transcription regulation concertedly determine gene activity are still poorly understood. This is in part due to the dynamic nature of the epigenome and due to the lack of techniques to resolve the structural aspects of epigenetic regulation. Moreover, a drawback of genome-wide biochemical analysis of the epigenome and transcriptome is that such methods do not allow the detection of cell-to-cell variation. The insertion of a single, non-endogenous engineered reporter gene cassette into the eukaryotic genome provides unique opportunities to directly influence the epigenetic state compared to the transcriptional state and offers a number of advantages to visually monitor the dynamics of epigenetic gene regulation. Such reporter gene cassette genomic integration approaches enable to obtain single cell and single gene analysis quantitative time-resolved data as input for computational simulations thereby advancing our understanding.

Scope of the thesis

Scope of the thesis

Cellular phenotypes rely on the correct expression of genes organized in complex networks. Gene expression regulation is a crucial mechanism to prevent gene over- or under expression. A diverse range of factors is involved in transcription regulation, such as transcription factors, chromatin remodellers, polymerases, histone modifying enzymes. Understanding how these factors act in concert within the nucleus to regulate gene activity or silencing remains a central challenge in molecular biology. The question when and where genes are expressed has been a major research focus. Large protein complexes (dis)assemble on genes within seconds whereas nucleosomes turnover within minutes to hours and gene activity shows temporal oscillatory and bursting behavior. New experimental advances enabled dynamic transcription measurements at single molecule and genome-wide levels.

In this thesis we use engineered reporter gene cassettes that are integrated in defined genomic loci in mammalian cells (Tumbar et al., 1999; Verschure et al., 2005) to measure the effect of altering the epigenetic chromatin state and to measure transcription dynamics in single living cells. The targeting of lacR or tetR tagged fluorescent epigenetic regulatory proteins to lac or tet operator DNA binding sequences provides a way to modulate the epigenetic chromatin state. The use of a reporter gene encoding bacteriophage MS2 hairpin repeats that are detected by a fluorescently tagged MS2 coat protein enables in vivo transcript imaging. The research described in this thesis focuses on the impact of the epigenetic chromatin composition on transcription repression dynamics. We focus on the role of methyl-CpG-binding protein 2 (MeCP2) as epigenetic chromatin regulatory protein. MeCP2 is a multifunctional protein involved in both transcription activation and repression. Mutations in MeCP2 play an important role in the developmental disorder known as Rett Syndrome. Rett syndrome is an inherited disease that almost exclusively affects females and causes severe mental and physical impairment.

In **chapter 1** we determined the transcription repression dynamics of a reporter gene array upon modulating the epigenetic chromatin state. We use a mammalian cell line containing a multicopy reporter gene cassette consisting of lac and tet operator binding

sequences and a CFP reporter gene containing MS2 hairpin sequences. We show a time-delayed response in the local decrease of MS2 tagged transcripts at the reporter gene compared to the rapid decrease of the transcriptional activator; our data indicate that endogenous transcription initiation is still ongoing in the absence of the transcriptional activator. MeCP2 lacR targeting to lacO binding sequences of the cassette diminished the delayed response while the transcript loss from the array appeared unaffected. Transcription repression exhibits a biphasic behaviour representing a delayed response followed by an actual transcript decrease. We propose that the local chromatin structure determines whether new transcription initiation events are performed thereby regulating the delay of transcription repression.

Chapter 2 describes the design and creation of a novel reporter gene cassette containing human cell line to quantitatively measure the contribution of the epigenetic chromatin state in regulating the rate of transcription at single gene level in single cells. We provide an overview of the set-up of our experimental approach and we discuss our design compared to current state-of-the-art to visualize mRNA with high temporal and spatial resolution.

In **chapter 3** we discuss the role of MeCP2 (dys)functioning focusing on MeCP2 mutations and duplication as noted in neurodevelopmental diseases Rett syndrome and Xq28 duplication syndrome, respectively. We show with a model-representation plotting the MeCP2 binding efficiency versus the general amount of MeCP2, the effect of an altered MeCP2 binding (MeCP2 mutations) or an increased MeCP2 concentration (MeCP2 duplication). We provide an overview of the numerous chromatin-related functions of MeCP2 considering the altered MeCP2 binding behavior in Rett and Xq28 duplication syndrome. Typically proper functioning of MeCP2 depends on the MeCP2 levels, its posttranslational modification state and its genomic binding.

In **chapter 4** we show an undiscovered functionality of MeCP2, i.e. its ability to induce extensive chromosomal unfolding. We used an engineered mammalian cell line consisting of a reporter gene containing a large amplified chromosomal domain. MeCP2-induced chromatin unfolding is triggered independently of the MeCP2 methyl-cytosine-binding

domain. Interestingly, MeCP2 binding triggers the loss of HP1γ at the chromosomal domain and an increased HP1γ mobility, which is not observed for HP1α and HP1β. Surprisingly, MeCP2-induced chromatin unfolding is not associated with transcriptional activation. We suggest a novel role for MeCP2 in reorganizing chromatin to facilitate a switch in gene activity.

Chapter 1

MeCP2 accelerates the transition rate of transcription repression dynamics measured at a defined chromatin locus in single cells

Diewertje G.E. Piebes, Hermannus Kempe, Ilona M. Vuist, Gijsbert J. van Belle, Adriaan B. Houtsmuller, Pernette J. Verschure

Abstract

Gene expression is regulated by the complex interplay of transcription factors and cofactors that directly or indirectly bind to DNA and alter chromatin composition. Here, we used time-lapse microscopy to analyze the repression kinetics when modulating chromatin state, employing a reporter gene array. The array consists of lac and tet operator binding sequences allowing targeting of fluorescent lac and tet repressors tagged with chromatin regulatory proteins of interest to control the expression of a CFP reporter gene, also encoding additional 3' UTR MS2 hairpins to allow quantification of newly synthesized transcripts in real-time. After inducing transcription repression by removing the targeted transcriptional activator, we observe that transcription initiation of the reporter gene transiently continues whereas the transcriptional activator is instantly lost from the array. Our data show a biphasic transcription repression response representing the actual decrease in transcripts at the reporter gene array and a preceding response time. We observe that targeting of the epigenetic reader protein methyl-CpG-binding protein 2 (MeCP2) significantly accelerates the transition rate of transcription repression, while the rate at which transcripts diffuse from the array is unaffected. We conclude that MeCP2 is able to facilitate the response to signals suppressing active transcription

Introduction

Epigenetic chromatin composition provides a dynamic means of creating chromatin with distinct features and properties that regulate chromatin-associated processes. Transcriptional activity (Hager et al., 2000; MacQuarrie et al., 2011) can be altered via binding of chromatin-associated proteins and local changes in chromatin structure (Akhtar et al., 2013; Van Kampen, 1992; Shahbazian and Grunstein, 2007). Transcription is not only regulated by recruitment of RNA polymerase II at promoters, but also by proteins regulating the ability of RNA polymerase II to penetrate chromatin barriers and facilitate its processivity (Dobrzynski and Bruggeman, 2009; Kwak and Lis, 2013; Mason and Struhl, 2005; Saunders et al., 2006; Svejstrup, 2004). Transcription regulatory elements, such as the transcription start site, promoter/enhancer regions, and body of

the gene exhibit defined histone modification patterns that are involved in regulating gene activation or repression (Barth and Imhof, 2010).

Methyl-CpG-binding protein 2 (MeCP2) is an epigenetic regulatory protein best described as a facilitator of setting gene expression programs (Linhoff et al., 2015) acting as a key chromatin structure regulator (Ghosh et al., 2010a; Linhoff et al., 2015; Schotta et al., 2004; Skene et al., 2010) and transcriptional regulator recruiting co-repressors (Lunyak et al., 2002; Lyst et al., 2013; Nan et al., 1998)(or activators (Chahrour et al., 2008; Mellén et al., 2012)). MeCP2 can alter chromatin folding as it binds chromatin-remodeling proteins such as Brahma and ATRX (Hu et al., 2006; Kernohan et al., 2014). Moreover, MeCP2 can bind methylated DNA and recruit repressive proteins such as mSin3a and histone deacetylases (HDACs) (Amir et al., 1999; Ghosh et al., 2010b; Nan et al., 1998; Shahbazian et al., 2002; Thatcher and Lasalle, 2006). In addition, the N-terminal domain of MeCP2 has been shown to bind Heterochromatin Protein 1 (HP1) (Agarwal et al., 2007), which is typically associated with the formation of transcriptionally silent chromatin as it binds through its chromodomain to tri-methylated histone H3 lysine 9 (H3K9me3) and recruits histone methyltransferase enzymes (Verschure et al., 2005). We recently showed that targeted binding of MeCP2 elicits chromatin unfolding and triggers the loss of HP1γ without any apparent change in expression of the genomically integrated reporter gene (Brink et al., 2013). In contrast, evidence has been provided that MeCP2 binds to promoters of active genes and induces gene activity via cAMP response element-binding protein (CREB) (Tao et al., 2009). Overall the connection between epigenetic chromatin composition and the precise role of regulatory proteins in transcription regulation and whether this is achieved via altering chromatin composition is unclear.

In this study, we took a single cell approach to investigate the dynamics of induced repression on a transcriptionally active reporter gene array. We used the U2OS 2-6-3 clone containing a multicopy integrated reporter gene cassette (Figure 1A-D) (Janicki et al., 2004), which consists of lac and tet operator (lacO and tetO) binding sequences, a CFP-SKL reporter gene, and a gene encoding MS2 hairpin loops. Binding of fluorescently tagged lac repressor (lacR) and tet repressor (tetR) to lacO and tetO binding sequences

allows visualization as well as modulation of the reporter gene array while the MS2 hairpin repeats enable visualization of newly synthesized transcripts by binding of YFP-tagged MS2 protein. MS2 tagging at reporter gene arrays has previously been explored extensively to study transcriptional activation (Ben-Ari et al., 2010; Bertrand et al., 1998; Brody and Shav-Tal, 2011; Darzacq et al., 2007; Huranová et al., 2010; Janicki et al., 2004; Larson et al., 2011; Martins et al., 2011; Mor et al., 2010; Rafalska-Metcalf et al., 2010; Schmidt et al., 2011; Shav-Tal et al., 2004; Zhao et al., 2011). However the dynamic behavior of transcripts and other involved factors when switching from a transcriptionally active to an inactive state has only recently started to be addressed (Bintu et al., 2016).

We measured induced repression of an activated reporter gene in absence and presence of the epigenetic modulator MeCP2. Briefly, we show that the decrease in the number of transcripts produced at the reporter gene array upon induction of repression significantly lags behind the rapid release of transcriptional activators. These findings suggest that new transcription initiation events transiently persist, in spite of the absence of the targeted transcriptional activator at the reporter gene array. Interestingly, when MeCP2 is targeted to the reporter gene array the transition rate is significantly shorter (while the transcript decrease kinetics are similar to those observed in non-targeted cells), suggesting that the role of MeCP2 when being associated with actively transcribed chromatin is to help keep actively transcribed chromatin in such a state that the response to signals suppressing transcription is accelerated.

Results

Experimental approach

We used time-lapse microscopy to analyze the dynamics of transcription repression when modulating chromatin state, employing a reporter gene array. We used the U2OS 2-6-3 cell line containing a multicopy integrated reporter gene cassette (Janicki et al., 2004), consisting of ~200 copies of a construct containing repeats of lacO (256x) and tetO (96x) sequences which allows for the visualization of the array by targeting fluorescently tagged

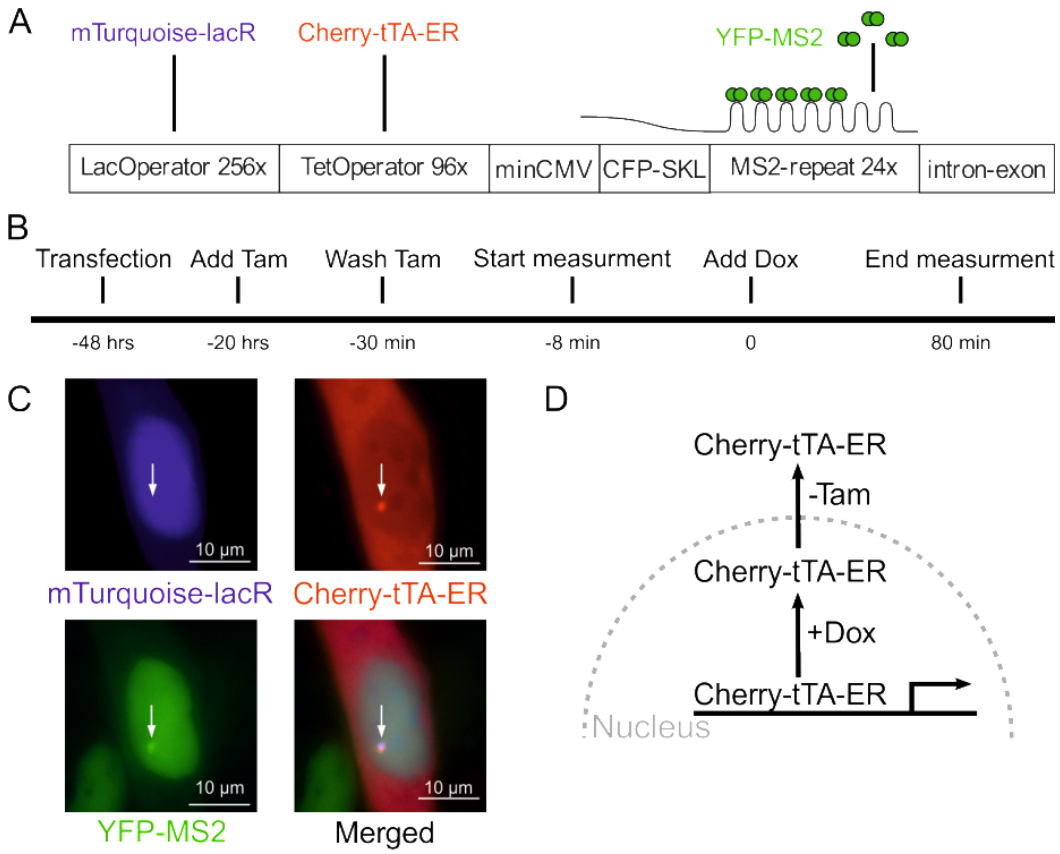

Figure 1: Experimental approach

A) Schematic representation of the reporter gene cassette. LacO is used for mTurquoise tagged lacR targeting and localization at the array. TetO Cherry-tTA-ER transcriptional activator binding is used to induce transcription of the CFP-SKL reporter gene consisting of a minimal CMV promoter, an SKL peroxisomal localization signal, and MS2 hairpin loops. YFP-MS2 coat protein binding to the MS2 repeat enables time-lapse microscopy transcription measurements at the reporter gene array. The intron-exon sequence attracts mRNA processing complexes.

B) Schematic representation of the experimental time line. Cells are transfected at -48 hours. The addition of Tamoxifen (20 hours) allows Cherry-tTA-ER to enter the nucleus and bind the tetO array in the absence of doxycycline thereby activating reporter gene activity. The medium is replaced by microscopy medium (-30 min) thereby removing Tamoxifen. The microscopy imaging is started at -8 min and addition of doxycycline is at t=0. Cells are imaged for 90 minutes.

C) The images show a typical representation of a cell expressing mTurquoise-lacR (blue), Cherry-tTA-ER (red) and YFP-MS2 (green). The arrow points to visualization of the reporter gene array by mTurquoise-lacR, Cherry-tTA-ER and YFP-MS2 levels immediately after doxycycline (Dox) induction (t=0). The image is a z-projection of a fluorescence microscopy stack, and the bar represents 10 µm.

D) Schematic representation of the treatments to release transcriptional activator (Cherry-tTA-ER) from the reporter gene array to measure transcription repression kinetics. Tamoxifen (Tam) regulates the localization of Cherry-tTA-ER in the nucleus while doxycycline interferes with tetO binding at the reporter gene array.

versions of lacR and tetR to binding sequences of the cassette (Figure 1A-D). In addition, lacR or tetR can be used to target additional fused transcription or chromatin modifying factors to the array to study their effect on transcription of a CFP-tagged SKL reporter gene extended with DNA encoding for MS2 RNA hairpin loops (Figure 1A-D). MS2 hairpins at the transcribed genes can in turn be used to quantify transcriptional activity of the system by measuring intensities of fluorescently tagged MS2 protein. To activate the reporter gene we used tetR tagged with the C-terminal domain of the tetracycline controlled transactivator VP16 (tTA), which increases and reduces gene activity in absence and presence of tetracycline (or its derivate doxycycline), respectively. To be able to regulate nuclear translocation, tTA was also fused to a Cherry tagged version of the estrogen receptor ligand binding domain (Cherry-tTA-ER). mTurquoise tagged lacR was used to visualize and track the reporter gene array.

In a typical experimental set-up, the U2OS 2-6-3 cells were treated overnight with Tamoxifen which binds to the ER ligand binding domain and thereby induces nuclear translocation of Cherry-tTA-ER. Cells were then imaged by confocal microscopy after removing Tamoxifen to stop Cherry-tTA-ER transport into the nucleus, and prior and after adding doxycycline to rapidly release it from the reporter gene array (Figure 1B and D). To study the effect of altering chromatin structure of the reporter gene array on transcriptional regulation, we targeted CFP-lacR fused to MeCP2 (Ausió et al., 2014; Brink et al., 2013; Chahrour et al., 2008; Skene et al., 2010) to the lacO binding sequences within the reporter gene array.

Biphasic transcription repression

We measured the decrease in transcriptional activator (Cherry-tTA-ER) and transcripts (YFP-MS2) at the array in real-time when inducing the removal of Cherry-tTA-ER from the array (-Tam/+Dox). As controls we measured the Cherry-tTA-ER, YFP-MS2 and mTurquoise-lacR levels at the reporter gene array in response to the presence and/or absence of Tamoxifen and doxycyline, i.e. +Tam/+Dox, -Tam/-Dox, +Tam/-Dox (Figure S1). Both Cherry-tTA-ER and YFP-MS2 data fitted well to an exponential decline function (Figure S2, table S1).

We observed that the abundance of Cherry-tTA-ER and YFP-MS2 at the reporter gene array decreased with a median half-life ($t_{½}$) of 2 minutes and 8 minutes, respectively (Figure 2A, B, C, D). As an additional control, we measured whether the decrease in Cherry-tTA-ER at the reporter gene array induces a decrease in the level of histone acetyl transferase (HAT) GCN5 at the array. GCN5 is a bromodomain containing HAT known to accompany VP16 at the multicopy array in U2OS 2-6-3 cells and to anchor chromatin-modifying complexes to promoter nucleosomes (Brink et al., 2013; Hassan et al., 2002; Stafford and Morse, 2001). We observed that the decrease in GCN5 at the reporter gene array (median $t_{½}$ is 3.4 minutes) is no different from the decrease in Cherry-tTA-ER (Figure 2G), indicating that transcription activator removal-induced gene repression accompanies a drop in transcription regulatory proteins such as HAT enzymes.

To fit the exponential decline of YFP-MS2 transcripts we included the possibility that this decline consists of a lag time between the release of Cherry-tTA-ER and the actual decrease in MS2-tagged transcripts (Figure 2F). We noted that the decrease in YFP-MS2 is preceded by a transition phase with a median time of 5 minutes (Figure 2E). Depending on the residence time of RNA polymerase II at the reporter gene we can infer whether transcription continues after removal of the transcriptional activator from the array. Darzacq et al. estimated that the mean residence time of RNA polymerase II is 517 seconds at this multicopy reporter gene array (Darzacq et al., 2007). The sum of the reported residence time of RNA polymerase II and the time at which transcriptional activator Cherry-tTA-ER is removed from the reporter gene array (dashed gray lines in Figure S3) provides a rough estimation for the expected time of complete YFP-MS2 transcript loss. We refer to this time as the fraction of enduring transcription. At this time point at which all transcripts are expected to be lost from the array, on average 23% of the initial number of YFP-MS2 transcripts are still present at the reporter gene array (Figure 2F).

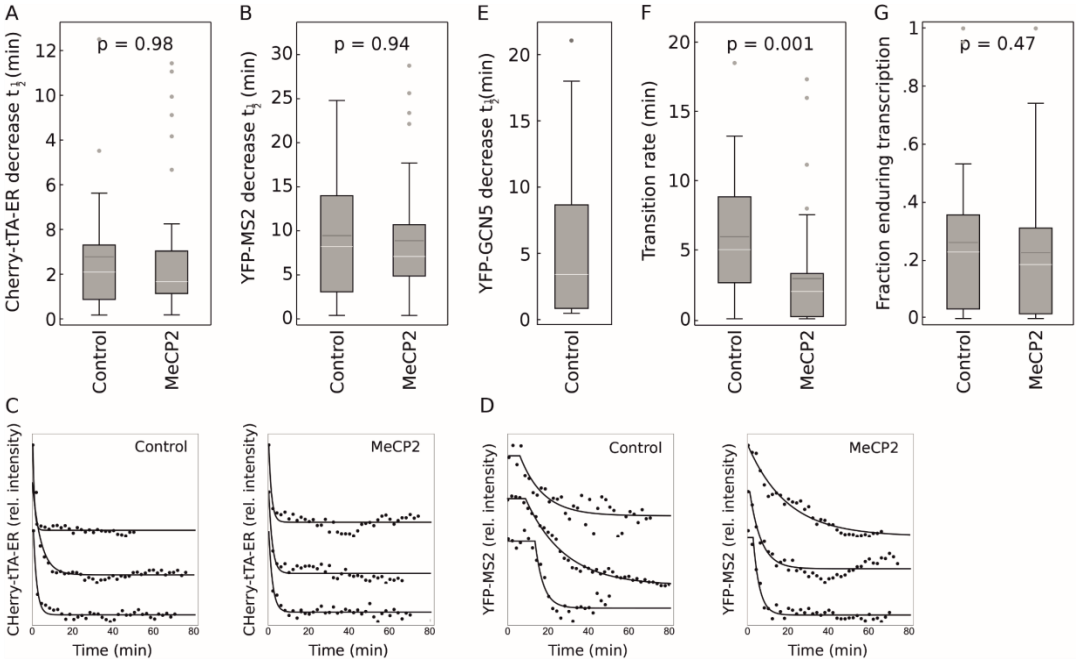

Figure 2: Transcription repression dynamics at the reporter gene array

Measurements at the reporter gene array in control and MeCP2 targeted U2OS 2-6-3 cells after doxycycline-induced release of Cherry-tTA-ER. The p-values shown are obtained by non-parametric Mann–Whitney U testing.

A) The half-life ($t_{1/2}$) for the decrease in transcriptional activator Cherry-tTA-ER localization at the reporter gene array.

B) The $t_{1/2}$ decrease in YFP-MS2 transcripts produced from the reporter gene array.

C) Representative single cell traces showing the decrease in Cherry-tTA-ER in control and MeCP2 targeted cells.

D) Representative single cell traces showing the decrease in YFP-MS2 in control and MeCP2 targeted cells at the reporter gene array.

E) The transition rate of transcription repression dynamics at the reporter gene array.

F) The fraction of enduring transcription at the reporter gene array. We interpret this fraction as the sum of the reported residence time of RNA polymerase II and the time at which transcriptional activator Cherry-tTA-ER is removed from the reporter gene array.

G) The $t_{1/2}$ decrease of acetyltransferase GCN5 at the reporter gene array

To determine if slow diffusion leads to underestimating the observed YFP-MS2 transcript levels, we applied fluorescence recovery after photobleaching (FRAP). Briefly, we bleached an area with a diameter spanning the reporter gene array and determined the

recovery of fluorescence at 1 second time intervals. The observed diffusion coefficients at the array for YFP-MS2 are 0.3 $\mu m^2/s$ and 0.03 $\mu m^2/s$ (Figure S6A, B, Table S2). These FRAP data indicate that the experimentally measured decrease in YFP-MS2 transcripts at the reporter gene array, upon removing Cherry-tTA-ER from the array (minute-scale), is much slower than the estimated second-scale YFP-MS2 transcript diffusion rate.

MeCP2 facilitates increased transcription repression responsiveness

To investigate the contribution of local chromatin structure on transcription repression dynamics, we measured the response of the system upon targeting MeCP2 to the reporter gene array (Figure S4). We observed that the abundance of Cherry-tTA-ER at the MeCP2 targeted gene array decreased with a median half-life of 1.5 minutes, slightly faster than the half-life of Cherry-tTA-ER in control cells (Figure 2A, C). Similarly, we noted that the decrease of YFP-MS2 at the MeCP2 targeted reporter gene array had a comparable median half-life to that observed in control cells (median $t_{½}$ is 6.8 minutes, Figure 2B, D). Also the percentage of YFP-MS2 transcripts at the MeCP2 targeted reporter gene array at the time point that Cherry-tTA-ER is expected to be lost from the array is similar to the percentage in control cells, 19 % versus 23 %, respectively (Figure 2F). Notably, when MeCP2 is present at the reporter gene array, we observed a significantly shorter transition time preceding the decrease in transcripts compared to the transition rate in control cells (median transition rate in MeCP2 targeted cells is 2 minutes versus 5 minutes in control cells) (Figure 2E). These data suggest that at the MeCP2 targeted array, accelerated repression is achieved via a change in the transition rate instead of the actual decrease in transcripts.

To explore whether MeCP2 targeting has an effect on the size, mobility and transcriptional state of the array, we tracked the motion of the MeCP2 targeted array and measured its size and levels of Cherry-tTA-ER and YFP-MS2 (Figure S4, S5). On average we observed an increased nuclear motion (Figure S4) but unaltered size of the array upon MeCP2 targeting (Figure S5C), whereas we did not observe a significant difference in

levels of Cherry-tTA-ER and YFP-MS2 at the array either in the presence or absence of MeCP2 (Figure S5 A-C). To further illustrate the correlation between Cherry-tTA-ER and YFP-MS2 levels, we plot the correlation between Cherry-tTA-ER levels in the nucleus and at the array as well as between Cherry-tTA-ER and YFP-MS2 levels both at the array. We observed a positive correlation between Cherry-tTA-ER nuclear and array bound levels in both control and MeCP2 targeted cells (ρ = 0.72 and 0.61, respectively), which indicates that in our experimental set-up Cherry-tTA-ER binding at the reporter gene array is not saturated. (Figure S5D). Plotting the correlation between Cherry-tTA-ER and YFP-MS2 levels at the reporter gene array in control and MeCP2 targeted cells (ρ = -0.32 and -0.13, respectively) shows in both cases a negative correlation. This suggests that the transcriptional response is saturated already at initial transcriptional activator levels before Cherry-tTA-ER is lost from the array, indicating that minor fluctuations in Cherry-tTA-ER do not affect the YFP-MS2 output. (Figure S5E).

Discussion

The U2OS 2-6-3 reporter gene array provides an effective tool to measure gene activity in a local chromatin context since it allows local transcription modulation without affecting global transcriptional outputs. We show biphasic transcription repression, i.e. a transition phase until transcripts are lost from the array after which transcript levels decrease exponentially. Targeting of MeCP2 to the reporter gene array accelerates the transition rate while the kinetics of the decrease in transcripts at the array are unaffected.

Our data point out that the observed transition rate in transcription repression compared to fast loss of transcriptional activator from the array cannot be explained by slow diffusion of YFP-MS2 transcripts that are produced by the reporter gene since the second-scale YFP-MS2 diffusion hardly contributes to the minute-scale measured decrease in YFP-MS2 transcripts. Our data suggest that endogenous transcriptional activators are still able to initiate ongoing transcription and that engaged RNA polymerase II continues producing mRNA and creating new binding sites for YFP-MS2 protein even beyond the point when the initial transcriptional activator is lost. We show that MeCP2 facilitates the transition

timeof single cells to become transcriptionally repressed. Our data show that the transcriptional activator levels at the array in MeCP2 targeted and control cells are very similar (Figure S6A). Moreover, we noted that the activated reporter gene array both in control and MeCP2 targeted cells is rather insensitive to a decrease in transcriptional activator (Figure S6E and Figure S3, S4). We conclude that once a gene is active, the period of activity is mainly determined by chromatin structural alterations thereby introducing a transition rate in transcription repression.

For instance histone exchange processes including incorporation of variant and/or canonical histones, and their posttranslational modifications, are efficient mechanisms to lengthen the response time in altering gene activity (Venkatesh and Workman, 2015). In principle, it is known that passage of RNA polymerase II over coding regions of genes is accompanied by a disruption of nucleosome structure. Depending on the level of gene transcription (low, moderate or high) chromatin structural alterations occur more frequently, but in all cases transcription shutdown is accompanied by re-formation of a more spaced nucleosomal state and histone exchange suppression (Kulaeva et al., 2013; Venkatesh and Workman, 2015). We propose that local chromatin context determines whether new transcription initiation events take place, or whether the chromatin first needs to change its structure thereby regulating transcription repression at the level of time delayed responsiveness (Figure 3). In this context, Bintu et al. illustrated the dynamic behavior in gene activity upon recruiting epigenetic regulatory proteins associated with a broad range of chromatin modifications (Bintu et al., 2016). The authors identified that different regulators evoke diverse modes of action via an altered initial transition rate and time scale of operation.

Since the studied reporter gene array is a multicopy array, we expected that MS2-tagged transcript measurements in single cells would represent an average transcript number of all single reporter genes within the array and that it would provide low cell-cell variability in reporter gene activity. However, we observe substantial variability in transcriptional activity and response time between single cell samples (Figure S2, S3, and 2E). This variation might be caused by variation in Cherry-tTA-ER expression levels, heterogeneity

in the cell-cycle status, or a combination of factors. Since transcription initiation events are known to correlate within the same locus (Gandhi et al., 2011; Raj et al., 2006) all genes within the reporter gene array might cycle simultaneously between 'on' and 'off' states. In this context, it should be noted that the locus of the reporter gene array spans 200 times 3.3 kb.

Determining the molecular aspects of transcription dynamics is still a central challenge to understanding eukaryotic gene expression regulation. Large protein complexes assemble and disassemble at genes within seconds (McNally et al., 2000), nucleosome exchange occurs in the order of minutes to hours depending on the genomic location (Dion et al., 2007), and transcript production is shown to follow complex bursting dynamics. Transcriptional kinetics of endogenous genes is characterized in single cells measuring transcription cycling of a short-lived luciferase reporter gene inserted into the mammalian genome (Chubb et al., 2006; Reid et al., 2009; Suter et al., 2011). By inferring dynamic on/off state kinetic parameters from a mathematical approach, Suter et al. showed that for each gene, specific endogenous regulatory sequences determine its set of kinetic transcription parameters. Many studies used a random telegraph model to describe transcriptional kinetics, stating that a gene can be in a transcriptionally active or inactive state (Peccoud and Ycart, 1995). Rybakova et al. and Schwabe et al. described transcription cycling according to a ratchet model, showing transitioning between 'on' to 'off' and 'off' to 'on' states via a multistep process (Rybakova et al., 2015; Schwabe et al., 2012). The progression through the ratchet in this model is locked by irreversible covalent reactions, representing for instance chromatin structural changes induced by posttranslational histone modifications. During the transition from the 'on' to 'off' state, transcription is still able to proceed. Therefore, a ratchet-like model predicts a delayed deactivation of transcription. Up until now experimental work has failed to show triggered transcriptional deactivation, hence the delay in response to transcriptional deactivation. In our experimental set-up, the U2OS 2-6-3 reporter gene array enabled us to experimentally measure triggered transcription repression in single cells of an activated reporter gene using time-lapse microscopy. Upon targeting MeCP2 to the reporter gene array, we observe a diminished transition rate in transcription repression,

indicating a more rapid transitioning from the 'on' to 'off' phase. Of interest, the transcriptional activation levels seem to be increased by targeting MeCP2 to the array. Since MeCP2 effectively decreased the 'on' phase, such an effect can only be obtained by faster transitioning through the 'off' phase. This would imply a double role for MeCP2 in transcription and might add to the much-discussed role of MeCP2 in gene expression.

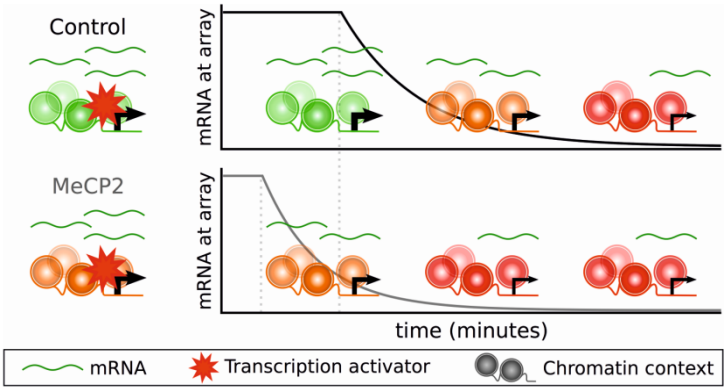

Figure 3: Single cell transcription repression indicates a chromatin-dependent transition rate

The cartoon illustrates the main characteristics of the measured repression dynamics, illustrating the decrease in transcripts (green lines) in real-time upon releasing a transcriptional activator (red star). Control cells (represented by the black line) display a prolonged transition time (dashed gray lines) compared to the repression in MeCP2 targeted cells (represented by the gray line). We propose that local chromatin context (represented by the colored DNA-nucleosome-promoter cartoon) sets the transition rate of transcription repression by temporally allowing new transcription initiation events.

Materials and Methods

CELL CULTURE

U2OS 2-6-3 YFP-MS2 expressing cells (Janicki et al., 2004) were cultured in DMEM, glutamax (Gibco, Thermo Fisher Scientific Inc.) 10% tet approved FCS (Clontech Laboratories, Inc., Takara biocompany), 1% PS (Gibco, Thermo Fisher Scientific Inc.) and 40µg/ml G418 (Gibco, Thermo Fisher Scientific Inc.) at 37°C under 10% CO2. Cells were transfected using lipofectamin 2000 according to manufacturer's instruction. Tamoxifen (Sigma) was added at 1mM concentration 20 hours prior to the experiment unless stated otherwise. Doxycycline was added to a final concentration of 1 ug/ml. The medium was replaced with Microscopy Medium, (137mM NaCl, 20mM D-glucose, 20mM Hepes, 5.4 mM KCl, 1.8 mM $CaCl_2$, 0.8 mM $MgSO_4$) 30 min before imaging.

PLASMIDS

Cherry-tTA-ER and YFP tagged GCN5 were gifts from SM Janicki and mTurquoise tagged lacR from MS Luijsterburg. CFP-lacR-MeCP2 was assembled with a Gibson assembly (Gibson et al., 2009) using EGFP-lacR-MeCP2 (Brink et al., 2013) and the CFPs3a (Clontech laboratories, Inc., Takara biocompany) vector using the following primers CCGGACTCAGATCTCGAGCATCCATGGTGAAATATGTAAC,
GGGCGATCGTCTAGAGTCGAGTTTAGTGAACCGTCAGATC and the Reverse complement sequence of both primers.

TIME-LAPSE MICROSCOPY MEASUREMENTS

For time-lapse microscopy imaging, U2OS 2-6-3 cells stably expressing YFP-MS2 were transfected with mTurqoise tagged lacR and tTA-Cherry-VP16 or together with YFP-GCN5 in Mattek dishes. 1mM Tam was added 20 h before the experiment to enable Cherry-tTA-ER diffusion into the nucleus allowing Cherry-tTA-ER binding at the tetO binding sites of the integrated reporter gene array. Prior to the single cell time-lapse microscopy measurements, Tam was washed away from the medium disabling Cherry-tTA-ER disabling transport to the nucleus. After ~30 minutes the cells are adjusted in the microscopy chamber and at t=0 doxycycline was added to an end concentration of 1µg/ml, inducing a fast release of Cherry-tTA-ER from the tetO binding sites. The amount of Cherry-tTA-ER at the reporter gene array is measured using time-lapse wide-field microscopy imaging for up to 90 minutes. The time-line of treatments is shown in Figure 1C. The accumulation of Cherry-tTA-ER and YFP-MS2 at the mTurqoise-lacR labeled reporter gene array can be measured by means of mCherry, mTurqoise, and YFP measurements using a wide field microscope. We used a Zeiss Axiovert 200m (Zeiss, Germany) with a Cairn xenon arc lamp (Cairn Research, UK) with a monochromator (0.30nm) and Zeiss 100x 1,4NA oil objective. The microscope is equipped with an incubator and an objective heater and heated to 37°C. Every 2 minutes images were taken with a cooled CCD camera (Coolsnap HQ, USA) using the following filters: CFP/mTurquoise: BP 470-30 YFP: BP 535-30 RFP: BP 620-60. Although we used both CFPs3a as well as mTurquoise, the same settings were used to ensure the same photography set-up for later comparison of time series.

IMAGE ANALYSIS

In the first image of each time series, all acquired channels (YFP-MS2, Cherry-tTA-ER and mTurquoise-lacR) were averaged to identify the center coordinates of the reporter gene array. These coordinates were used in the ”SpotTracker2D” (Sage et al., 2005) extension in ImageJ to track the reporter gene array at all time points. The obtained center coordinates of the reporter gene array were used to measure YFP, mCherry, and mTurquoise or CFP intensities averaging over an area of 5 by 5 pixels (= 0.934µm × 0.934µm) centered at these coordinates. At each time point, we corrected for background intensity by subtracting the average of an equally sized background spot from within the nucleus. When the default background spot did not fall in the nucleus, we manually selected another one. Each single-cell time series was normalized to the maximum and minimum intensity spot of the image series.

FLUORESCENCE RECOVERY AFTER PHOTOBLEACHING (FRAP)

We used a Leica SP5 confocal laser-scanning microscope equipped with a 40x/1.2NA HCX PL APO CS oil-immersion objective (Leica), an argon laser and an AOTF. For FRAP analysis, a cell was scanned at 514 nm excitation with short intervals (585 ms) at low laser power (zoom 8 with 68.9 nm pixel size). After 10 scans a high intensity (100% laser power) 650 ms bleach pulse at 488 nm was applied to a photobleaching spot with a diameter of 2.5 µm spanning the reporter gene array. Subsequently, the recovery of the fluorescence intensity of the photobleached spot was followed for another 20 seconds at 1s intervals and 300 seconds at 3s intervals. All curves were normalized to baseline fluorescent intensity post-bleach and averaged. The Lecia LASAF software was used for image acquisition and data extraction. We analyzed the FRAP data by fitting bi-exponentially the mRNA bound fraction and the non-bound freely diffusing YFP-MS2 fraction.

$$I(t) = 1 + A_1 e^{-\lambda_1 t} + A_2 e^{-\lambda_2 t}$$

We constrained both fits to use the same recovery rates (λ1 and λ2) since both fits consider the same YFP-MS2 molecules and YFP-MS2 bound transcripts.

MS2 DIFFUSION MODEL

From the FRAP data, we calculated the diffusion coefficient using: (Kang et al., 2012)

$$D = 0.224\ \frac{\omega^2}{t_{1/2}},$$

in which D is the diffusion coefficient in $\mu m^2 s^{-1}$ and ω is the diameter of the bleached spot of the FRAP experiment. We constructed a two-dimensional finite difference diffusion model that provides diffusion in space and time. The model calculates the concentration at a certain time point and position based on the concentrations at this position and its direct surroundings at the previous time point. We generated a circular shaped grid with a diameter of 15 µm and we used a grid size of 0.1 μm^2. The transcription site is considered to have the same size as the average reporter gene array size within our experiments (2.45 μm^2, data not shown) and the reporter gene array is considered to be located at the center of the nucleus. We did not consider degradation or transport to the cytoplasm in the model.

From the FRAP data we extracted the ratio between mRNA-YFP-MS2 and YFP-MS2 in the nucleus (0.25:0.75) and the transcription spot (0.73:0.27). From the FRAP data, we can also calculate the average intensity ratio between the nucleus and the transcription spot. (0.27:0.73). Scaling the ratios obtained from the bi-exponential fit with the spot intensity ratio shows that there is as much of YFP-MS2 present in the nucleus as at the transcription spot. However, mRNA-YFP-MS2 is almost 8 times more abundant at the transcription spot. These ratios are summarized in Table S2 and used as starting conditions of the model.

Acknowledgements

We would like to thank S.M. Janicki, D.S. Spector and R. Singer for kindly providing cell clones and constructs used in these experiments.

Supplementary Material

Table S1

The half-life (t1/2) decrease in Cherry-tTA-ER from the reporter gene array in minutes.

A rapid decrease in Cherry-tTA-ER localization at the reporter gene array is achieved by the presence of doxycycline and absence of Tamoxifen. This setup disables transport of Cherry-tTA-ER to the nucleus and inhibits its binding to the gene array.

	- Tam	**+ Tam**
- Dox	76.5 min.	160.3 min.
+ Dox	2.1 min.	21.3 min.

Table S2

Relative amount of MS2 fractions in the nucleus and at the reporter gene array

The data show the calculated start condition measurements used for the diffusion model. MS2-YFP fractions are based on pre-bleach intensities of FRAP data and fractions ($A_{1\ and}\ A_2$) from the fitted bi-exponential functions.

Molecule	**Location**	**Relative Amount (a.u)**
MS2-YFP	Nucleus	0.206
mRNA-MS2-YFP	Nucleus	0.067
MS2-YFP	Reporter array	0.193
mRNA-MS2-YFP	Reporter array	0.533

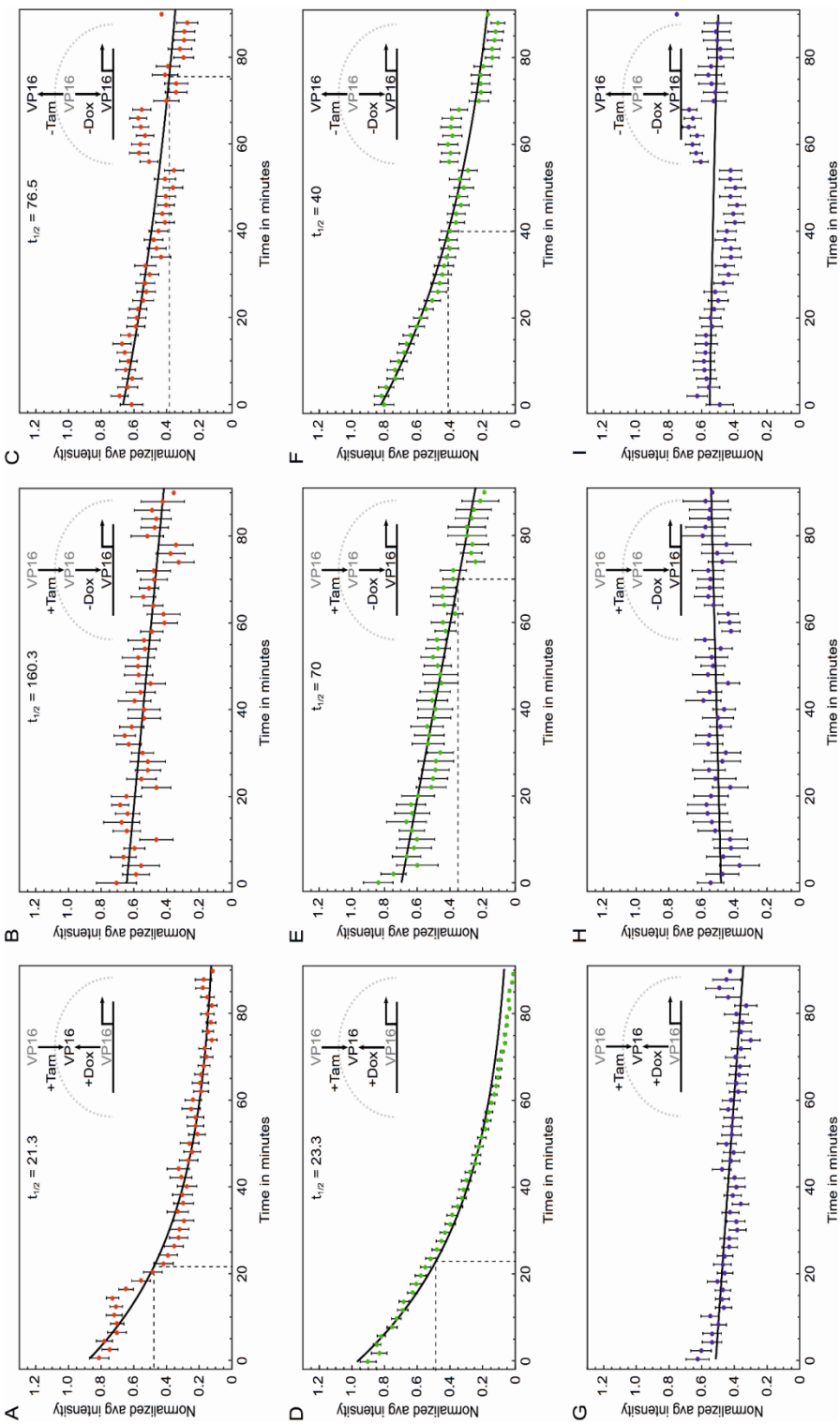

Figure S1: Cherry-tTA-ER, YFP-MS2 and mTurquoise-lacR time-lapse microscopy measumrements in the presence and/or absence of doxycycline and Tamoxifen

Figure S1: Cherry-tTA-ER, YFP-MS2 and mTurquoise-lacR time-lapse microscopy measurements in the presence and/or absence of doxycycline and Tamoxifen

A, D, G) The decrease in Cherry-tTA-ER transcriptional activator (A), MS2-YFP transcripts (D), and mTurqoise-lacR (G) from the reporter gene array in U2OS 2-6-3 cells in the presence of both Tamoxifen and doxycycline (+Tam/+Dox).

B, E, H) The decrease in Cherry-tTA-ER transcriptional activator (B), MS2-YFP transcripts (E), and mTurqoise-lacR (H) at the reporter gene array in U2OS 2-6-3 cells in the presence of Tamoxifen and absence of doxycycline (+Tam/-Dox).

C, F, I) The decrease in Cherry-tTA-ER transcriptional activator (D), MS2-YFP transcripts (F), and mTurqoise-lacR (I) at the reporter gene array in U2OS 2-6-3 cells in the absence of both Tamoxifen and doxycycline (-Tam/-Dox).

The cartoon insert represents the experimental set-up of different subfigures. The dots show the mean normalized intensity at each time point. The error bar shows the standard error of the mean. The half-life ($t_{1/2}$) of the decrease in Cherry-tTA-ER transcriptional activator and MS2-YFP transcripts at the reporter gene array is shown at the top-center of each plot and is indicated by the dashed lines.

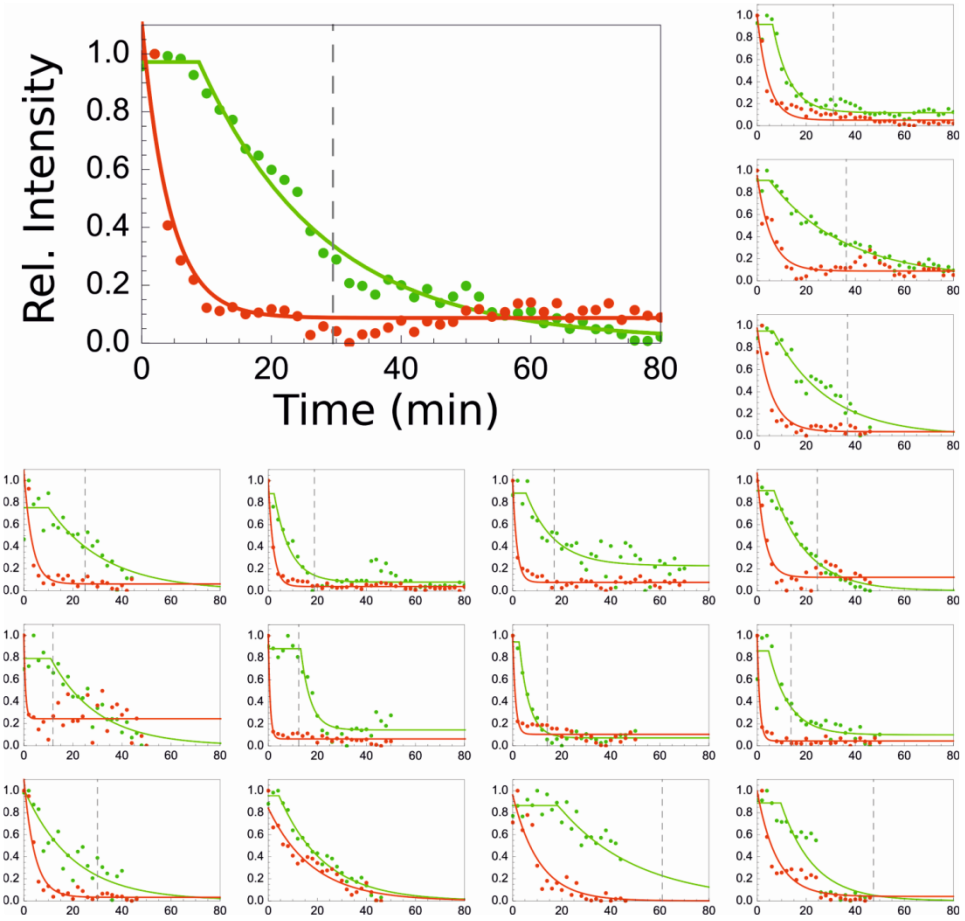

Figure S2: Single cell measurements of the decrease in Cherry-tTA-ER transcriptional activator and YFP-MS2 transcripts in U2OS 2-6-3 control cells

The plots show the decrease in YFP-MS2 transcripts (green) and Cherry-tTA-ER transcriptional activator (red) at the reporter gene array in U2OS 2-6-3 cells upon removing Cherry-tTA-ER from its tetO binding sequences in the presence of doxycycline and absence of Tamoxifen. The data is fitted to an exponential function with or without a delay for YFP-MS2 and Cherry-tTA-ER dynamics, respectively. The dashed line gives the time point at which Cherry-tTA-ER is depleted from the reporter gene array with an additionally added 517 seconds representing the average RNA polymerase II residence time at the reporter gene. The fitted curves that deviated on average more than 10% from each data point were not used for further analyses.

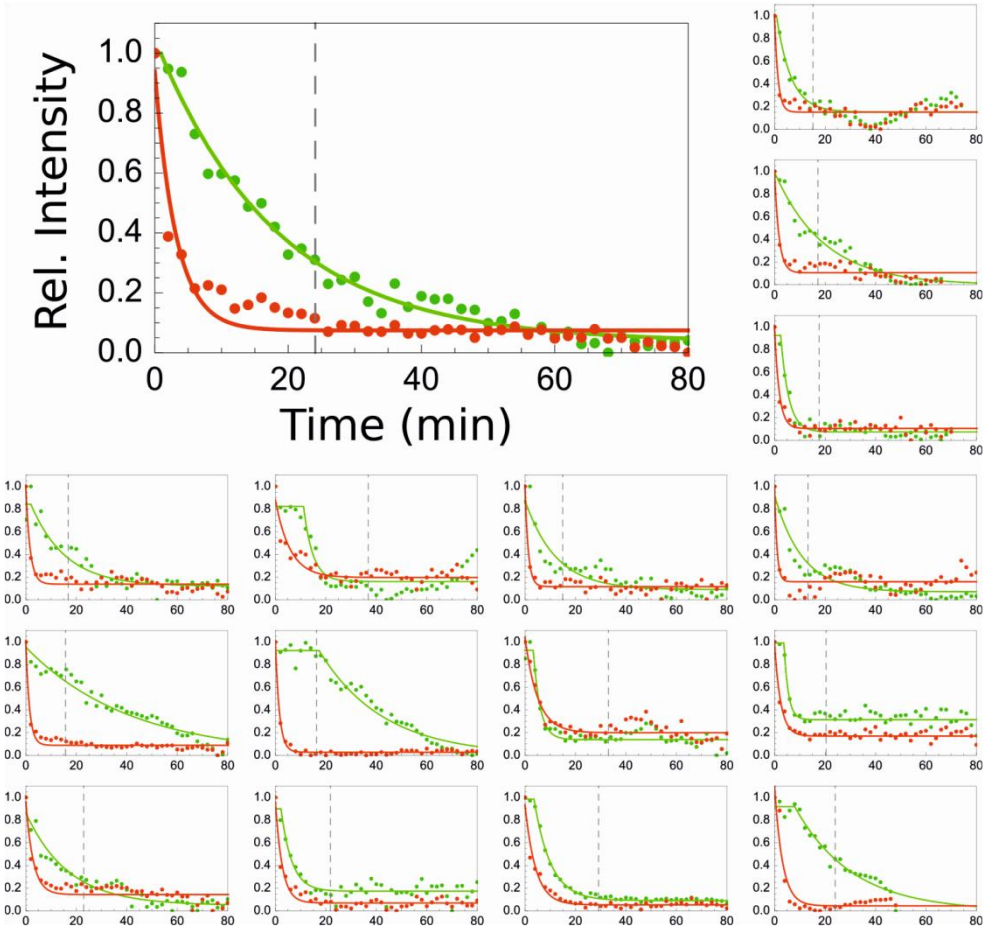

Figure S3: Single cell measurements of the decrease in Cherry-tTA-ER transcriptional activator and YFP-MS2 transcripts in U2OS 2-6-3 MeCP2 targeted cells

The plots show the decrease in YFP-MS2 transcripts (green) and Cherry-tTA-ER transcriptional activator (red) at the reporter gene array in U2OS 2-6-3 cells upon inducing the removal of Cherry-tTA-ER from its tetO binding sequences in the presence of doxycycline and absence of Tamoxifen. The data is fitted to an exponential function with or without a delay for YFP-MS2 and Cherry-tTA-ER dynamics, respectively. The dashed line gives the time point at which Cherry-tTA-ER is depleted from the array with an additionally added 517 seconds of the average RNA polymerase II residence time at the reporter gene. The fitted curves that deviated on average more than 10% from each data point were not used for further analyses.

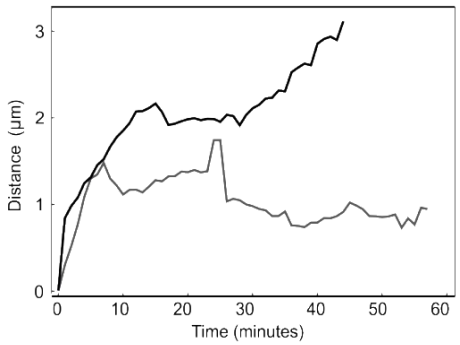

Figure S4: Mobility of the transcription spot during transcription repression

The average displacement of the reporter gene array in U2OS 2-6-3 cells upon inducing the removal of Cherry-tTA-ER from its tetO binding sequence is shown in time for both control (grey) and MeCP2 targeted (black) cells.

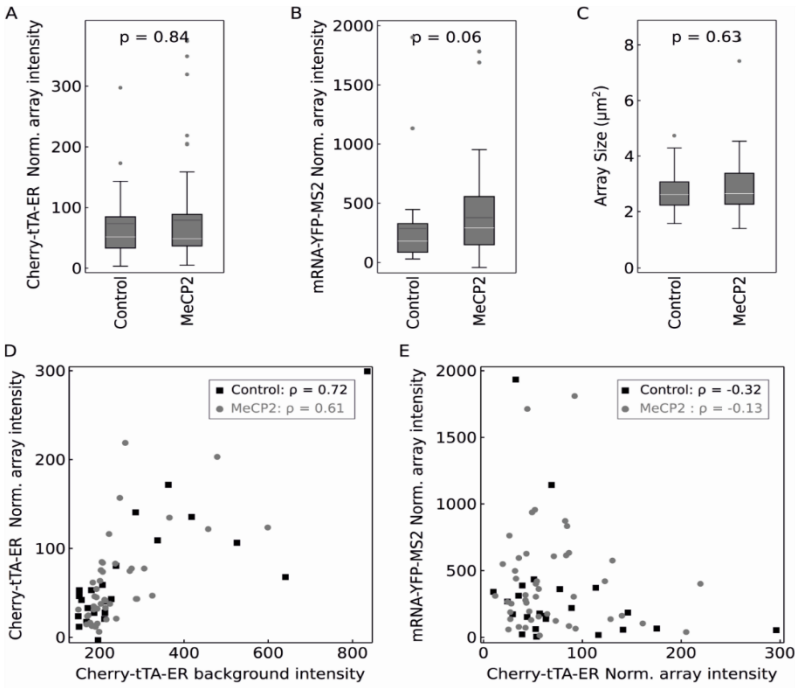

Figure S5: Reporter gene array measurements at control and MeCP2 targeted reporter gene array in U2OS 2-6-3 cells

A) The background-normalized amount of Cherry-tTA-ER transcriptional activator at the reporter gene array in the control and MeCP2 targeted array.

B) The background-normalized amount of YFP-MS2 transcripts at the reporter gene array in control and MeCP2 targeted cells.

C) The size of the transcription array in control and MeCP2 targeted cells. D) The correlation between transcriptional activator (Cherry-tTA-ER) on the reporter gene array versus random nuclear levels in control cells (circles) and the targeted cells (squares).

E) The correlation between transcriptional activator (Cherry-tTA-ER) versus transcript (YFP-MS2) levels at the reporter gene array in control (circles) and MeCP2-targeted cells (squares).

In A-C, the p-value shown is obtained with the Mann-Whitney U test. In D and E correlation coefficients are given in the inset.

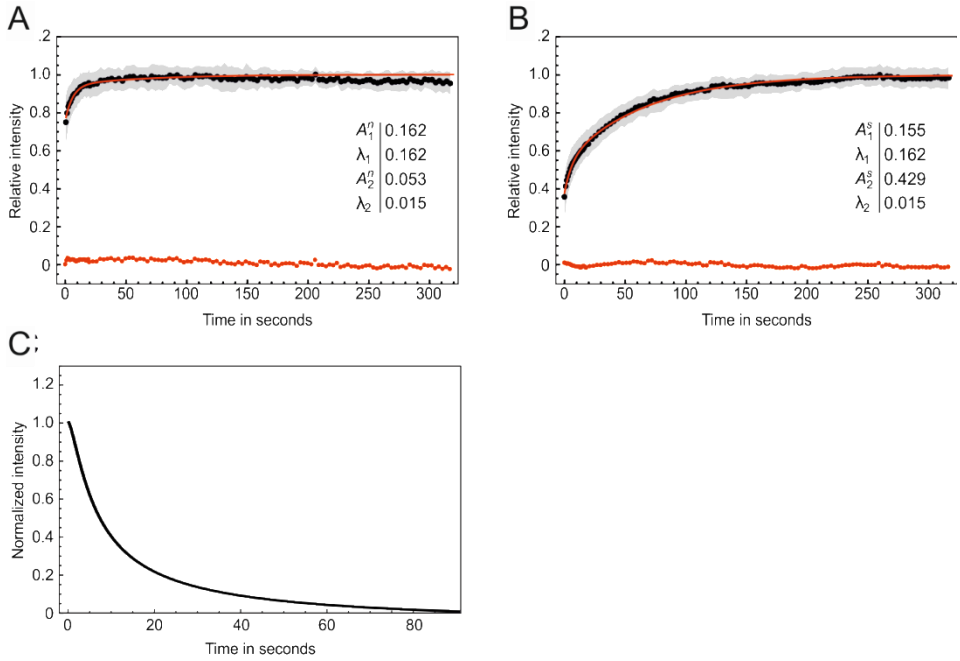

Figure S6: YFP-MS2 diffusion kinetics

A) FRAP measurements of YFP-MS2 in the nucleus of U2OS 2-6-3 cells. Two different YFP-MS2 fractions can be distinguished representing freely diffusing and bound YFP-MS2.

B) FRAP measurements of YFP-MS2 at the gene array in U2OS 2-6-3 cells. Two different YFP-MS2 fractions can be distinguished representing freely diffusing and bound YFP-MS2.

The black dots show the mean of 20 individual FRAP experiments. The gray shaded areas show the standard deviation around this mean. The red line gives the least squares fit to the data points with the residual shown by the red dots. Table 1 summarizes the parameters of the bi-exponential fit, with the fractions of YFP-MS2 (A1) and mRNA-YFP-MS2 (A2) of either the nucleus denoted by (n) or the reporter gene array denoted by (s) and the rate constants denoted by λ1 and λ2.

C) Based on the diffusion parameters, the data are simulated with a diffusion model. The diffusion model simulation shows that upon instant transcription termination the intensity of the transcription spot exhibits a half-life of 7.9 seconds.

Chapter 2

Generating cell clones to measure transcription dynamics in an induced variable epigenetic chromatin state

Diewertje G.E. Piebes, Pernette J. Verschure

Abstract

To investigate the influence of the chromatin context on transcription regulation in single cells at the level of single genes we created a reporter gene cassette to be inserted into defined genomic sites of human cells. The cassette is equipped with a readout to measure real-time mRNA and protein level kinetics of a reporter gene upon modulating the epigenetic chromatin state of the reporter gene. The reporter gene is driven by a mammalian promoter that induces constitutive gene expression. The reporter gene cassette containing cells with a single integration site are designed to measure the mRNA and protein levels in real-time and the response time to alter the transcription output upon modulating the epigenetic chromatin state of the cassette. This approach should enable us to determine the gene-specific kinetic characteristics of transcription and the contribution of epigenetic regulation. Here we provide an overview of the set-up of our experimental approach and we discuss our design compared to the current state-of-the-art to visualize mRNA with high temporal and spatial resolution. Here we show that the reporter gene cassette is being expressed when transfected in human cells and that the target constructs bind to a tet operator repeat. In future studies we plan to integrate the cassette via homologous integration in the human genome and measure single gene, single cell real-time transcription upon modulating the chromatin structure.

Introduction

Epigenetic gene regulation is essential to orchestrate gene expression patterns and plays a major role in determining cellular identity. Epigenetic regulatory mechanisms, such as histone modifications and DNA methylation, have been directly linked with transcriptional regulation and changes in higher-order chromatin folding (Deng and Blobel, 2014; Rafalska-Metcalf et al., 2010; van Steensel, 2011; Wendt and Grosveld, 2014). Currently, we lack quantitative understanding of these complex interactions. Mechanistic interactions of individual epigenetic factors that determine single gene transcription dynamics, are largely unknown. Such regulatory networks are often simply represented as all-or-none, i.e. gene silencing or activation.

Gene regulatory networks are inherently noisy due to the low amount of reacting components. The noise caused by the transcription regulatory network is considered to represent a form of intrinsic noise. Noise can be propagated from one cellular compartment to another within the same cell (Maheshri and O'Shea, 2007). Such propagated noise is considered to represent an extrinsic noise source (Johnston et al., 2012; Maheshri and O'Shea, 2007). Noise in transcription kinetics is still largely unexplored, but an important factor when measuring at the single cell, single gene level. In a previous theoretical study the role of noise in transcription regulation is explored studying nonexponentially distributed lifetimes of gene states (Schwabe et al., 2012). Schwabe et al. represented a stochastic model entitled 'the molecular ratchet' that considers the concerted action of several proteins assuming an ordered, multistep and cyclic mechanism involving a sequence of transitions between distinct chromatin states. The molecular ratchet transitions are assumed to involve reversible protein complex formation on chromatin followed by irreversible posttranslational histone modifications. To experimentally test this theoretical model, single gene transcriptional measurements are inevitable. In the present study, we set-out to develop a reporter gene cassette containing cell line to quantitatively study the contribution of the epigenetic chromatin state in regulating the rate of transcription at single gene level in single cells. Using this cell line we are able to test the behavior of the theoretical molecular ratchet model. The integration of such theoretical transcription regulation models with transcription real-time single cell imaging will undoubtedly provide more insight into the complex regulation and stochastic nature of transcription.

We constructed a reporter gene cassette consisting of a reporter gene that consists of MS2 tagged RNA which can be detected by constitutively expressed fluorescently tagged MS2 protein and that contains DNA binding sequences allowing to target epigenetic regulatory proteins to modulate the chromatin structure of the cassette. We engineered the reporter gene cassette such that we can perform systematic quantitative measurements allowing to plot the transcription rate as function of (i) the integration of the reporter gene cassette in a defined genomic chromatin context, (ii) targeting and accumulation of epigenetic regulatory proteins to the reporter gene cassette and (iii) the

local chromatin structure of the reporter gene cassette. This set-up will enable us to interpret transcriptional cell-cell variability and the contribution of the epigenetic chromatin state to transcriptional noise. In the present study, we show the cloning and transient transfection of this reporter gene cassette and the creation of epigenetic targeting constructs to modulate the chromatin structure of the cassette.

Results

Design of the reporter gene cassette

To quantitatively study the contribution of the epigenetic chromatin state in regulating the rate of transcription, we designed a cell line consisting of a reporter gene cassette containing several features. These features represent (i) an array of tet operator (tetO) binding sequences allowing binding of tetracyclin-induced Cherry tet repressor (tetR)-tagged transactivator VP16 (tTA) fused to the ligand binding domain of the estrogen receptor (ER), i.e. Cherry-tTA-ER targeting, (ii) a mTurquoise-NES-PEST tagged reporter gene driven by a phosphoglycerate kinase (PGK) promoter and (iii) a bacteriophage MS2 hairpin repeat to detect RNA transcripts via YFP tagged MS2 protein binding (Figure 1A and B).

To measure the effect of both transcriptional repressors and activators at protein level, we used a reporter gene coding for a short-lived fluorescent protein. Short-lived proteins allow to measure changes in their protein level upon transcriptional repression in time. Many short-lived proteins have a life time shorter than 2 hours and they consist of a degradation signal, e.g. a PEST sequence, named after the amino acids they represent. The PEST sequence is present in short-lived proteins such as mouse ornithine decarboxylase (MODC), which has a life time 30 minutes. Li et al. noticed that fusion of the PEST part of the MODC protein to a GFP reporter gene drastically reduced the life time of the reporter gene (Li, 1998). We fused this PEST signal to the mTurquoise reporter gene to reduce the life time of the mTurquoise reporter gene. In addition, we added a nuclear export signal (NES) to the mTurquoise reporter gene to export the fluorescent

protein outside of the nucleus and measure its protein levels in the cytoplasm (Figure 1A and B).

We selected the mammalian PGK promoter to drive the exon-only sequence of mTurquoise. This cyan fluorescent protein has a respective high Quantum Yield, providing bright fluorescence and relatively low photo toxicity (Goedhart et al., 2010). The PGK promoter is known to induce constitutive gene expression in cultured cells and in transgenic mice (McBurney et al., 1994).

To allow visual single cell transcription measurements of the reporter gene in real-time, we integrated a hairpin-bearing MS2 bacteriophage sequence into the reporter gene coding DNA that upon transcriptional activation is rapidly bound with high specificity and affinity to constitutively expressed YFP-tagged MS2 bacteriophage capsid protein (Ben-Ari et al., 2010).

The reporter gene cassette contains a FRT site enabling integration of the cassette via homologous recombination with a FRT Flipase site. A series of human embryonic kidney (HEK) cells were previously created by Gierman et al, containing a FRT Flipase site and a GFP reporter gene at known genomic sites. A nested-PCR was used to identify the exact integration of the FRT Flipase containing reporter gene. The expression levels of the GFP reporter gene at these integration sites is identified in a previous study (Gierman et al., 2007)(Anink-Groenen et al. unpublished results). Our reporter gene cassette was designed such that these defined FRT Flipase containing genomic sites could be used as landing platform allowing to insert our cassette into previously examined genomic sites.

The integration of a 84x tetO tandem repeat upstream of the reporter gene enables us to modulate the epigenetic chromatin state of the reporter gene cassette via targeting of tetR binding proteins fussed to epigenetic regulatory proteins. The reporter construct, consisting of the PGK promoter, the mTurquoise reporter gene, MS2 repeats and the FRT Flipase site was synthesizes by Genescript©. The Genscript© synthesized construct was

cloned into the transfection vector pPur to add the 84x tetO tandem repeat. The final DP15 construct has a size of 11.312 kb.

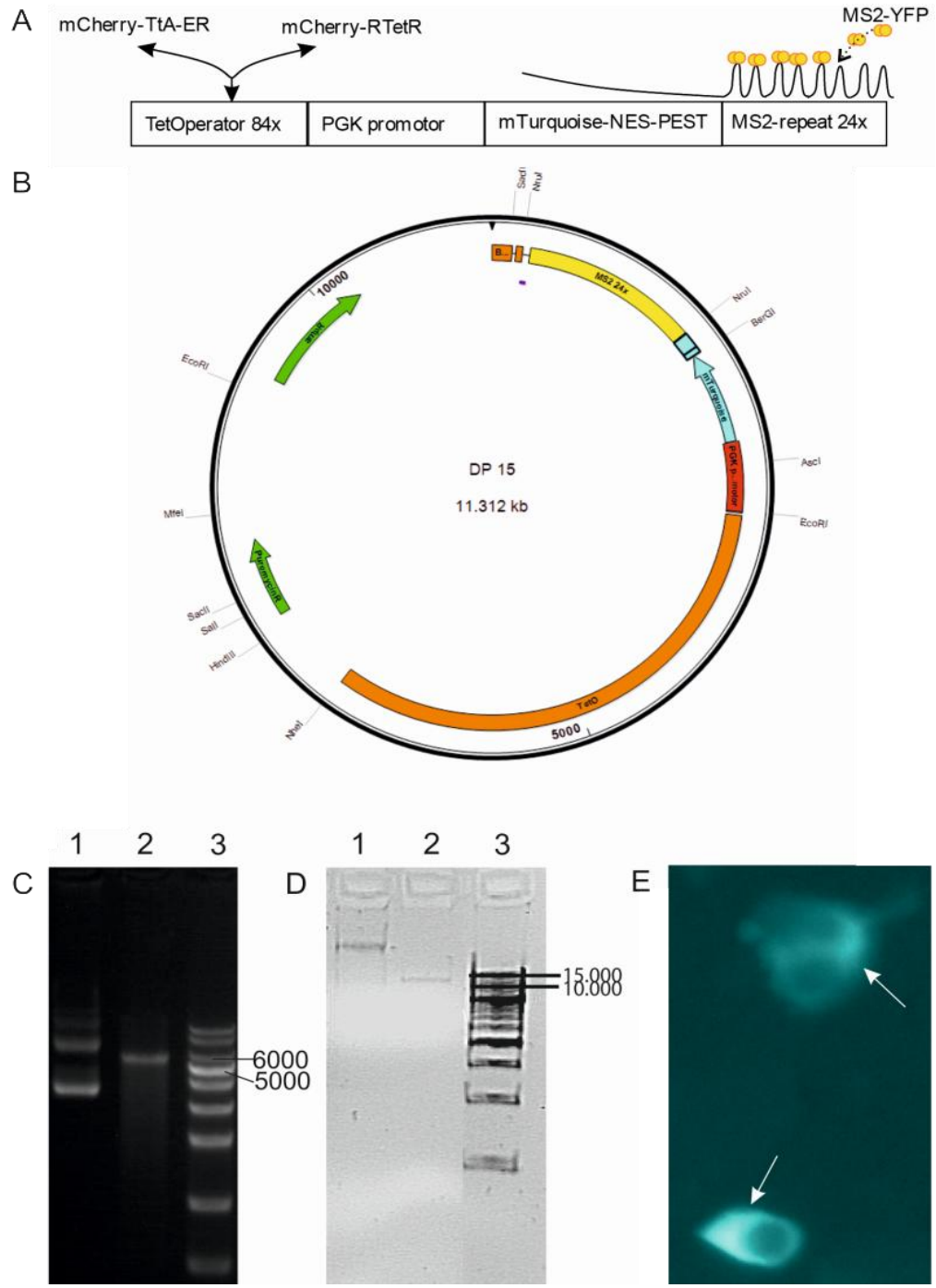

Figure 1: Reporter gene cassette

Figure 1: Reporter gene cassette

1A) The reporter gene cassette containing a 84x tandem tetO repeat sequence allowing targeting of the tetR and rtetR constructs (i.e. Cherry tagged TtA containing an ER binding domain and Cherry tagged rtetR). The mTurquoise reporter gene containing a nuclear export signal (NES) and a PEST degradation signal as well as a 24x MS2 repeat is driven by a PGK promoter. The MS2 hairpin repeat allows microscopic detection of the MS2-tagged transcripts at the reporter gene cassette via the binding of YFP tagged MS2 binding protein.

1B) The engineered transcription unit and the tetO 84x tandem repeat cloned in a pPur plasmid. The entire DP15 construct has a size of 11.312 kb. The MS2 24x repeat sequence (yellow), the mTurquoise-NES-PEST gene (blue), the 84x tetO tandem repeat (orange) and the ampicillin and puromycin resistance genes (green) are indicated. The unique restriction sites of DP15 are shown.

1C) Restriction digestion analysis of the Genescript© synthesized construct consisting of the PGK promoter, mTurquoise reporter gene, MS2 repeats and FRT Flipase site. An agarose gel analysis of the HindIII restriction digested Genescript© synthesized construct is shown. The construct is cloned into the Puc57 vector exhibiting a combined size of 5622 bp (insert: 2912 bp and puc57: 2710 bp). Lane 1 shows the undigested vector, lane 2 the construct digested by HindIII. Lane 3 shows a restriction digestion DNA 'KB' ladder provided by Genescript.

1D) Agarose gel analysis of the NheI restriction digested DP15 construct. Lane 1 shows the entire non-digested DP15 construct. In lane 2 the DP15 construct is digested with NheI. NheI cuts DP15 immediately adjacent to the tetO 84x tandem repeat. The single band shows that the DP15 construct is intact and approximately 12 kb. Lane 3 shows the restriction digestion DNA 'large' ladder provided by MRC Holland.

1E) Widefield image of Hek H100 cells transfected with the DP15 construct. The mTurquoise-NES-PEST reporter gene is located in the cytoplasm of the cells. Arrows depict three cells expressing the DP15 construct in the cytoplasm one day after transfection.

The 84x tetO tandem repeats are known to exhibit genomic instability via recombination events (Al-Allaf et al., 2012). The tetO sequence and eventually the created DP15 construct are therefore cultured in specialized Stbl2^{TM} competent *E.Coli* cells. The Stbl2^{TM} cells are highly efficient chemically competent bacterial cells that contain a unique set of markers to allow stable cloning of direct repeats and retroviral sequences and tandem array genes. We noticed that even in these Stbl2^{TM} cells the tetO repeat is unstable. Figure 1C and D illustrate the agarose gel testing of respectively the synthesized construct and the full DP15 construct. Figure 1C shows the cassette integrated in a Puc57 vector resulting in a band of 5622 bp after restriction digestion with HindIII. Figure 1D shows

that the NheI restriction digested construct results in a band of 11.312 kb, illustrating that the DP15 construct remained intact after multiplying the construct in Stbl2^{TM} cells.

We tested the transient expression of the DP15 construct in Hek H100 cells and visualized the expression of the mTurquoise reporter gene in living cells using a wide field microscope equipped with CCD camera. Figure 1E shows 2 typical representations of cells transfected with the DP15 construct. Since the mTurquoise reporter gene is tagged with a NES, the fluorescent protein is observed in the cytoplasm of the transfected cells. The next step is to integrate the DP15 construct into the FRT Flipase site of the Hek H100 cells and perform selection and correct single integration of clones with the inserted construct. Due to time constraints we did not manage to create clones with the singly integrated DP15 construct.

Targeting epigenetic regulatory proteins

To modulate the transcriptional activity of the reporter gene, we created fusion proteins consisting of tetR fluorescently tagged regulatory proteins. The tetR-tetO binding can be reversed at minute time-scale upon treating the cells with tetracyclin or doxycyclin (Gossen and Bujard, 1992) allowing to determine the effects of the targeted regulatory proteins upon their binding or release from the tetO binding sequences (tet-on or tet-off induction). The tandem tetO repeat sequences can also be used to visualize the compaction of the chromatin structure upon targeting tetR tagged proteins (Brink et al., 2013; Tumbar et al., 1999; Verschure et al., 2005). We used mCherry-tTA-ER (a gift from SM Janicki (Rafalska-Metcalf et al., 2010) consisting of the mCherry tagged transactivator tTA and the ligand binding domain of the estrogen receptor (ER) to modulate the nuclear versus cytoplasmic localization of the targeting construct upon addition of Tamoxifen.

The commercially available TtA and reverse TtA (rTtA) are fusions of the tetR and rtetR, respectively with the acidic activation domain (AAD) of VP16. We annotated the tetR binding protein and the VP16 AAD (Figure 2A) in the sequence of rTtA and we designed a PCR to obtain only the rtetR domain from this construct. We fused the rtetR to mCherry in a low expression vector entitled p3'SS, containing a polyomaF9 promoter. We used this

vector to create a fusion construct consisting of rtetR tagged mCherry fused to either Heterochromatin 1β (HP1β) protein or methyl-CpG binding protein 2 (MeCP2) (Figure 2B). Both HP1 and MeCP2 are proteins are known to be particularly enriched at pericentromeric chromatin. HP1 is a chromatin-binding protein that bridges via its chromo- and chromoshadow domain H3 lysine 9 tri-methylated histones with other chromatin associated proteins thereby advancing the 'spreading' of a transcriptionally silent heterochromatin structure (Verschure et al., 2005). MeCP2 was originally found to bind methylated DNA and to act as a transcription repressor (Nan et al., 1997). The regulatory protein targeting constructs were designed to modulate the transcriptional activity of the reporter gene cassette. Figure 2C shows an agarose gel with the mCherry-lacR vector that was used to replace lacR with rtetR. The newly cloned mCherry-rtetR, mCherry-rtetR-MeCP2 and mCherry-rtetR-HP1 were digested at a unique site in the rtetR construct to discriminate the presence of rtetR instead of lacR, shown in Figure 2C, lane 1. To verify the presence of HP1β (700bp) and MeCP2 (1400bp) all constructs were digested with Asc1, as shown in Figure 2C, lane 3 upon performing a single digestion in the backbone of the vector.

To test the created targeting proteins we used U20S 2-3-6 cells containing a reporter gene cassette consisting of tetO tandem repeats, as well as an adjacently placed lacO tandem repeat (Rafalska-Metcalf et al., 2010). We transiently co-transfected the rtetR constructs together with a lacR-EGFP construct (Brink et al., 2013; Verschure et al., 2005), to verify the binding properties of the rtetR constructs.

We visualized the tetO array of the mCherry-rtetR transfected U2OS 2-6-3 cells with the confocal microscope (Figure 2D). Upon addition of doxycyclin the rtetR construct is released from the tetO repeat, whereas eGFP-lacR binding at the lacO array is maintained since lacR-lacO binding is unaffected by the presence of doxycyclin. We show that mCherry-rtetR binds to the tetO array in presence of doxycylin and that mCherry-rtetR is released from the tetO array after removing doxycyclin from the medium. We show the presence of eGFP-lacR at the lacO array both in the presence and absence of doxycyclin. Figure 2C and D show the presence of the mCherry-rtetR construct fused to MeCP2 or HP1 at the reporter gene cassette in the nucleus before addition of doxycyclin.

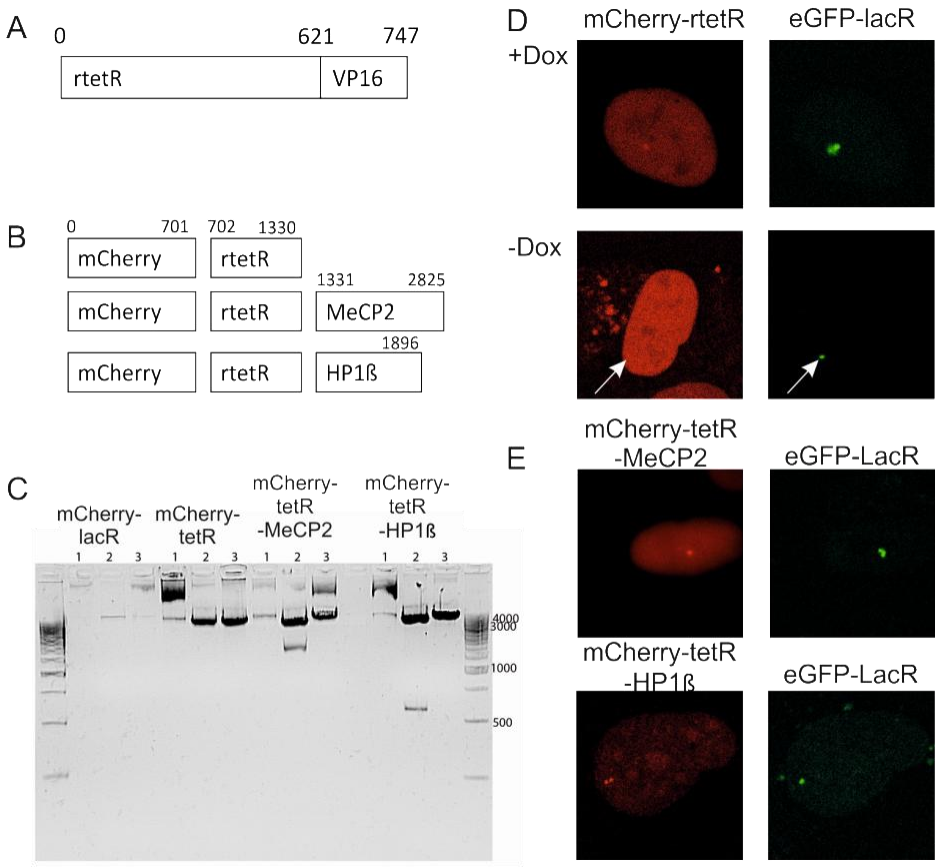

Figure 2: Targeting constructs

Figure 2: Targeting constructs

2A) Representation of the rTtA construct. The rTtA construct consists of the rtetR and 3x the VP16 AAD domain exhibiting sizes of 621 and 126, respectively. Primers were designed to PCR only the rtetR domain, this part of the construct is used for the creation of the rtetR constructs represented in Figure 2B.

2B) A representation of the mCherry-rtetR tagged constructs. The targeting constructs were created to modulate the epigenetic chromatin structure of the DP15 reporter gene cassette and hence to measure the effect on the transcriptional activity of the mTurquoise reporter gene.

2C) Agarose gel of the restriction enzyme digestions of mCherry-lacR, mCherry-rtetR, mCherry-rtetR-MeCP2 and mCherry-rtetR-HP1β to check the correct cloning of the fusion proteins. The following restriction digestions are shown: 1) NruI digestion makes a single cut in the rtetR protein, 2) AscI digestion isolates the insertion of HP1β (~700bp) or MeCP2 (~1400bp) and 3) SacII makes a single cut in the plasmid backbone.

2D) Confocal images of U2OS-2-6-3 cells containing a 84x tandem tetO repeat transfected with mCherry-rtetR (red) and eGFP-lacR (green). The cells treated with doxycycline (+dox) for 24 hours and the cells treated with doxycyclin for 24 hours are subsequently cultured in dox depleted for 1 hour (-dox). +Dox treated cells show that the rtetR is bound to the tetO-array. -Dox treated cells show that rtetR is lost from the tetO array. EGFP-lacR binding at the lacO array is shown in both +dox and -dox treated conditions.

2E) Confocal images of U2OS 2-6-3 cells transfected with either mCherry-rtetR-MeCP2 or mCherry-rtetR-HP1β and eGFP-lacR. The reporter gene cassette is visualized by the binding of eGFP-lacR to the lacO array and the tetO array is visualized by the binding of mCherry-rtetR-MeCP2 or mCherry-rtetR-HP1β.

Discussion

In the present study we created an engineered reporter gene cassette that should enable the measurement of transcription dynamics in a single gene in single cells, using real-time microscopy imaging. To visualize synthesized transcripts a MS2 repeat was placed immediately adjacent to a mTurquoise-NES-PEST reporter gene. To measure the effect of modulating the chromatin composition on transcriptional dynamics in single cells, we created a set of tetO targeting proteins fusing rtetR to mCherry or to the regulatory proteins MeCP2 and HP1β. In addition, we designed the reporter gene cassette such that it can be integrated in a single genomic location using FRT Flipase integration. We show the molecular design of the DP15 cassette and its cytoplasmic localization in Hek H100 cells. Moreover, we show the molecular design of mCherry rtetR tagged MeCP2 and HP1 epigenetic regulatory proteins and their nuclear localization in U2OS 2-6-3 cells. We

discuss the design of our reporter gene cassette containing cell line compared to the current state-of-the-art to measure mRNA with high temporal and spatial resolution.

Transcription cell population measurements

Biochemical transcription cell population measurements (e.g. time-resolved quantitative RT-PCR, chromatin immunoprecipitation, ChIP) have generated multiple models of transcription regulation that are often interpreted in terms of sequential molecular events (Coulon et al., 2013). The general view is that recruitment of different molecular partners progressively stabilizes the eventually formed protein complex and facilitates recruitment of other factors in a static and well-ordered manner. The complication of such population snapshot measurements is that transient events and events occurring only in a subset of cells are not identified. Typically live-cell experiments provide kinetic aspects of transcription regulation over a broad range of time scales that are much shorter than most gene-induction population studies.

An indirect approach to uncover temporal gene expression variability among genes is to analyse the steady-state distribution of fluorescent reporter protein levels in sub cell populations. For example first performing flow cytometry cell population selection and subsequently count the distribution of protein levels (Hoppe et al., 2014; Viñuelas et al., 2013). In addition, nowadays single cell biochemical high-throughput analysis technologies such as single cell RNA-seq, are becoming more common and reliable (Stegle et al., 2015). A second indirect approach to determine transcriptional dynamics regards measuring the fluorescent protein levels in single cells using time-lapse microscopy and reconstruct the RNA time-traces (Harper et al., 2011; Suter et al., 2011). These studies revealed that a significant amount of cell-cell variability in gene expression exists. Such noise in gene expression is shown to correlate with gene functioning, promoter features and genomic positioning of a gene. Information about cell-cell transcription variability and hence cell population heterogeneity, not only impacts fundamental research but is also important for medical applications (Navin et al., 2011). Cellular heterogeneity in gene

activity is an important factor to infer tumor cell behavior, specially with respect to the upcoming field of personalized medicine (Murtaza et al., 2013).

Spatial localization of transcripts

RNA detection using in situ hybridization provides a method to quantify RNA levels in fixed cells, allowing single cell and also high-resolution detection when coupled with ultrathin sectioning and electron microscopy (Weil et al., 2010). With single molecule RNA FISH (smRNA FISH) multiple fluorescent probes are hybridized to a single mRNA enabling single molecule transcript detection levels (Raj et al., 2008). smRNA FISH revealed that a large cell-to-cell heterogeneity exists in transcript levels. Based on these observations it suggested that genes exhibit pulsitile behavior fluctuating between 'on' and 'off' states, i.e. transcriptional bursting (Rybakova et al., 2015; Suter et al., 2011). Currently, smRNA FISH is optimized such that it allows fast, multi-plexed automated and also high throughput transcript analysis (Battich et al., 2013). FISH sequencing of RNA (FISSEQ) or multiplexed error-robust FISH (MERFISH) are new technologies for visualizing RNA at subcellular single molecule level providing information on the localization of thousands of RNA species, including splice variants and single nucleotide polymorphisms (Chen et al., 2015; Lee et al., 2014).

Transcription dynamics

Transcription dynamics can be measured in cells expressing a reporter gene cassette such as designed in the present study (Bertrand et al., 1998; Larson et al., 2009; Rafalska-Metcalf and Janicki, 2007). Transcript tagging is enabled via genomic integration of a reporter gene encoding the RNA of interest with stem bacteriophage stem loop sequences such as MS2, PP7 or λ-phage N-protein boxB that bind with high affinity to their fluorescently tagged coat protein (Bertrand et al., 1998). Combining two transcript tagging systems allows live-cell imaging of two mRNA species simultaneously (Hocine et al., 2013; Lange et al., 2008). The initial mammalian cell lines expressing MS2 tagged transcripts exhibited multiple copies of a reporter gene cassette (Rafalska-Metcalf et al.,

2010). Such a multicopy reporter gene cassette integration improves detection of MS2 fluorescently tagged transcripts but exhibits the drawback that transcriptional measurements represent averaging of the transcript levels of the multicopied reporter genes (Rafalska-Metcalf and Janicki, 2007). Synchronized expression of the reporter genes within a multicopy reporter gene cassette enables to approximate the transcription dynamics of single genes. Previous studies showed that targeting of the acidic amino acid domain (AAD) of a transcriptional activator (i.e. VP16) to a multicopy reporter gene cassette boosts synchronous transcriptional activation of multicopy reporter genes (Rafalska-Metcalf et al., 2010). The MS2 transcript tagging has nowadays also been extended to a single gene copy integration for instance using the Flp-In system (Yunger et al., 2010) and even as an endogenous knock-in mouse harboring one tagged allele of the β-actin gene (Lionnet et al., 2011).

A major drawback of microscopic single cell and especially of real-time transcription measurements is that they are time-consuming and technically demanding. In general, microsopic detection methods have constraints regarding the production of large data sets. Moreover, both biological and technical variability between the cells further complicates single cell microscopical data interpretation. Moreover, experimental cell modulation tools, can induce large cell-to-cell biological variability in the response time of cells. Also experimental technical factors such as variations in culture conditions, the exact temperature of the set-up and timing in sample preparations can induce experimental variability. The reproducibility of the set-up of single cell microscopic measurements is essential such that multiple experiments can be compared. Akthar et al. (2013) developed a multiplexing approach to enable parallel monitoring of transcriptional activity of thousands of randomly integrated reporter genes. This multiplexing enables massive upscaling of reporter gene transcriptional screening at various genomic sites. In addition, the approach enables the screening of different kind of constructs for instance constructs with different promoters and other sequential differences.

Genomic integration of reporter gene cassette

Our reporter gene cassette is designed to be singly integrated in any mammalian cell line or transgenic mouse making use of the FRT Flipase site via homologous recombination. The main reason to use the FRT-Flipase recombinant cloning method for integration of our engineered reporter gene cassette was the availability of a large set of Hek H100 clonal cell lines containing an FRT site integrated in pre-determined genomic sites with known transcriptional activity (Gierman et al., 2007). Nowadays the CRISPR/Cas9 system provides a very efficient way to induce homologous recombination (Boettcher and McManus, 2015; Hsu et al., 2014; Liu et al., 2015). A major advantage of the CRISPR/Cas9 method could be to fuse a MS2 repeat directly to an endogenous gene instead of integrating a large reporter gene cassette. A possible challenge of the CRISPR/Cas9 method for transcription dynamics measurements might be interference of the guide RNA with MS2 hairpin loops. Another drawback of using the CRISPR/Cas9 for genomic integration is their off target integration.

Conclusion

A substantial component of transcriptional variability has been linked to molecular dynamics occurring at the local gene level involving the epigenetic chromatin state. To study the contribution of epigenetic regulation on transcription dynamics at single gene level it is inevitable to perform dedicated real-time microscopy imaging but also to create testable quantitative and predictive models. To minimize technical fluctuations affecting cell-cell variability measurements it is important to use a well defined experimental platform and to perform multiple measurements within a relatively short time frame. We show the design, engineering and transient expression of our constructed reporter gene cassette in living Hek H100 cells. As a next step we plan to integrate the reporter gene cassette via homologous integration in the human genome of Hek H100 cells. We created epigenetic regulatory targeting constructs and show their ability to bind and release from the tetO array by doxycyclin treatment.

Materials & Methods

ISOLATION OF RTETR

The TetOn advanced construct was annotated using DNAstar. PCR was performed with following primers: forward primer: tgtacagcAtgtctagactggacaagagc, Reverse primer: ggcgcgccccgccgctttcgcactttgc @62°C. Taq polymerase from MRC Holland was used in an applied biosystem gene amp PCR system 2700.

CONSTRUCTION OF DP15

The reporter gene cassette was created in two stages. The promotor, gene and signal sequences together with the MS2 repeat and the FRT site were synthesized by Genescript© as one construct. The tetO repeat was cloned into the pPur transfection vector. Subsequently, the Genescript© synthesized construct was cloned into pPurTetO1.84.

RESTRICTION DIGESTION AND GEL ANALYSIS

Restriction digestion was performed according to the conditions provided by Fermentas. Fermentas enzymes and buffers were used for exactly one hour at 37°C. 1% TBE or TAE agarose (Sigma) gels were run at 90V until DNA was properly separated (Biorad electrophoresis) (60-90 min). Images of the gels were made using a Genius imager. DNA was cut from the gel and isolated using Fermentas purification kit and ligated 16-20 hours at 16°C with Roche T4 ligase.

TRANSFECTION AND CELL CULTURE

DNA was extracted using Fermentas miniprep kit, and transfected with Invitrogen Lipofectamin 2000 using the Invitrogen provided conditions. U2OS 2-6-3 cells were cultured in Glutamax DMEM, supplemented with 10% Tet-approved FCS serum (Clontech), 1% PS (Gibco). Hek H100 cells were cultured in Glutamax DMEM supplemented with 10% FCS serum and 1% PS (Gibco). For imaging the cells were grown in Mattek dishes or Alcian Blue coated coverslips. Coverslips are fixed in 4% formaldehyde diluted in PBS and embedded in Vectashield. Mattek dishes were washed and covered in Microscopy Medium and imaged in real-time.

MICROSCOPY

Fixed cells were imaged using a Zeiss LSM510 (Zeiss, Germany), equipped with a Zeiss plan neofluar 636/1.25 NA oil objective. We used multitrack scanning, employing an UV laser (364 nm), an argon laser (488 nm) and a helium-neon laser (543 nm) to excite DAPI staining and green and red fluorochromes. Emitted fluorescence was detected with BP 385-470, BP 505–550 and 560 LP filters. Three-dimensional (3D) images were scanned at 512 by 512 pixels averaging 4 times using a voxel size of 200 nm axial and 60 nm lateral.

Zeiss S100 axiovert was used for wide-field imaging of the reporter protein, using a 40 x 1.3 n/a oil objective. mTurquoise was excited with a HBO 50 HG mercury lamp ~430 nm. CCD camera Images were taken using and an axiocam 1CM (Zeiss, Germany).

Chapter 3

The balancing act of MeCP2: A multi-tasking protein

Diewertje G.E. Piebes, Pernette J. Verschure

Abstract

Methyl CpG binding protein 2 (MeCP2) contains several binding domains and it is known to exhibit chromatin remodeling activities. Depending on its folding the MeCP2 protein binds to specific DNA target sites and attracts several different proteins triggering a variety of functions in the nucleus. MeCP2 does not contain a catalytic domain but it typically is able to guide regulatory proteins to its DNA target sites. Genome-wide transcription is coordinated by the complex interplay of proteins that directly or indirectly interact with DNA to form the chromatin fiber. This network of interactions underlies the cell type specific epigenetic chromatin composition of the genome. MeCP2 plays an important role as epigenetic 'reader protein' in chromatin-related gene expression regulation having a strong affinity for methylated CG dinucleotides and MeCP2 exhibits chromatin remodeling activities via MeCP2 bound epigenetic regulatory proteins. Mutations in the MeCP2 coding sequence or MeCP2 duplication as observed in neurodevelopmental disorders such as Rett syndrome and Xq28 duplication syndrome affect the network of chromatin-related interactions thereby altering gene expression regulation.

MeCP2 is ubiquitously expressed in somatic cells and particularly enriched in the brain. Throughout the years many different functions of MeCP2 have been discovered, illustrating the functioning of MeCP2 in the nucleus specifically in brain cells. Here, we provide a chronological overview of the discoveries regarding MeCP2 molecular (dys)functioning. Moreover, we discuss steady state MeCP2 binding to DNA or regulatory proteins as a result of MeCP2 mutations and duplication considering an altered MeCP2 binding or MeCP2 cellular concentration.

Introduction

Folding of the eukaryotic genome into higher-order chromatin structures and gene expression patterns are tightly related with each other (Li et al., 2007). The genome is partitioned into distinct functional chromatin domains delineated by regulatory elements that help to assure cell type-specific gene expression (Bodnar and Spector, 2013; Ernst

and Kellis, 2010; Gierman et al., 2007; Noordermeer and Duboule, 2013; van Steensel, 2011; Yadon et al., 2013). Gene expression is coordinated by the complex interplay of proteins that modulate the epigenetic chromatin composition (e.g. DNA methylation and histone modifications). The affinity of chromatin binding proteins is determined by their interactions with specific histone modifications, DNA binding proteins and co-regulators. Vice versa, the location of histone modifications is modulated by the DNA sequence and the presence of chromatin binding proteins. CpG binding proteins such as methyl CpG binding protein 2 (MeCP2) are typical proteins that provide a link between histone modifications and DNA methylation (Nan et al., 1998b).

MeCP2 is a multifunctional protein exhibiting chromatin remodeling properties. MeCP2 is ubiquitously expressed and abundantly present in mature neuronal brain cells (Skene et al., 2010; Song et al., 2014). Moreover, MeCP2 is present in normal brain in all types of glia, including astrocytes, oligodendrocyte progenitor cells and oligodendrocytes. Mutations in the MeCP2 gene located on the X chromosome give rise to the postnatal neurodevelopmental disorder known as *Rett syndrome*. Rett syndrome is a rare genetic neurological disorder almost exclusively affecting girls. Rett syndrome at first does not show large phenotypic changes in affected children, but 6 - 12 months after birth the second stage of the disorder manifests itself through rapid regression of neuronal and motor functioning which stabilizes when children are around 4 years old. After a long plateau phase of the disease the final disease phase is recognized by severe motor dysfunctioning (Neul and Zoghbi, 2004). Duplication of the *MeCP2* gene inducing upregulation of cellular MeCP2 levels causes another neurodevelopmental disorder, named *Xq28 duplication syndrome* showing a disease outcome that is very similar to Rett syndrome. Rett syndrome symptoms starting gradually during childhood include loss of purposeful hand use, slowed brain and head growth, movement and breathing problems, seizures, and intellectual disability (Anderson et al., 2014; Neul and Zoghbi, 2004). Xq28 duplication syndrome distinguishes itself from Rett syndrome by the prompt development and the recurring infections. Similarities in Rett and Xq28 duplication syndrome symptoms include aberrant breathing, gastroesophageal reflux, hypotonia, epilepsia, speech problems and disability to walk (Anderson et al., 2014; Van Esch, 2012).

MeCP2 is expressed in brain cells, both in neuronal cells and also in glial cells that support and exhibit protection for the nervous sytem. Recent studies indicate that in MeCP2 deficient cells showing a Rett syndrome phenotype, MeCP2 is not expressed in astrocytes, in contrast to its expression in wild type mice. It is noted that neuronal growth is compromised and that the morhopholy and density of neurons is decreased, when astrocytes from MeCP2 deficient mice are co-cultured with hippocampal neurons from wild type mice (Ballas et al., 2009). The authors showed that upon restoring the expression of MeCP2 in astrocytes from MeCP2 deficient mice caused a non-cell-autonomous growth inducing effect on neurons from MeCP2 deficient mice thereby re-establishing the dendritic morphology and reducing Rett syndrome symptoms of the mice such as abbarent breathing (Lioy et al., 2011).

The history of observations regarding MeCP2-related disorders started in the early 50's last century when the Austrian physician Andreas Rett (1924-1997) first encountered patients with a not yet described postnatal developmental disorder. It took at least a decade before Andreas Rett published his findings. The first molecular biological questions regarding Rett syndrome were not answered until Adrian Bird discovered the MeCP2 protein in 1992 (Meehan et al., 1992; Nan et al., 1993), although the link between MeCP2 and Rett syndrome was discovered in 1999 (Amir et al., 1999). Since this discovery alterations in MeCP2 functioning as a chromatin remodeling protein were reflected against downstream neuronal and muscle-related Rett syndrome symptoms.

In this review, we provide an overview of research findings related to the functioning of MeCP2 and MeCP2 involved disorders (see Table 1). We outline the DNA binding sites and protein binding partners of MeCP2 indicating their relationship with molecular effects of MeCP2 (dys)regulation within MeCP2-related neurological disorders. In this context, we provide a minimal model-representation showing the affinity of MeCP2 binding and its bound functional fraction (Figure 1).

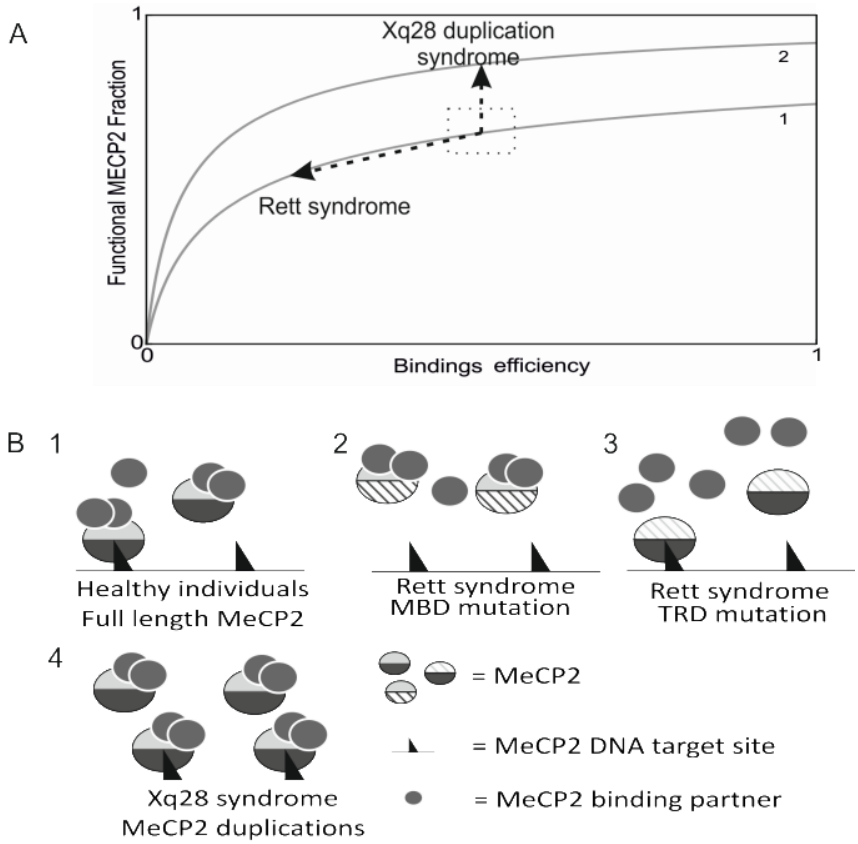

Figure 1: Effects of MeCP2 binding properties.

A) This figure provides the model-representation of the steady-state behavior of MeCP2 binding as a result of MeCP2 binding parameters and MeCP2 concentration. In Rett syndrome the MeCP2 functional bound fraction is decreased due to the lower binding efficiency (lower k_b) of MeCP2 at DNA target sites or at MeCP2 protein binding partners. In Xq28 duplication syndrome an increase in the amount of MeCP2 (relative to the amount of target DNA), causes an increase in the MeCP2 functional bound fraction.

B) The cartoon illustrates the MeCP2 bound fraction for different MeCP2 binding efficiencies. 1. In individuals without Rett or Xq28 syndrome, full length MeCP2 binds its DNA targets and MeCP2 binding proteins allowing the formation of a functional MeCP2 bound fraction. Since protein-protein and protein-DNA binding is a dynamic process not all sites are continuously occupied. 2. In Rett syndrome MBD or TRD mutations both interfere with the formation of a functional MeCP2 bound fraction (i.e. binding of MeCP2 to DNA target sites and to protein binding partners) compared to the situation in individuals carrying full length MeCP2. 3. In Xq28 syndrome, MeCP2 duplication induces an increase in the amount of MeCP2 (relative to the amount of target DNA), thereby causing an increase in the MeCP2 functional bound fraction.

MeCP2 is a multifunctional protein with multiple binding sites

Nowadays MeCP2 is accepted to represent a multifunctional protein that can exhibit different functions e.g. the ability to repress as well as to activate gene expression (Chao and Zoghbi, 2009). MeCP2 is a protein that can bind to DNA and that is able to bind a variety of regulatory proteins. MeCP2 is reported to represent a rather unstructured protein, implicating that a large part of MeCP2 can adapt a different 3D protein structure depending on its binding partners. Only 35-40% of the MeCP2 protein represents a structured part i.e. parts of the methyl binding domain (MBD) and an AT-hook domain in the transcription repression domain (TRD) (Adams et al., 2007; Martı et al., 2014). The rest of the MeCP2 protein including the C-terminal part are proposed to represent the 'disordered' part of the protein exhibiting structural folding depending on the association with defined proteins or posttranslational protein modifications (Adams et al., 2007). MeCP2 binds with its MBD to DNA (Nan et al., 1993), having affinity for both methylated and non-methylated CG dinucleotides (CpGs) and DNA in general. The MeCP2 MBD largely overlaps with a nuclear domain that is suggested to represent a matrix attachment binding region (MAR) that is supposed to be part of a nuclear cytoskeleton or scaffold. MeCP2 binds with its TRD to proteins involved in transcription regulation thereby either turning genes on or off. The C-terminus of MeCP2 is theoretically shown to cover several binding sites of which at least two have been proven experimentally (see Table 1) (Buschdorf and Strätling, 2004; Dintilhac and Bernués, 2002). The C-terminal domain is known to facilitate both binding of MeCP2 to DNA and to contain a WW domain that is predicted to play a role in protein-protein interactions (Buschdorf and Strätling, 2004).

MeCP2 has increased affinity for methylated compared to non-methylated C nucleotides (Ghosh et al., 2010b). Moreover, the enrichment in A and T nucleotides adjacent to methylated CpGs is known to involve high-affinity binding of MeCP2 to DNA target sites (Klose et al., 2005). The binding of MeCP2 to hydroxymethylated C nucleotides includes another level of complexity in MeCP2 functioning. Several assays showed that the affinity of MeCP2 for hydroxylated and non-methylated C nucleotides is similar. Moreover, an A nucleotide following a hydroxymethylated C nucleotide has been noted to provide high

affinity MeCP2 binding (Kinde et al., 2015; Mellén et al., 2012). Hydroxymethylation is often a result of oxidative damage, possibly hampering the binding of MeCP2 (Kinde et al., 2015; Valinluck et al., 2004). Kinde et al. showed that MeCP2 also binds to both hydroxymethylated and methylated CA dinucleotides. The genomic profile of methylated CG, AC or hydroxymethylated CG dinucleotides has important implications to understand the functional role of MeCP2 at methyl and hydroxymethyl-specific binding sites. Methylated CA dinucleotides largely parallel the profile of methylated CG dinucleotides across genomic elements, including intergenic regions, regulatory elements of inactive genes, promoters and gene bodies of lowly expressed genes and repetitive DNA sequences,. Hydroxymethylated C nucleotides typically demarcate active regulatory elements, i.e. hydroxymethylated CG dinucleotides are preferentially enriched throughout gene bodies of highly expressed genes and are depleted from transcriptional start sites (Lister et al., 2013). In neuronal cells hydroxymethylation is suggested to represent an intermediate epigenetic state marking sites of subsequent CG demethylation (Guo et al., 2011; Lister et al., 2013). Hydroxymethylation is considered to also denote a stable epigenetic state, playing a role in learning, memory, neurogenesis and neuronal activity-regulated gene expression.

MeCP2 is a protein that has a large set of binding partners. In Figure 2 we highlight MeCP2 DNA and protein binding partners indicating the multifunctional role of MeCP2. Identifying downstream molecular and cellular targets that are affected by MeCP2 (dys)functioning will help to interpret the role of MeCP2 in brain development and maintenance of brain function.

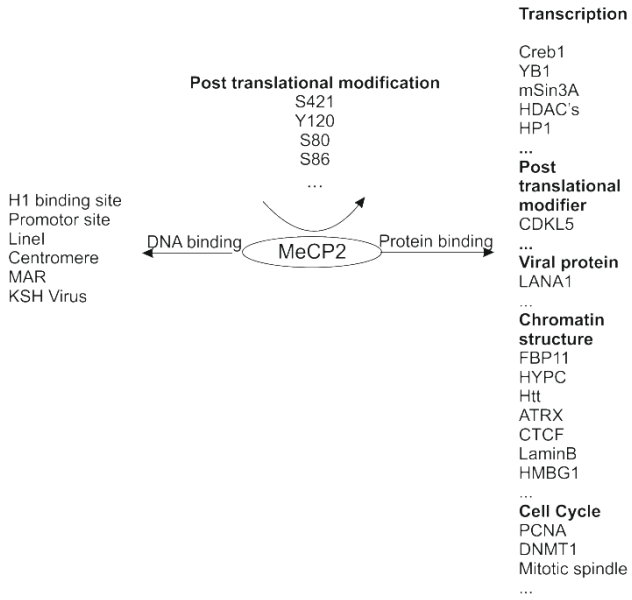

Figure 2. MeCP2 is a multi-functional protein.

MeCP2 has a directing functionality on regulation of the chromatin structure, it binds various DNA targets with its MBD and recruits with its TRD regulatory proteins towards MeCP2 bound DNA target sites. MeCP2 binds to proteins that involve various functionalities, i.e. transcription regulation, chromatin structural changes, cell cycle regulation and even viral activities. MeCP2 is a disordered protein that gains its functionality upon posttranslational modifications and protein binding.

MeCP2 dysfunctioning: an altered balance

A large body of evidence indicates that mutations in chromatin remodeling or chromatin structural proteins are related to neurological disorders (Lv et al., 2013). Examples of such neurological disorders are mutations in ATRX causing *Alpha-thalassemia mental retardation syndrome* (Ratnakumar and Bernstein, 2013), mutations in cohesion proteins such as SMC leading to *Cornelia the Lange syndrome* (Revenkova et al., 2009), CDKL5 mutations giving rise to clinical features similar to those noted in Rett syndrome, also being diagnosed as *West syndrome* and *X-linked infantile spasms* (Kato, 2006)**.** Moreover, several other duplicated loci show a correlation with chromatin structural alterations and neurological-related disorders such as *autism spectrum disorders* (ASD) and/or *schizophrenia* (Nomura and Takumi, 2012). Mutations and amplification in the coding sequence of MeCP2 give rise to Rett syndrome and Xq28 duplication syndrome,

respectively. A wide variety of MeCP2 mutations causes a more severe or milder Rett syndrome disease outcome largely depending on the effect of the mutation on the MeCP2 protein structure. Table 1 shows a historical overview of the research related to an (altered) functioning of MeCP2 involving Rett syndrome, Xq28 duplication syndrome and other MeCP2-related disorders. Note that some recent studies envision a role for MeCP2 that is contradicting MeCP2-related findings of earlier days.

More than 2000 MeCP2 mutations have been reported in females with Rett syndrome. Eight common MeCP2 mutations are known to result in loss of function due to truncated, unstable or abnormally folded MeCP2, whereas more recently, large MeCP2 rearrangements including deletions were reported (Amir et al., 1999; Bienvenu and Chelly, 2006). MeCP2 mutations affect the affinity of MeCP2 for its binding partners. Structural analysis of MeCP2 mutations at defined sites of the TRD show an improper formation of the AT-hook of the TRD. These AT-hook TRD MeCP2 mutations can still bind DNA, although transcriptional patterns are changed, indicating that the MeCP2 protein is not properly functioning. These TRD MeCP2 mutations are known to produce a severe Rett phenotype and to disrupt a large part of the structural ordered part of MeCP2. MeCP2 mutations just outside the AT-hook TRD are known to cause a mild Rett phenotype suggesting that TRD mutation-induced alterations in MeCP2 folding play a role in the disease outcome (Baker et al., 2013). It has been noted that the R113C MeCP2 mutation in the MBD disrupts H-bonds required for MBD DNA target binding. This R113C MeCP2 mutation is known to induce only a mild form of Rett syndrome (Kucukkal and Alexov, 2015), whereas MeCP2 gene duplication as noted in Xq28 duplication syndrome will cause a general increase in the cellular MeCP2 concentration thereby affecting saturation of MeCP2 binding to DNA or regulatory proteins, or possibly inducing a competition with other chromatin binding proteins (Baker et al., 2013; Christodoulou et al., 2003; Fyfe et al., 2003). In the brain MeCP2 is suggested to be required for the reactivity of neuronal responses. In Rett syndrome, MeCP2 is associated with a low density of dendritic spine (Na et al., 2013). In Xq28 duplication syndrome dendritic spine occurs in larger numbers after birth and spine numbers drop a few weeks after birth, although the size of the dendritic spine is smaller compared to the size in healthy mice

(Jiang et al., 2013). Of importance, it is known that introduction of full length MeCP2 in a knock-out Rett syndrome mouse model induces partial recovery from the Rett syndrome symptoms (Guy et al., 2007). This indicates that development of the Rett syndrome phenotype most likely occurs post developmentally, which is of interest for treatment strategies.

Molecular behavior of MeCP2 functional binding

We created a simplified model-representation illustrating the impact of MeCP2 mutations and MeCP2 duplication on the amount of functional MeCP2, i.e. the MeCP2 bound fraction (Figure 1). In this model-representation we simplified the cellular complexity of MeCP2 binding, the cellular MeCP2 distribution, the MeCP2 target site distribution and the MeCP2 binding kinetics, whereas we take into account the concentration of MeCP2, MeCP2 binding sites and two parameters for respectively the binding and dissociation of MeCP2. The ordinary differential equations associated with this model are the following:

$$\frac{dCpG}{dt} = \frac{dMeCP2}{dt} = -MeCP2 \cdot \ CpG \cdot k_a + k_d \cdot MC$$

$$\frac{dMC}{dt} = MeCP2 \cdot \ C \cdot k_a - k_d \cdot MC$$

MC represents the concentration of MeCP2 bound to MeCP2 binding sites, i.e. (non)methylated dinucleotides, hydroxymethylated cytosines, any DNA or MeCP2 binding proteins. K represents the MeCP2 binding constant and k_d the MeCP2 dissociation constant. Since the ratio between the number of MeCP2 proteins and the number of MeCP2 binding sites is unknown, we assume that both variables are equimolar. Different MC ratios do not alter the curve of the plot. In Xq28 duplication syndrome it is expected that somatic and neuronal cells exhibit elevated cellular MeCP2 levels and hence an increased pool of MeCP2 is able to bind DNA target sites or proteins binding sites. In contrast, in Rett syndrome the amount of MeCP2 target binding (either the DNA target site or MeCP2 binding proteins) is lower due to mutations in the MBD, TRD or other parts of the MeCP2 coding sequence. We only take into account MeCP2 point mutations that

affect a change in the MeCP2 coding sequence. Decreased binding affinity of MeCP2 for DNA or MeCP2 binding proteins will induce a drop in the overall amount of functional MeCP2. The model-representation illustrates the impact of an altered MeCP2 binding and an altered MeCP2 concentration on the MeCP2 functional fraction, plotted as the MeCP2 bound fraction. This model-representation indicates that the molecular behavior of the two MeCP2-related neurodevelopmental syndromes are strikingly different although the phenotypic outcome of these disorders shows some overlap.

MeCP2 downstream functioning

As described in Table1 various observations have been made in relation to MeCP2 functioning and MeCP2-related disorders. Here we illustrate some of the MeCP2 downstream functioning involved phenomena and their relationship with MeCP2 related disorders.

MeCP2 related to genome stability, immunity and circadian rhythms

The ability of MeCP2 to bind hydroxmethylated and methylated dinucleotides as well as other genomic sites illustrates the complexity of MeCP2 functioning for neuronal gene expression and hence neuronal development, plasticity and disease. Specially mutations in the MeCP2 MBD affecting the ability of MeCP2 to bind methylated and hydroxymethylated sites will alter gene expression patterning and genomic stability. During replication MeCP2 associates with the replication fork and binds to DNA methyltransferase DNMT1 thereby restoring the DNA methylation pattern after replication (Kimura and Shiota, 2003). Moreover, MeCP2 is known to exhibit DNA methylation-induced silencing of retro-transposable elements such as Line-1 (Muotri et al., 2010), thereby providing genomic stability preventing retro-transposable elements to cause insertional mutagenesis. Of interest, MeCP2 is upregulated in virally infected cells, for instance infected by John Cunningham Virus (Shirai et al., 2011). In this context, MeCP2 is known to upregulate IFNγ cytokine levels in infected cells thereby supporting

innate and adaptive immunity (Yang et al., 2012). MeCP2 has been shown to interact with viral proteins involved in viral latency (Chiang et al., 2013; Matsumura et al., 2010). In this context, HIV-1 can regulate expression of miRNA132 which downregulates the expression of MeCP2 allowing HIV to become viral (Chiang et al., 2013). MiRNA132 also regulates circadian rhythm involved proteins, i.e. histon acetylase activity of CLOCK, and binding of CLOCK to PERIOD genes Per1 and Per2. Moreover, miRNA132 is known to regulate MeCP2 expression and hence expression of Per1 and Per2 via a CREB dependent pathway. Interestingly, MeCP2 is circadianly regulated and circadian MeCP2 levels are noted to have important consequences on the chromatin structure and transcription of MeCP2 dependent genes. It is tempting to propose that MeCP2 is able to facilitate a light-induced CREB-dependent circadian transcription regulation. Circadian alterations in MeCP2 levels could be responsible for sleep disturbances as noted in autism and Rett syndrome (Alvarez-Saavedra et al., 2011; Martínez de Paz et al., 2015). In conclusion, the MeCP2 domain that binds to DNA affects a wide variety of effects ranging from genome stability, DNA replication, immunity to circadian rythm regulation. It is intruiging to connect these different functional effects of MeCP2 in one regulatory layer.

Posttranslational modifications of MeCP2 as basis for multifunctionality

Although MeCP2 does not explicitly contains a catalytic domain, MeCP2 is demonstrated to contribute to binding and recruitment of other, catalytically active protein complexes. MeCP2 can exhibit both gene activation and repression depending on its genomic and protein binding profile (Tao et al., 2009). MeCP2 posttranslational modifications (e.g. phosphorylation at S80 and de-phosphorylation at S421) largely influence the genomic and protein binding profile of MeCP2 and thereby its biological functioning (Bellini et al., 2014). S421 phosphorylation occurs in response to neuronal activity, mutations at S421 influence dendritic growth and regulation of genes involved in neuronal connectivity. MeCP2 S421 phosphorylation is suggested to be specifically connected to neurodegenerative features of Rett syndrome and Xq28 duplication syndrome (Zhou et al., 2006). Moreover, S80 phosphorylation is noticed to be associated with an increased

MeCP2 binding at promoters of a set of genes, e.g. Rab3d, Vamp3 and Igsf4b, with a reduced transcriptional activity of these genes and with a rested neuronal state. Deficient S80 phosphorylation exhibits reduced MeCP2 binding and increased transcription of Rab3d, Vamp3 and Igsf4b. SCDKL5 is a protein that is known to phosphorylate MeCP2. Intriguingly, mutations in CDKL5 lead to a syndrome (West syndrome) often diagnosed as Rett syndrome showing disease symptoms that are very comparable to Rett syndrome symptoms (Weaving et al., 2004). Alteration in posttranslational modification states of MeCP2 has been connected with MeCP2 nuclear location and functioning (Bergo et al., 2014). It has been noticed that phosphorylation of Y120 is associated with an accumulation of MeCP2 at the centrosome and the mitotic spindle regulating cell growth and cytoskeleton stability. Y120 is located within the MeCP2 MBD domain and it is a highly conserved site in mammals. A patient affected by a variant form of Rett syndrome was found to harbor a MECP2 mutation, possibly mimicking a constitutively phosphorylated Y120 state. This mutation was shown to cause decreased affinity of mutated MeCP2 at compact chromatin domains causing deficient spindle morphology, microtubule nucleation and prolonged mitosis. These studies indicate that posttranslational MeCP2 modifications play a major role in the ability of MeCP2 to interact with its DNA and protein partners thereby regulating functional activities of MeCP2.

MeCP2 and its opposite functionality: transcriptional activity versus repression

MeCP2 is described to be able to recruit transcription regulatory proteins that are associated with opposite effects. The MeCP2 TRD recruits proteins that exhibit histone deacetylation transcription repressive activities such as NCor/HDAC3 and Sin3a corepressor complexes (Nan et al., 1997, 1998b). On the other hand, the MeCP2 TRD recruits Creb1 protein and Creb1 binding partners causing transcriptional activation instead of repression (Tao et al., 2009). Creb1 is a protein that binds a cAMP response element, a nucleotide sequence present in many viral and cellular promoters causing gene activity (Chao and Zoghbi, 2009). MeCP2 has been shown to interact with YB1, a

protein involved in alternative RNA splicing (Young et al., 2005). An interaction of MeCP2 with gene body DNA methylation is shown to induce alternative splicing thereby excluding methylated exons from the synthesized transcripts (Lev Maor et al., 2015). This abillity of MeCP2 to cause splicing of methylated exons might represent a 'repressive' action on actively transcribed genes. Moreover, MeCP2 is proposed to play a role in chromatin folding as it binds chromatin remodeling proteins such as Brahma and ATRX. The best evidence of the involvement of MeCP2 in chromatin structural changes is based on chromatin capture analysis of the imprinted Dlx5/Dlx6 locus implicating a role for MeCP2 in silent chromatin loop formation. The N-terminal domain of MeCP2 has been shown to bind Heterochromatin protein 1 (HP1) (Agarwal et al., 2007) a protein that is typically associated with the formation of transcriptionally silent chromatin as it binds with its chromodomain to histone H3 lysine 9 tri-methylation (H3K9me3) and recruits with its chromoshadow domain histone methyltransferase enzymes (Verschure et al., 2005). During mouse myogenesis cellular MeCP2 levels are largely increased and an abundant colocalization of MeCP2 together with HP1 (especially HP1γ) is noted at largely clustered and compact MeCP2 stained chromatin, i.e. chromocenters (Agarwal et al., 2007). We recently showed that MeCP2 targeting induced chromatin unfolding and that this chromatin unfolding is related with displacement of HP1γ from compact chromatin (Brink et al., 2013). These examples illustrate that MeCP2 can evoke an opposite effect on the chromatin composition and the transcriptional state. In a recent study a novel high-resolution microscopy imaging approach is used to compare the chromatin structure in neuronal tissues from MeCP2 null mice compared with tissues in wild type mice (Linhoff et al., 2015). It was noted that the chromatin of MeCP2 null cells represents a more compacted chromatin structure and a redistribution of various histone modifications related to pericentromeric heterochromatin was noted in cells of MeCP2 null cells. The chromatin structural changes in cells from MeCP2 null versus wild type MeCP2 mice is not observed in all neuronal cells, suggesting cell-type specific chromatin structures. For instance during myogenesis it was noted that MeCP2 caused compaction of chromocentres, suggesting that these events enable these cells to fullfill their specific tasks during development. MeCP2 functionality might act as a key facilitator to ensure

correct chromatin structural functionalities that are needed for cell-specific and moment speciic neuronal tasks, i.e. tasks during neuronal development or neuronal maintenance provided by proper interactions between neuronal and glia cells.

Competition of MeCP2 with nuclear binding proteins impacts nuclear integrity

The increased cellular MeCP2 levels noted in Xq28 duplication syndrome are expected to largely affect the binding efficiency of chromatin binding proteins that are seemingly unrelated to the functioning of MeCP2. For instance it has been shown that the naturally observed binding competition between MeCP2 and histone H1 at MeCP2 binding sites is lost in MeCP2 knockout mice causing a general upregulation of histone H1 levels (Skene et al., 2010). In principle histone H1 upregulation might represent a compensation for the lack of functional MeCP2 to evoke a total collapse of the nucleosomal chromatin structure.

Incorrect assembly of the nuclear envelope together with a decreased proliferation and cellular viability represents another cellular phenotype of cells in which MeCP2 is knocked down (Babbio et al., 2012). This fits well with the role of MeCP2 to interact via its MBD with Lamin B receptor (LBR) located at the nuclear periphery (Guarda et al., 2009; Nan et al., 1993; Weitzel et al., 1997). Nuclear lamins are major components of the lamina playing a role in maintaining nuclear envelope integrity, orchestrating mitosis and apoptosis, regulating DNA replication and transcription and providing chromatin domain anchoring sites.

Summary

MeCP2 is a multifunctional protein consisting of at least 3 binding domains without a typical catalytic domain. MeCP2 plays an important role in altering the binding affinity of regulatory proteins for their chromatin or DNA binding sites. Moreover MeCP2 plays an important role in maintaining a correct DNA methylation profile of importance for proper chromatin folding, transcription patterning and genomic stability. MeCP2 is able to facilitate gene expression programs at two levels. MeCP2 acts as a key regulator of

chromatin structure by preventing the formation of compact chromatin (Linhoff et al., 2015; Schotta et al., 2004) and by competing with binding of histone H1 at methylated nucleosomal linker chromatin (Ghosh et al., 2010a; Skene et al., 2010). Moreover, MeCP2 functions as a transcriptional regulator either by recruiting co-repressor (Lyst et al., 2013; Nan et al., 1998b) or co-activator proteins (Chahrour et al., 2008; Mellén et al., 2012) i.e. having an opposing 'Yin-Yang' regulatory effect, which is subject to the phosphorylated state of MeCP2. The type of functional activity of MeCP2 seems to depend on its protein structure that is for a large part intrinsically disordered. MeCP2 is involved in providing nuclear integrity and hence nuclear functionality such as replication, transcription, mitosis and genome stability. Disturbed binding of MeCP2 is proposed to have a crucial effect on the ability of MeCP2-bound catalytic proteins to find their correct target sites. MeCP2 plays an important role in facilitating genome structural functionalities. The dual functionality of MeCP2 helps to assure long-lived neurons to adapt their gene expression programs upon exposure to changed conditions such as an altered synaptic activity or injury.

Interestingly, Rett and Xq28 duplication syndrome show large similarities in their disease symptoms. We show with a model-representation that Rett and Xq28 duplication syndrome exhibit very different molecular behavior. In Xq28 duplication syndrome the relative increase in the amount of cellular MeCP2 levels compared to the amount of MeCP2 binding sites causes an increased MeCP2 functional bound fraction, whereas in Rett syndrome the MeCP2 functional bound fraction is lower due to a decrease in the binding efficiency of the mutated MeCP2 protein.

MeCP2 facilitates chromatin functioning by its ability to bind to DNA target sites and to bind to catalytic active proteins. The dynamics of MeCP2 DNA or protein interactions has large impact on MeCP2 functioning. Almost all MeCP2 mutations lead to neurodegeneration, although only one phosphorylation site, up until now, is identified to be involved in neuronal connectivity. In general after depolarisation of the neuronal membrane, MeCP2 becomes phosphorylated at S421 and binds to its target genes such as BDNF in order to regulate dendritic spine density (Mellén et al., 2012; Zhou et al., 2006).

Following the model of functional binding as depicted in Figure 1B, a Rett syndrome mutation in the MBD will hamper binding of MeCP2 to its target genes and will therefore alter the MeCP2-induced target gene regulation. A Rett syndrome mutation in the TRD will prevent MeCP2 to bind to its protein binding partners required to change the transcriptional activity of its target gene, eventhough MeCP2 would have been phosphorylated upon the depolarisation. In principle a mutation in any of the MeCP2 domains will result in improper regulation of denditric spine density. In duplication syndrome, the binding affinity of MeCP2 for its target sites is expected to increase and this will result in more, but smaller dendritic spines. Although MeCP2 related diseases have a different molecular backgroundthe different MeCP2 mutations seem to induce the same kind of symptoms possibly all due to the changes in denditric spine density.

Clinical treatment of MeCP2-related disorders is not trivial since MeCP2 is involved in many different pathways. Treatment of MeCP2 related disorders typically concentrates on distant disease symptoms such as seizures and lung infections and also on treatment of symptoms related to deficiency in neuronal development such as dendritic spine formation and neuronal connectivity (Xu et al., 2014) for more details, see Gadalla et al (Gadalla et al., 2011). Regarding a more direct treatment of MeCP2, mice studies showed that replacing mutated MeCP2 with full-length MeCP2 is able to recover the Rett syndrome phenotype. Moreover, it was recently established that systemic delivery of MeCP2 cDNA in female mouse models rescues behavioral and Rett syndrome cellular symptoms (Garg et al., 2013). In this context, introduction of MeCP2 non-coding siRNA posttranslationally downregulating MeCP2 levels could provide a means to temper MeCP2 production in Xq28 duplication syndrome. Restoring correct MeCP2 functioning in glia could play an important role in ameliorating robust features Rett syndrome symptomes. Identifying key molecules to restore MeCP2 expression in glia may provide further clues in the mechanism of recovery, providing potential targets for therapeutic intervention. There is still a long road ahead to realize direct MeCP2 targeted treatments in humans and especially in diseased children.

Table 1: The history of MeCP2 functioning

Chronological overview of different findings on MeCP2 molecular functioning

Year and Reference	Description of findings
1966 (Rett, 1966)	Without any knowledge of the MeCP2 gene the Austrian physician Rett discovered a syndrome in girls. This syndrome is named **Rett syndrome**. Until today no cure for Rett syndrome has been discovered. Rett syndrome treatment includes treatment treatment of disease symptoms such as seizures and aberrant breathing.
1992 - 1993 (Meehan et al., 1992; Nan et al., 1993)	In the early 90's the research team of Adrian Bird discovered a new protein referred to as methyl-CpG-binding protein 2 (MeCP2). MeCP2 is characterized to **bind methylated CG dinucleotides** (CGs). MeCP2 contains a **methylated DNA binding domain** (MBD) being part of the MBD protein family. MeCP2 is described to bind in vitro to single methylated CpGs requiring symmetrical methylation. Moreover, MeCP2 is reported to exhibit no association with hemi-methylation or methylation at CpG islands. MeCP2 is also characterized to have a domain that binds the DNA helix in the large groove.
1997 (Weitzel et al., 1997)	The MeCP2 (rat) MDB is shown to exhibit a **matrix attachment region** (MAR). A homologue of MeCP2 has previously been described in chickens, the ARBP protein also having a MAR. MARs are supposed to attach to a nuclear matrix of scaffold region that would belong to a nuclear cytoskeleton. This MAR binding is the first indication of MeCP2s contribution to nuclear and chromatin structure as described later in more detail when studying MARs.
1997-98 (Nan et al., 1997, 1998b)	The **transcriptional repressive function** of MeCP2 is described to be located in the **transcription repression domain** (TRD). This TRD is shown to interact with Sin3a thereby forming a repressive complex attracting histone deacetylases (HDACs). Besides the attraction of a repressive complex, MeCP2 is noted to compete with histone H1, thereby interfering with the chromatin structure.
1999 (Lubs et al., 1999)	A disease characterized as **X-linked mental retardation** is shown to exhibit **duplication of the distal arm of the X chromosome.** The disease shows besides neurological deterioration an increase in pulmonary infections. Three months later the presence of MeCP2 at this locus was confirmed.

1999-2000 (Amir et al., 1999; Buyse et al., 2000)	**Genetic Rett syndrome mutations** are discovered for the first time linking MeCP2 to Rett Syndrome**.** A year later a new diagnostic tool is presented making use of DHPLC and direct sequencing. This tool allows **Rett syndrome genetic diagnosis** rather than diagnosing the phenotypic outcome.
2000-present (Christodoulou et al., 2003)	**MeCP2 mutations are not site specific**, i.e. a wide variety of genotypes and phenotypes exist. The international Rett syndrome foundation funded a database where (anonymously) single patient data are stored for open access named 'Rettbase'.
2001 (Guy et al., 2001)	**MeCP2 deficient mice** are developed showing a Rett syndrome phenotype. The first mouse strain containing mutated *MeCP2* under control of a lox-cre site shows the Rett phenotype when mutated MeCP2 is ubiquitously expressed. The original MeCP2 deficient mouse strain developed by the research team of Adrian Bird is named after the Bird-lab.
2001/2002 (Colantuoni et al., 2001; Tudor et al., 2002)	**mRNA profiling of MeCP2 deficient mouse strains** (expressing mutant MeCP2 or MeCP2 knock-out) shows that a large number of genes are affected. The noticed gene expression landscape in the MeCP2 mouse strains was rather unexpected. Since MeCP2 is shown to act mainly as a repressor, it was expected that MeCP2 mutations would mainly cause gene expression upregulation. It is concluded that MeCP2 affects several transcriptional regulators and not only the synaptic pathway that is regressing during late disease development.
2002 (Dintilhac and Bernués, 2002)	MeCP2 is noticed to bind high-mobility group B1 protein (HMGB1) based on a sequence in the MeCP2 C-terminal region. A pull-down assay proved that the **MeCP2 C-terminal domain binds to HMGB1** a protein that binds to histone proteins and recruits other protein complexes to chromatin. HMGB1 is able to bend DNA thereby enabling DNA-protein binding. HMGB1 is ubiquitously expressed in the nucleus and has a multifunctional role in chromatin organization.
2002 (Yntema et al., 2002)	Since the *MeCP2* gene is located on the X-chromosome (Xq28), it is speculated that Rett syndrome only occurs in females because in male MeCP2 mutations are not viable. MeCP2 mutations causing a mild or carrier phenotype in girls are noted to cause **Rett syndrome in males in a more severe phenotype.**
2003 (Kimura and Shiota, 2003)	**MeCP2 is shown to interact with DNMT1 as well as PCNA at the replication fork** during S phase. DNMT1, the maintenance DNA methyltransferase, follows the replication fork and methylates the hemi-methylated new strands immediately. The manner of recognition by

	DNMT1 with the hemi-methylated DNA is not explained.
2004 (Kriaucionis and Bird, 2004; Mnatzakanian et al., 2004)	**A second splice variant of MeCP2, MeCP2a** is identified which contains an extra sequence at the N-terminal of exon 1 and it contains no part of exon 2. This new variant is noted to be expressed in elevated amounts in the brain compared to the earlier described MeCP2. This new variant is named MeCP2a, because it turned out to be more abundant in the brain than the previously described isoform.
2004 (Weaving et al., 2004)	***Cyclin dependent kinase like 5 (CDKL5)* mutations** are described to be **associated with Rett syndrome.** Mutations in CDKL5 involve other autism related disorders.
2004 (Valinluck et al., 2004)	**MeCP2 is found to bind hydroxymethylated CGs**. The affinity of MeCP2 for hydroxymethylated CGs is shown to be lower than the affinity for methylated CGs. Affinity of MeCP2 for unmethylated CGs and hydroxymethylated CGs are reported to be similar.
2004 (Luikenhuis et al., 2004)	**A non-mutated *MeCP2* gene is introduced in the MeCP2 null mice** to recover the MeCP2 depleted phenotype. After this experiment using knock-in techniques, several studies have been conducted using strategies of importance for Rett syndrome clinical treatment.
2004 (Buschdorf and Strätling, 2004)	Annotation based on sequences revealed a **WW group II domain in the C-terminal region of MeCP2**. The WW group II domain is shown to bind FBP11 and HYPC RNA splicing involved proteins in vivo. C terminal WW group II domain mutations that are known to exist in Rett syndrome patients are identified to influence MeCP2 binding properties. This WW group II domain is not exactly the same C-terminal MeCP2 domain that was previously described to bind to HMGB1. The WW group II domain and the C-terminal domain that binds HMBG1 overlap and differ in only a few amino acids.
2004 (Collins et al., 2004)	**Mild over expression of MeCP2 in mice resembles the Rett disease phenotype.** Both MeCP2 overexpression and MeCP2 mutations cause postnatal neurological disorders, indicating a tight regulation of MeCP2 expression in mature neurons.
2005 (Mari et al., 2005)	**CDKL5** is shown to phosphorylate itself and **to mediate MeCP2 posttranslational modifications**. The expression patterns of CDKL5 and MeCP2 are shown to overlap in similar tissues.
2005	**Duplication of the Xq28 (*MeCP2*) locus is noted to cause a neurodegenerative disease in boys**. The onset of the Xq28 duplication syndrome is progressive and not delayed as noted in Rett syndrome. A very

(Meins et al., 2005)	notable difference between Rett and Xq28 duplication syndrome is the high susceptibility of Xq28 duplication syndrome for pneumonia. These phenotypic differences were first explained by the duplication of a neighboring gene Interleukin-1 receptor-associated kinase 1 (IRAK-1). Later it was noticed that patients with no IRAK-1 duplication also show immune deficiency. It is noted that *IFNy* is a target gene of MeCP2 and aberrant regulation of this protein is also involved in the recurring lung infections.
2005 (Young et al., 2005)	MeCP2 is shown to **interact with the RNA splicing factor YB-1.** In the brain, many genes undergo alternative splicing. YB-1 has several functions in chromatin and RNA regulation and binds to Y boxes in promoter regions.
2006 (Zhou et al., 2006)	**MeCP2 S421 phosphorylation** in response to neuronal activity is required for transcription of the brain derived neurotrophic factor BDNF, for dendritic growth and for the maturation of spine. It is noted that MeCP2 is involved in neuronal activity and required for the connectivity of neurons, and is likely connected to the neurodegeneration observed in Rett syndrome and duplication syndrome.,
2007 (Guy et al., 2007)	**The Rett syndrome phenotype can be rescued in MeCP2 knock-out mice by re-introducing full length MeCP2**. This suggests that the effect of MeCP2 deficiency in Rett syndrome is post-developmental. For this experiment Lox-Cre mice were created, thus this treatment is not yet applicable in humans. Only one mouse in this experiment did not recover from the treatment, possibly due to a recombination in the locus resulting in a skewed MeCP2 protein.
2007 (Adams et al., 2007)	MeCP2 is shown to represent an **intrinsically disordered protein** having only 35-40% ordered structure i.e. MeCP2 requires dimerization, complex formation or posttranslational modifications to stabilize the protein structure. The disordered protein organization is expected to give rise to a lot of other possible functional folding states of the MeCP2 protein. Of interest, the earlier described WW II domain is shown to be part of the disordered C-terminal of MeCP2, therefore only functioning in combination with other regulatory proteins.
2008 (Chahrour et al., 2008)	Microarray gene expression analysis of MeCP2 mice is performed by several groups, most notable in this study is the fact that **MeCP2 binds to promoter regions of genes that are actively expressed**.
2009 (Tao et al., 2009)	It is noted that **MeCP2 S86 phosphorylation** is associated with the functioning of **MeCP2 as an activator** instead of a repressor thereby inducing the binding of MeCP2 with Creb1 at promoters of target genes. The MeCP2 phosphorylated or non-phosphorylated state inducing the

	activator versus repressor state is noted as the 'Yin-yang effect' of MeCP2.
2009 (Ballas et al., 2009)	**Astrocytes from MeCP2 knock-out mice (exhibiting Rett syndrome phenotype) do not support growth of neuronal cells.** In brains from wild type mice MeCP2 is expressed in both neurons and glial cells. Wild type neuronal cells, co-cultured with astrocytes from MeCP2 deficient mice show a compromised growth.
2009 (Guarda et al., 2009)	MeCP2 is shown to **colocalize with the Lamin B receptor** and to interact with LaminB by the MAR region. The inner membrane of the nucleus is described to provide a structural function as part of the nuclear cytoskeleton and chromatin close to the nuclear periphery and is described to represent silenced chromatin (Reddy et al., 2008).
2010 (Skene et al., 2010)	It is shown that **neuronal MeCP2 levels are similar to histone-octamer levels** and small changes in MeCP2 concentrations are noted to alter the chromatin structure. MeCP2 is noted to compete with the binding of H1 in neuronal cells, replacing almost half of them. In case of MeCP2 deficiency, H1 levels are noted to be upregulated to replace the missing MeCP2 as in other non-neuronal cells, expressing MeCP2 at a much lower level.
2010 (Ghosh et al., 2010b)	It is noted that in vivo the **binding affinity of MeCP2 at methylated CpGs versus non-methylated CpGs** differs only 3-fold.
2010 (Muotri et al., 2010)	**MeCP2 binding at retrotransposon Line-1 repetitive elements** is shown to **repress its replicative potential**, whereas Alu retrotransposons are unaffected by MeCP2 binding. An important role for MeCP2 in maintaining chromatin stability is proposed. Retrotransposons that replicate and integrate in the genome can cause mutagenesis.
2010 (Kernohan et al., 2010)	MeCP2 is noted to **interact with ATRX** (a protein associated with mental retardation alpha thalassemia syndrome) **and** with **cohesion at the maternal imprinted gene *H19***. The involvement of MeCP2 in transcription regulation of *H19* at sites distal or proximal from the gene promoter is suggested to occur via **chromatin looping**.
2011 (Lioy et al., 2011)	In MeCP2 deficient mice exhibiting a Rett syndrome phenotype, astrocytes do not express MeCP2. **Re-introduction of MeCP2 in astrocytes of MeCP2 deficient cells restores dendritic complexity in the brain** and reduces Rett symptoms such as abbarent breathing and hypoactivity and prevents premature lethality.
2011	**John Cunningham Virus (JCV)** is noted to trigger **transcriptional activation of MeCP2 in infected brain cells.** JCV is carried latent in brain cells in a

(Shirai et al., 2011)	large part of the world population. The presence of this virus can cause progressive multifocal leukoencephalopathy (PML) in immunodeficient individuals.
2011 (Agarwal et al., 2007)	MeCP2 is noted to be able to **induce the clustering of compact chromatin domains during myogenic differentiation** in mice. The N-terminal domain of MeCP2 and HP1β are noted to interact and induce clustering of compact chromatin domains, i.e. chromocenters.
2012 (Mellén et al., 2012)	The relative binding affinity of MeCP2 for methylated CGs, hydroxymethylated CGs en unmethylated CGs is described. The **affinity of MeCP2 for hydroxymethylated and methyldated CGs is similar**, in contrast to findings in earlier studies. This study takes in account possible nucleotide combinations in the neighborhood of the C nucleotide. MeCP2 Is shown to have a higher affinity for the CA combination.
2013 (Matsumura et al., 2010)	MeCP2 is noted to **bind with Latency Associated Nuclear Agent LANA-1, of the herpes virus KSHV**. This interaction is found to occur outside of the viral genome, indicating a collaboration between LANA-1 and MeCP2 to regulate gene expression of both the viral and endogenous genes.
2013 (Chiang et al., 2013)	It is noted that HIV infected CD4+ cells overexpress miRNA 132, which represses, among others, MeCP2. **HIV-induced MeCP2 repression is noted to enhance the HIV replication potential.**
2013 (Brink et al., 2013)	Targeting of **MeCP2 is noted to be able to induce significant chromatin decondensation** accompanied by the eviction of Heterochromatin protein 1 (HP1γ) as measured in cells carrying an amplified chromosomal domain. MeCP2-induced chromatin decondensation is noted to be comparable to targeting of a transcriptional activator VP16, although it does not alter the transcriptional activity of the reporter gene within the chromosomal domain.
2013 (Baker et al., 2013)	**Mutations in an AT-hook in the MeCP2 TRD domain** are noted to cause **a more severe Rett phenotype** than other TRD mutations. It is noted that this AT-hook has structural similarity with the high-mobility group AT-hook (HMGA). It is suggested that the chromatin structure plays an important role in this AT-hook related Rett phenotype through alteration of the local enrichment of nucleosomes.
2014 (McFarland et al., 2014)	**MeCP2 is shown to interact with Huntingtin protein (Htt).** In mutant Htt CAG repeats in the Htt protein encoding an enlarged polyQ tract are known to cause Huntington's disease. Htt is shown to bind to proteins that are also binding partners of MeCP2. Mutant Htt is noted to have an increased

	binding interaction with MeCP2.
2014 (Song et al., 2014)	**MeCP2 levels** are identified **in different cells of different tissues and at several stages of early life development**. MeCP2 is noted to be expressed in almost all body cells except the intestine and colon, microglial cells and mature gonads.
2014 (Khrapunov et al., 2014)	The **binding of MeCP2 with its MBD** is in vitro noted to be highly correlated with **salt concentrations in the nucleus**. The affinity of MeCP2 for either methylated or unmethylated CpGs is shown to be dependent on the nuclear salt concentration.
2014 (Bergo et al., 2014)	**Phosphorylation of MeCP2 at Y120** is noted to induce **colocalization at centromeres** and to play a role in **mitotic spindle formation**, **proper microtubule nucleation and progression through mitosis**.
2015 (Lev Maor et al., 2015)	An **interaction of MeCP2 with CTCF and HP1 is noted to direct RNA splicing**. CTCF and MeCP2 binding is noted to be regulated by DNA methylation facilitating exon exclusion or inclusion dependent on the DNA methylation levels, via the presence of RNA polymerase II and HP1 directed splicing factors.
2015 (Martínez de Paz et al., 2015)	MeCP2 is noted to be **circadianly regulated.** MeCP2 protein levels fluctuate with the rhythm of CLOCK genes and chromatin structure alterations are directly correlated with MeCP2 fluctuating levels. It is shown that when MeCP2 levels are increased the chromatin is in a more condensed state. miRNA 132 was reported to regulate MeCP2 as well as HAT activity of CLOCK proteins.
2015 (Linhoff et al., 2015)	A high resolution microscopy imaging approach (entitled chromATin) is used to examine the chromatin compaction and epigenetic chromatin composition in MeCP2-null mice brains compared to wild type mice. **MeCP2 null neurons showed an increased density of the compact chromatin** and a striking redistribution of various histone modifications related to pericentromeric heterochromatin (e.g. H4K20me3) compared to the chromatin of wild type neurons. The chromatin structure changes are not observed in all neuronal cell types illustrating the cell-type specific differences in chromatin structure in complex tissues.

Chapter 4

A Role for MECP2 in Switching Gene Activity via Chromatin Unfolding and HP1γ Displacement

Diewertje G.E. Piebes, Maartje C. Brink, Marloes L. de Groote, Martijn S. Luijsterburg, Corella S. Casas-Delucchi, Roel van Driel , Marianne G. Rots, M. Cristina Cardoso, and Pernette J. Verschure

This Chapter was published as:

Brink, M.C., Piebes, D.G.E., de Groote, M.L., Luijsterburg, M.S., Casas-Delucchi, C.S., van Driel, R., Rots, M.G., Cardoso, M.C., and Verschure, P.J. (2013). A role for MeCP2 in switching gene activity via chromatin unfolding and HP1γ displacement. PLoS One *8*, e69347.

DGE Piebes and MC Brink contributed equally to this paper

Abstract

Methyl-CpG-binding protein 2 (MeCP2) is generally considered to act as a transcriptional repressor, whereas recent studies suggest that MeCP2 is also involved in transcription activation. To gain insight into this dual function of MeCP2, we assessed the impact of MeCP2 on higher-order chromatin structure in living cells. We used a mammalian cell system harbouring a lactose operator and reporter gene-containing chromosomal domain to assess the effect of lactose repressor-tagged MeCP2 (and partial domains) binding in living cells. Our data reveal that targeted binding of MeCP2 elicits extensive chromatin unfolding. MeCP2-induced chromatin unfolding is triggered independently of the methyl-cytosine-binding domain. MeCP2 binding triggers the loss of HP1γ at the chromosomal domain and an increased HP1γ mobility, which is not observed for HP1α and HP1β. Surprisingly, MeCP2-induced chromatin unfolding is not associated with transcriptional activation. Our study suggests a novel role for MeCP2 in reorganizing chromatin to facilitate a switch in gene activity.

Introduction

Gene activity is governed by the interplay between various proteins that modulate the epigenetic composition of chromatin (e.g. DNA methylation, histone modifications) (van Steensel, 2011). Histone modifications and DNA methylation are linked by CpG-binding proteins such as methyl-CpG-binding protein 2 (MeCP2) (Fuks et al., 2003) through, for instance, cross-talk between MeCP2 and heterochromatin protein 1 (HP1) isoforms (Agarwal et al., 2007). MeCP2 is ubiquitously expressed in human tissues and particularly enriched at pericentromeric heterochromatin domains in brain cells (Shahbazian et al., 2002b; Skene et al., 2010). MeCP2 plays a role in neuronal maturation and impaired MeCP2 function results in neurodevelopmental disorders such as Rett syndrome (Lam et al., 2000; Yusufzai and Wolffe, 2000). HP1 is a chromatin-binding protein that bridges H3K9-methylated histones with other chromatin-associated proteins thereby advancing the 'spreading' of heterochromatin (Groner et al., 2010; Hines et al., 2009). Both the clustering of pericentromeric heterochromatin domains and the relocalization of HP1 (in

particular HP1γ) occur during myogenic differentiation when the level of methyl-CpG-binding proteins is up-regulated (Agarwal et al., 2007; Brero et al., 2005).

MeCP2 was originally found to bind methylated DNA and to act as a transcriptional repressor (Jones et al., 1998; Lewis et al., 1992; Nan et al., 1998b). More recent work demonstrated that MeCP2 also binds at actively transcribed genes and promotes activation of DNA-methylated genes, suggesting a role as a transcriptional activator (Ben-Shachar et al., 2009; Chahrour et al., 2008; Ego et al., 2005; Matsumura et al., 2010; Yasui et al., 2007). Currently, MeCP2 is considered a multifunctional protein (Ghosh et al., 2010b), i.e. MeCP2 is known (i) to bind methylated DNA (Jones et al., 1998; Lewis et al., 1992; Nan et al., 1998b), (ii) to recruit a wide range of proteins (e.g. chromatin-remodeling proteins Brahma, ATRX) (Georgel et al., 2003; Ghosh et al., 2010a; Harikrishnan et al., 2005; Horike et al., 2005; Hu et al., 2006; Kernohan et al., 2010; Nan et al., 2007), (iii) to induce the formation of repressive chromatin (Eivazova et al., 2009; Nikitina et al., 2007a; Skene et al., 2010) and change the number and size of pericentromeric heterochromatin domains (Singleton et al., 2011), (iv) to be involved in histone H1 displacement (Amir et al., 1999; Ghosh et al., 2010a; Nan et al., 1997; Nikitina et al., 2007b), (v) to play a key role in neurological disease (e.g. Rett syndrome) involving both gene activation and repression (Amir et al., 1999), (vi) to be implicated in regulation of imprinted genes (LaSalle, 2007). To unambiguously assess how MeCP2 contributes to epigenetic gene regulation within the context of the mammalian genome, we targeted MeCP2, an MeCP2 Rett mutant (R133C) or partial MeCP2 domains as EGFP-lac repressor (lacR)-tagged fusions in cells harbouring a lac operator (lacO) and reporter gene-containing genomic domain (Belmont et al., 1999). Using this methodology, we previously showed that HP1 targeting is sufficient to induce local chromatin condensation and recruitment of histone methyltransferase SETDB1, concomitant with increased tri-methylation of H3K9 (Verschure et al., 2005). Here we show that MeCP2 targeting causes extensive chromatin decondensation of the targeted genomic domain, which acts independently of the MeCP2 methyl-cytosine-binding domain (MBD) and results in eviction of the HP1γ isoform without an alteration in the transcriptional activity of the targeted chromatin.

Results

MeCP2 targeting causes local chromatin unfolding

To investigate the effect of MeCP2 targeting on chromatin folding we used cell lines that enable targeting of (EGFP-lacR-tagged) MeCP2 and partial MeCP2 domains to an integrated lacO genomic region, which are present in a highly amplified chromosomal domain in hamster cells (the AO3_1 and RRE_B1 clones) or as a multicopy genomic integration in human cells (the 2-6-3 clone). While the AO3_1, RRE_B1 as well as the 2-6-3 cells allow measurements of visual changes in 3-D chromatin folding upon targeting to the lacO array, it should be noted that the AO3_1 and RRE_B1 cells harbor a much larger array (80 Mpb) (Robinett et al., 1996; Tsukamoto et al., 2000; Tumbar et al., 1999; Verschure et al., 2005) compared to the 2-6-3 cells (2 Mbp). Therefore, the impact of induced chromatin changes in 3-D folding are more striking in the AO3 and RRE cells. Importantly, the 2-6-3 clone exhibits less genomic instability then the AO3_1 and RRE_B1 clones, which makes it more suitable to study cell-cycle-dependent chromatin folding. Moreover, the 2-6-3 clone harbors a reporter gene containing 24 tandem MS2 repeats allowing visualization and measurement of changes in the transcript levels using YFP-tagged MS2 coat protein.

We generated EGFP-lacR-tagged full-length MeCP2 or partial domain fusion proteins and expressed these fusions in the different cells lines harboring lacO arrays. Analysis of 3-D confocal images revealed that MeCP2 targeting induced extensive unfolding of the lacO array compared to targeting lacR in AO3_1, RRE_B1 and 2-6-3 cells (Figure 1A). MeCP2 targeting induced unfolding of the lacO array in AO3_1 and 2-6-3 cells to the same extent as targeting of the viral activator VP16, which is known to cause extensive chromatin unfolding (Figure 1A) (Robinett et al., 1996; Tsukamoto et al., 2000; Tumbar et al., 1999; Verschure et al., 2005). We measured the expression level of exogenously expressed MeCP2 to verify the effect of the amount of MeCP2 on chromatin folding. Fluorescent immunolabeling using MeCP2 specific antibodies showed that mCherry-lacR tagged MeCP2 contained a ~25% higher MeCP2 level than the endogenous MeCP2 level in non-transfected cells (Figure 1B, C). Moreover, we determined the effect of over-expression of

exogenous MeCP2 on chromatin folding. We show that cells with highly over-expressed MeCP2 levels visually exhibit a comparable level of chromatin unfolding (Figure 1D).

FISH labeling of the lacO array in AO3_1 cells using lacO probes confirmed that the MeCP2-induced unfolded structure overlapped completely with the unfolded lacO array (Figure 1E), showing that the EGFP-lacR visualized unfolded structure resembles the decondensed lacO array. Since the lacO chromosomal domain exhibits an extended fibrillar chromatin conformation in RRE_B1 cells and a compact chromatin (heterochromatic) structure in the AO3_1 and 2-6-3 cells, we used the AO3_1 and 2-6-3 cells for investigation of the effect of MeCP2 on epigenetic regulation (de Leeuw et al., 2006; Verschure et al., 2005).

To study whether MeCP2-induced chromatin unfolding is cell-cycle dependent, we analyzed cells in S-phase based on the known accumulation of proliferating cell nuclear antigen (PCNA) into foci in replicating cells. These experiments were performed in human U2OS 2-6-3 cells containing a 200-copy lacO array (Janicki et al., 2004). Our data show that MeCP2-induced unfolding occurred as frequently in S-phase cells as it did in non S-phase cells based on transfections with mCherry-PCNA or staining for endogenous PCNA. These results illustrate that the MeCP2-induced chromatin structural changes are independent of the cell-cycle stage (Figure 2A, B). (Leonhardt et al., 2000).

MeCP2 chromatin unfolding acts independent of the MBD domain

MeCP2 harbors a methyl-binding domain (MBD), a transcription-repression domain (TRD) and a poorly characterized C-terminal domain (Nan et al., 1993, 1997, 1998a). We tagged various MeCP2 subdomains and regions spanning the MBD, TRD, the C-terminus and MeCP2 lacking its C-terminus (ΔC-terminus) or mutant MeCP2^{R133C} (Rett Syndrome point mutation in the MBD domain) (Ballestar et al., 2000) to EGFP-lacR to identify which MeCP2 subdomain is responsible for unfolding of the lacO chromosomal domain upon targeting. First we tested the nuclear localization of the EGFP-lacR-tagged MeCP2 full-

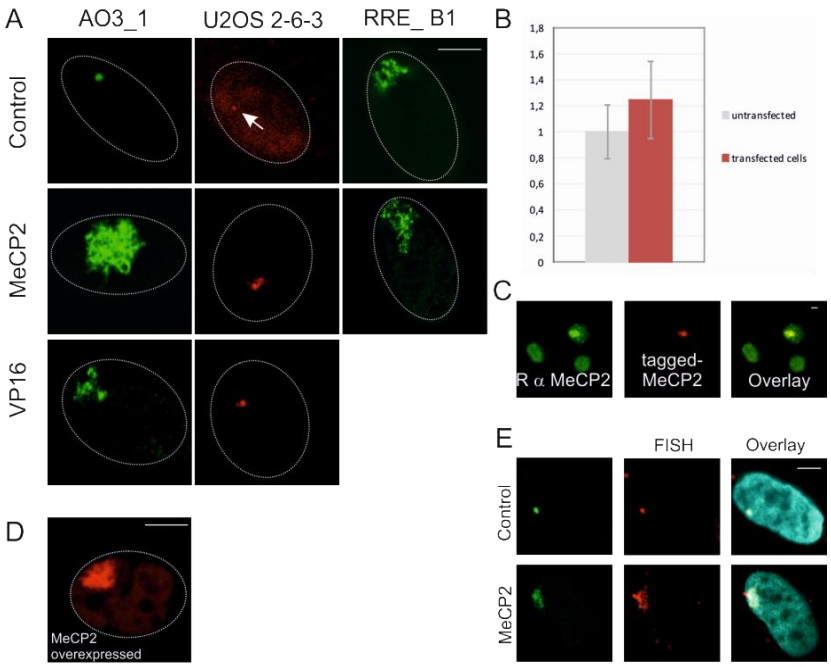

Figure 1. MeCP2 unfolds chromatin.

The effect of MeCP2 lacR-lacO targeting on 3D chromatin folding was measured in AO3_1 and RRE_B1 clones (CHO derived, containing an amplified chromosomal region consisting of DHFR cDNA transgene, 256 lac operator repeats and flanking DNA) and the 2-6-3 clone (U2OS derived, containing lacO repeats and a tetracycline inducible reporter gene encoding cyano fluorescent protein and 24 repeats of the MS2 bacteriophage translational operator). The images show a typical representation of cells 48 hours after transfection. We imaged at least 100 cells per transfection and for quantitative measurents approximately 30 cells per transfection were imaged under comparable microscopical set-up (see Figure 4).

A) The images show individual optical sections of AO3_1 cells transfected with EGFP-lacR (control), EGFP-lacR-tagged MeCP2 or VP16, 2-6-3 cells transfected with EGFP-lacR (control), mCherry-lacR tagged MeCP2 or VP16 and RRE_B1 cells transfected with EGFP-lacR (control) or EGFP-lacR-tagged MeCP2.

B) AO3_1 cells expressing mCherry-lacR tagged MeCP2 (n = 138) (shown in C) contain ~25% more MeCP2 levels then endogenous MeCP2 (in non-transfected cells, n = 249). The error bars show the standard deviation of the analyzed cells.

C) The images (a thick slice taken with open pinhole setting) to quantify endogenous/exogenous MeCP2 levels (shown in B), show AO3_1 cells transfected with mCherry-lacR tagged MeCP2 and immunolabeled with an antibody against MeCP2.

D) The images show an individual optical section of an AO3_1 cell highly over-expressing tagged MeCP2 (5.3 times higher than representative cells shown in (A). Representative cells are the cells that allow the Argos image analysis programme to select the lacO array from nuclear background, i.e. the cells on which we performed our quantitative measurements (see Figure 4 and S1). This analysis of MeCP2 over-expression illustrates that in cells exhibiting overexpressed MeCP2 levels a visually unfolded lacO chromatin array is observed similar as in the cells expressing representative MeCP2 levels. (E) The images show AO3_1 cells transfected with EGFP-lacR (control) and EGFP-lacR tagged MeCP2 (green signal), FISH-labeled with a fluorescent lacO probe (red signal) and DAPI-stained (blue signal). The images represent individual optical sections. Bars = 5 μm.

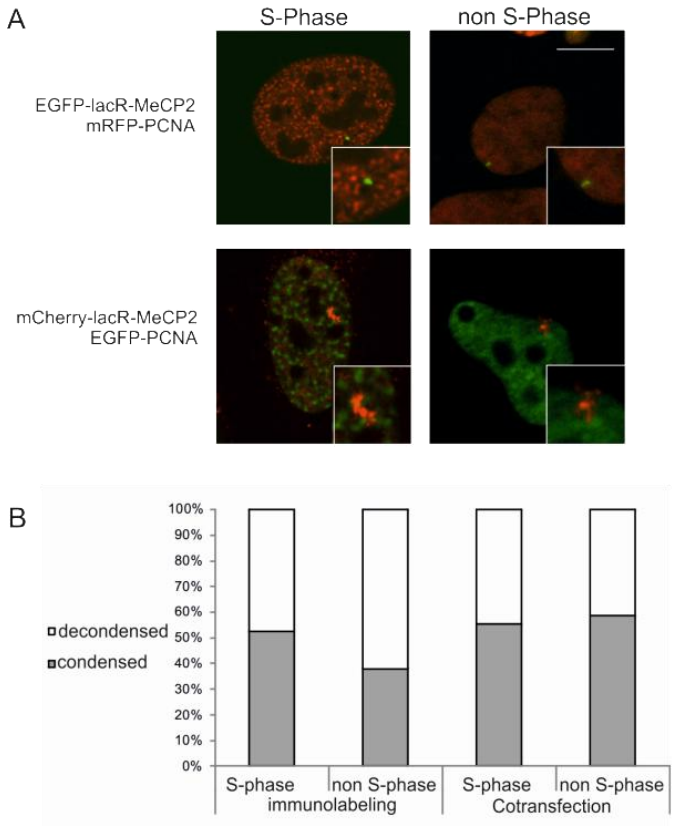

Figure 2. MeCP2-induced chromatin unfolding is independent of cell-cycle stage.

A) The images show 2-6-3 cells (U2OS derived clone containing a 200 copy chromosomal array of 256 lacO repeats and a reporter gene harboring 24 repeats of the MS2 bacteriophage) that were co-transfected with mCherry-tagged (red signal) or EGFP-tagged (green signal) lacR-MeCP2 and EGFP-tagged (green signal) or mRFP-tagged (red signal) PCNA. PCNA localizes at replication foci during S phase. The images represent individual optical sections of fixed cells. Bar = 5 μm.

B) The histogram shows quantification of the number of lacR-MeCP2 transfected cells showing a condensed (grey bar) or decondensed (white bar) chromosomal array in either S or non-S phase based on PCNA expression or immunolabeling (on X-axis noted as immunolabeling, n = 74 and cotransfection, n = 68). A χ^2 test was performed on PCNA immunolabeled (resulting in p = 0.25) and cotransfected cells (p = 0.81). Random variation probabilities show a high random variation between the decondensation and the cell cycle phase

length and MeCP2 partial domain constructs in mouse fibroblasts lacking a lacO array. Similar to native full-length MeCP2, all lacR-tagged MeCP2 fusion proteins localized to pericentromeric heterochromatin in the mouse fibroblasts, except for the lacR-tagged C-terminus, which was homogeneously distributed in the nucleus (Figure 3). Next, we analyzed the effect of targeting EGFP-lacR tagged MeCP2 full-length, MeCP2 partial

domains or VP16 versus EGFP-lacR (control) in the lacO-containing AO3_1 cells (Figure 4). Targeting of lacR-tagged MBD, TRD or ΔC-terminus domains did not cause chromatin unfolding into an extended fibrillar stucture as observed with full-length MeCP2 targeting, while targeting of MeCP2^{R133C} did result into mild chromatin structural changes. Targeting of the lacR-tagged MeCP2 C-terminus caused chromatin fibrillar unfolding but also to a much lesser extent than targeting of full-length MeCP2. Figure 4A shows typical representations of cells transfected for 48 hours with the respective constructs. For quantitative analysis approximately 30 nuclei per condition were imaged with a comparable microscopical set-up (Figure 4B, C, Table S1). We quantitatively assessed the change in chromatin structure by measuring the surface of the lacO chromatin domain relative to surface of a sphere with equal volume. A perfectly spherical structure, has a designated surface factor of 1, whereas a fibrillar unfolded chromatin structure will have a lower surface factor, due to its furrowed surface with equal volume. The quantitative measurements mirrored our visual observations: the degree of chromatin unfolding as observed in full-length MeCP2 (and VP16) was most pronounced in the cells targeted by partial MeCP2 domains containing the MeCP2 domains downstream of the MBD (i.e. MeCP2^{R133C} , C- terminus and TRD), while MBD and ΔC-terminus show almost a similar chromatin structure as observed upon EGFP-lacR control targeting (Figure 4B, Table 1, Table S1). To verify the effect of the amount of MeCP2 on chromatin unfolding we measured the fluorescence intensity of the transfected constructs in the lacO chromosomal array and we compared them with the surface factor measurements. Our intensity measurements show that there is no significant correlation between the amount of transfected construct and the changed chromatin structure as measured by the surface factor (Figure 4C, Table S1). Our findings reveal that the MeCP2 regions downstream of the MBD are involved in MeCP2-induced chromatin unfolding whereas the MBD itself is dispensable for this phenomenon.

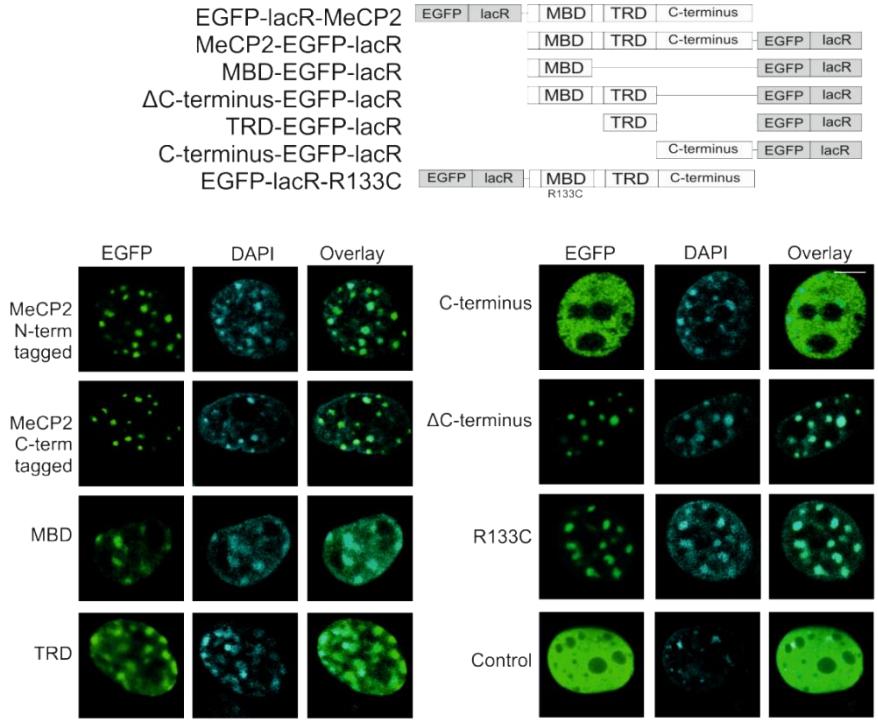

Figure 3. Nuclear distribution of EGFP-lacR-tagged MeCP2 domains in mouse fibroblasts.

A) The illustration shows a schematic representation of the tested constructs: EGFP-lacR tagged (grey boxes) full-length MeCP2, C- and N- terminally-tagged, MeCP2 partial domains (MBD, ΔC-terminus, TRD, C-terminus) and R133C Rett syndrome mutation (white boxes).

B) The images show EGFP-lacR-tagged DAPI (blue signal). MeCP2 and MeCP2 partial domains localize at DAPI dense chromocenters, except for the ΔC-terminus. We imaged approximately MeCP2 and partial MeCP2 domains (green signal) that were expressed for 48 hours in NIH/3T3 cells and stained with 100 cells per condition. The images represent individual optical sections of DAPI stained cells. Bar = 5 μm.

MeCP2-associated factors: MeCP2 targeting interferes with HP1γ binding

Through targeting to the lacO array in AO3_1 cells, we subsequently analyzed the accumulation or displacement of a variety of previously reported MeCP2-associated factors including proteins and epigenetic marks related to a transcriptionally active chromatin state (i.e. the Brahma subunit of the SWI/SNF complex (Harikrishnan et al., 2005; Hu et al., 2006; Wang, 2003), TFIIB, CREB1 (Chahrour et al., 2008; Kaludov and Wolffe, 2000), RNA polymerase II, RNA splicing factor SC35 (Buschdorf and Strätling, 2004), H3K4 di-methylation and H4K16 acetylation and CpG methylation) (Table 2). While

the distribution of most of these factors or epigenetic marks was not altered by targeting MeCP2, we confirmed that MeCP2 targeting interferes with chromatin binding of linker histone H1 (FRAP data not shown), which is compatible with the observed chromatin unfolding (Amir et al., 1999; Ghosh et al., 2010b; Nan et al., 1997; Nikitina et al., 2007b). Moreover, we detected MeCP2-induced changes in the distribution of HP1γ and decided to study this in more detail.

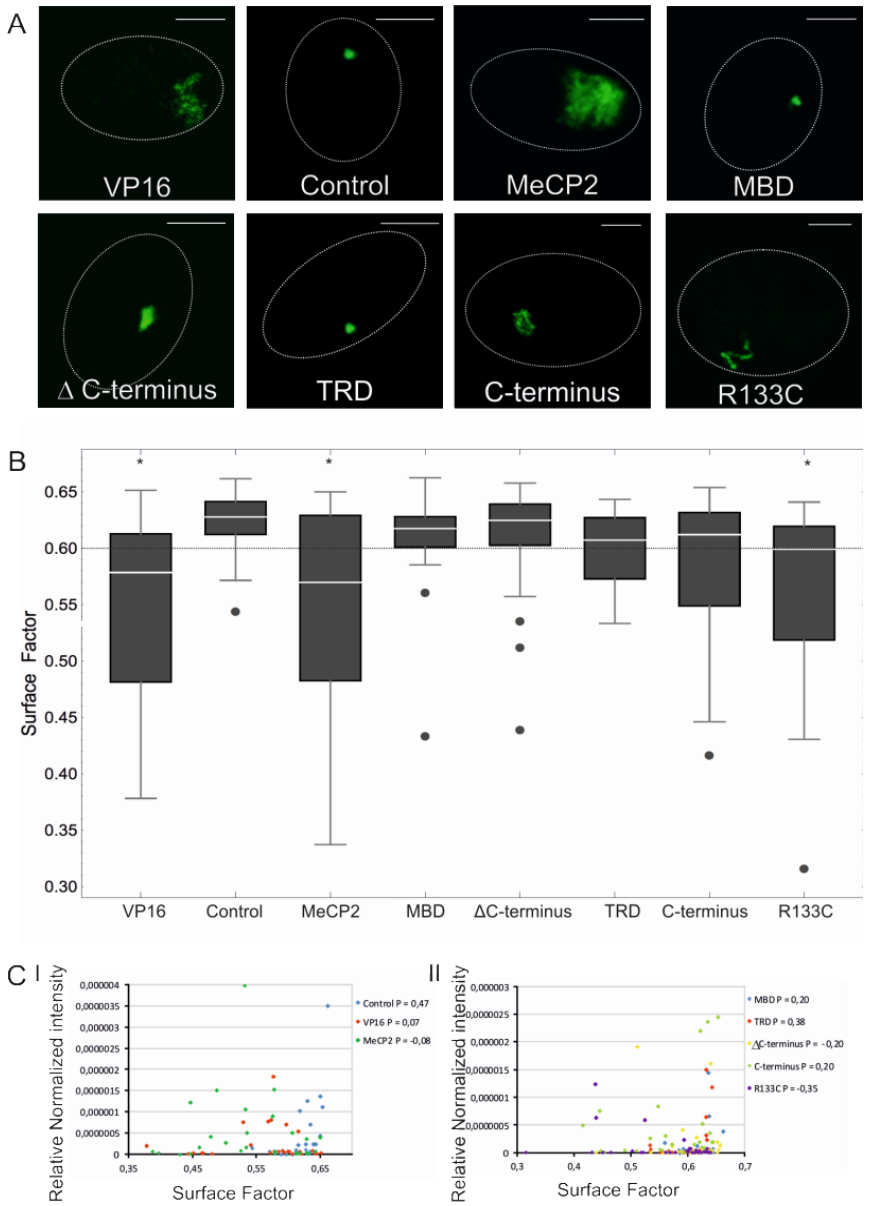

Figure 4. MeCP2-induced chromatin unfolding acts independently of the methyl-cytosine-binding domain.

Figure 4. MeCP2-induced chromatin unfolding acts independently of the methyl-cytosine-binding domain.

A) The images show AO3_1 cells (CHO-derived clone containing an amplified chromosomal region consisting of the DHFR cDNA transgene and 256 lac operator repeats) that were transfected (green signal) with EGFP-lacR (control) or EGFP-lacR-tagged full-length MeCP2, -VP16 and -MeCP2 partial domains (i.e. MBD, ΔC-terminus, TRD, C-terminus and R133C Rett syndrome mutation). The images show a typical representation of cells transfected for 48 hours. For quantitative analysis 30 nuclei per condition were measured with comparable microscopical set-up. The images represent examples of individual optical sections. Bar = 5 μm.

B) The figure shows the changes in lacO array large-scale chromatin structure measured with a 3D image analysis tool, i.e. the surface factor. The surface factor determines the surface of a given chromosomal domain/object normalized to the surface of a sphere with an equal volume (Rottach et al., 2008). The distribution of the surface factor measurements is plotted as a box-plot. The second and third quartiles of the observed values are within the box, the median value is shown by the white horizontal line, the whiskers show the first and fourth quartiles of the observed values, dots are the outliers.

The dotted line represents the ~20% of cells in the EGFP-lacR control population that exhibit a mildly decondensed array (see also (Li et al., 1998)). Considering a population (20%) of control cells exhibiting a decondensed configuration as the threshold of MeCP2-induced decondensation, the following percentages are found for lacR control 18%, VP16 68%, MeCP2 full length 47%, MBD 23%, ΔC-terminus 23%, C-terminus 47% and R133C 50%). We scored the chromatin structure based on the surface factor in the full cell population. Based on our statistical analysis the EGFP-lacR tagged VP16, MeCP2 (full length) and the R133C population are significantly different from EGFP-lacR control, whereas EGFP-lacR tagged MBD, TRD, C-terminus and ΔC-terminus, are not significantly different from EGFP-lacR (for p values see Table 1).

C) The figure shows the intensity of the transfected constructs measured within the lacO chromsomal array and plotted versus the chromatin surface factor measurements of the respective cells (I: Control, VP16 and MeCP2, II: MBD, TRD, C-terminus, ΔC-terminus and R133C). The Pearson correlation coefficient (P) of the intensity of the transfected constructs and the determined surface factor are given.

We recently identified an interaction between MeCP2 and the HP1 proteins in mouse myoblast cells (Agarwal et al., 2007). Co-transfection of mCherry-lacR and EGFP-tagged HP1α, β or γ in A03_1 cells showed enrichment of all HP1 isoforms at the lacO array (Figure 5A-C). Indeed, FRAP measurements on the mobility of HP1γ at the lacO array (visualized by mCherry-LacR) or elsewhere in the nucleus showed that HP1γ has a slower exchange rate at the array (Figure 5D). The measured binding kinetics of HP1γ at the lacO array is in accordance with previous findings on the binding dynamics of HP1 at pericentromeric heterochromatin (Schmiedeberg et al., 2004). Therefore, our findings imply that HP1γ binding at the lacO array in the AO3_1 cells reflects binding at heterochromatin, which is in agreement with the heterochromatic nature of the array

(Figure 5A-D). Strikingly, while HP1α and β remained bound (Figure 5C), HP1γγaccumulation at the lacO array was lost upon MeCP2 targeting (Figure 5A, B). We determined the HP1γ exchange rates using fluorescence loss in photo bleaching (FLIP) (Figure 5E), which identified two dynamic HP1γ pools corresponding to a freely diffusing (t1/2~3 s) or a transiently chromatin-bound population (t1/2~50 s) (Figure 5E). LacR-transfected cells displayed reduced HP1γ mobility at the array (37%, t1/2=52 s), indicating efficient retention of HP1γ at the array. Strikingly, the proportion of the freely diffusing HP1γ population went up to 97% (t1/2 = 1.5 s) after targeting of lacR-tagged MeCP2. These results confirm that MeCP2 effectively antagonizes binding of HP1γ to chromatin.

Populations analyzed	p-value
Control - VP16	p = 0.00003
Control - Full length MeCP2	p = 0.0001
Control - $MeCP2^{R133C}$	p = 0.0003
Control - MeCP2 C-terminus	p = 0.012
Control - MeCP2 TRD	p = 0.013
Control - MeCP2 MBD	p = 0.15
Control - MeCP2ΔC-terminus	p = 0.33

Table 1. Statistical evaluation of the chromatin structural analysis.

Statistical evaluation of the differences in chromatin structure after targeting EGFP-lacR tagged constructs. Rows 1 through 7 show the comparison between control cells transfected with EGFP-lacR and cells transfected with EGFP-lacR-tagged full-length MeCP2, EGFP-lacR-tagged VP16 and EGFP-lacR-tagged MeCP2 partial domains (i.e. C-terminus, MBD, TRD, ΔC-terminus, R133C Rett syndrome mutation). Since the data are not normally distributed and do not have a shared variance, we used Wilcoxon nonparametric statistical testing corrected for multiple testing (Bonferoni) (Sokal and Rohlf, 2011). The p-values are shown, indicating the probabilities that two populations are different choosing a cut-off value of p = 0.007. Based on this analysis the EGFP-lacR tagged VP16, MeCP2 (full length) and the R133C population are significantly different from EGFP-lacR control, whereas EGFP-lacR tagged MBD, TRD, C-terminus and ΔC-terminus, are not significantly different from EGFP-lacR.

To verify our observations that MeCP2 induces HP1γ dissociation from the lacO array in AO3_1 cells, we also analyzed this phenomenon in U2OS 2-6-3 cells (Figure 6A-E). Although the 200 copy lacO array in the 2-6-3 clone is smaller compared to the large amplified domain in the AO3_1 clone, we were able to confirm the MeCP2-induced HP1γ loss from the 200 copy lacO array in the 2-6-3 clone (Figure 6A). Similar to our analysis in AO3 cells, FLIP analysis in the 2-6-3 cells also revealed two dynamic HP1γ pools corresponding to freely diffusing (78% $t_{1/2}$~ 12.6s) and chromatin-bound (22%, $t_{1/2}$~86.6s) HP1γ pools. As in AO3 cells, MeCP2 targeting markedly shifted the proportion of freely diffusing HP1γ molecules towards 99.9 % in 2-6-3 cells, while 0.1% remained chromatin bound (Figure 6D). Similar to MeCP2 targeting, we found that the viral activator VP16 induced a comparable shift in HP1γ mobility in 2-6-3 cells (i.e. 98% freely diffusing and 2% chromatin-bound; Figure 6A, D).

To gain more insight into the MeCP2-induced HP1γ dissociation from the lacO array upon chromatin unfolding, we analyzed the ability of MeCP2 to displace two partial HP1γ domains, the chromo domain, CD (1-75), which mediates HP1 binding to H3K9 tri-methylation, and the chromo shadow domain, CSD (92-173), which mediates HP1 dimerization and binding to a number of other proteins (Hayakawa et al., 2003). The HP1γ CSD domain localized at the lacO array upon targeting mCherry tagged lacR whereas MeCP2 targeting triggered the displacement of the HP1γ CSD from the lacO array (Figure 6B, C). The distribution of the HP1γ CD was not affected upon MeCP2 targeting. FLIP analysis confirmed these findings and revealed that the mobility of the HP1γ CSD at the lacO array in control cells was similar to the full-length HP1γ as freely diffusing (73% t1/2~ 8.77s) and chromatin-bound (27%, t1/2~57.8s) pools could be detected. Upon targeting mCherry-lacR tagged MeCP2, a striking shift towards freely diffusing HP1γ CSD molecules (92%) could be measured, while only a small fraction remained chromatin bound (8%; Figure 6E). These experiments suggest that MeCP2-induced displacement of HP1γ associated with the presence of its CSD.

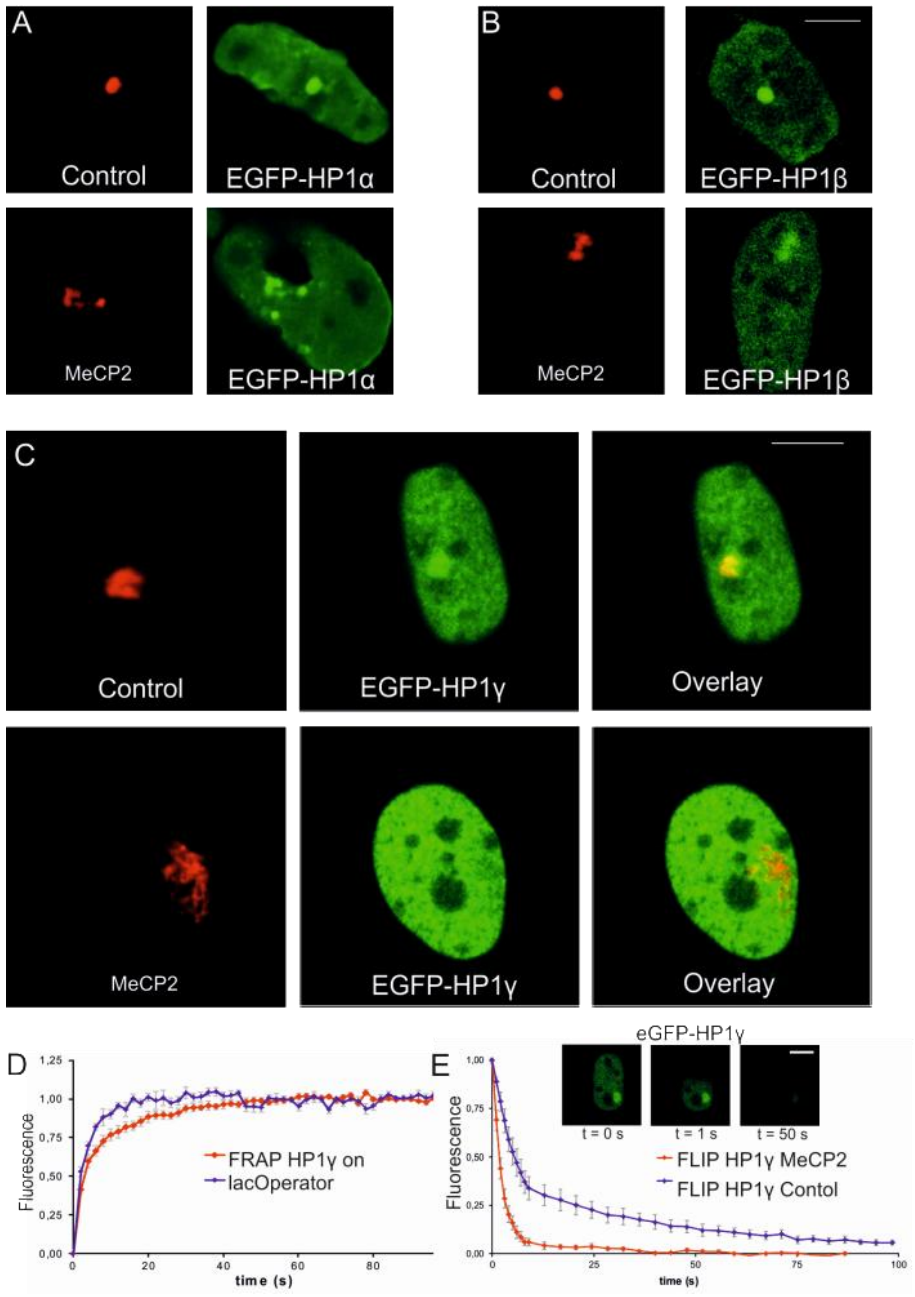

Figure 5. MeCP2 interferes with HP1γ binding.

Figure 5. MeCP2 interferes with HP1γ binding.

AO3_1 cells (CHO-derived clone containing an integrated lacO array) were co-transfected with EGFP-tagged HP1 α, β or γ (green signal) and mCherry-tagged lacR or lacR-MeCP2 (red signal).

A-C) Pictures show 3D images that were recorded of living cells. The images represent individual optical sections and nuclei have the same scale. Bar = 5 μm.

D) The curves show Fluorescent Recovery After Photobleaching (FRAP) data of HP1 γ at the lac operator (red curve) as well as at the overall nuclear localization (blue curve)

E) The graphs show FLIP curves of EGFP-HP1γ in the presence of mCherry-lacR-MeCP2 (red line) or mCherry-lacR (blue line). The insets show an EGFP-HP1γ and mCherry-lacR targeted cell of which half of the nucleus is continuously bleached (only green channel is shown). Bar = 5 μm. FLIP was measured in the bottom half of the nucleus.

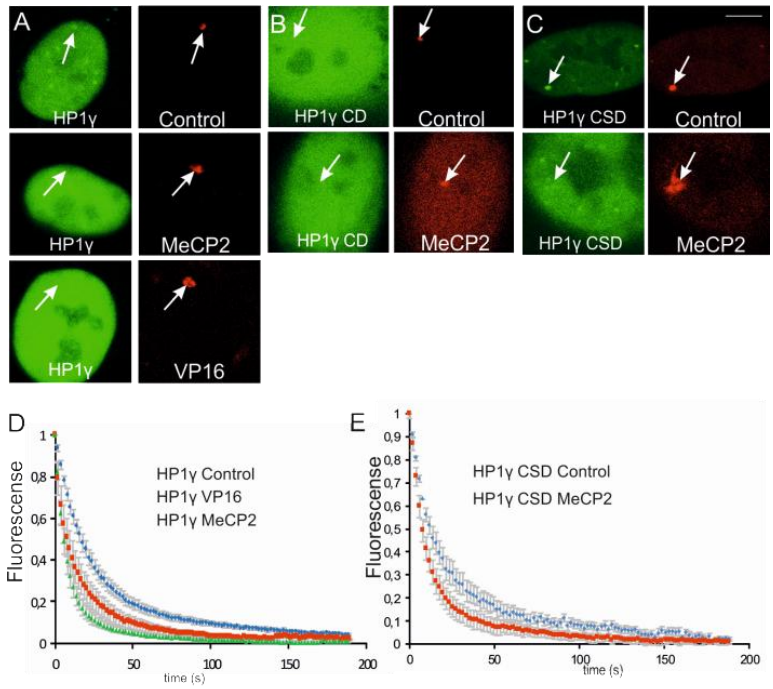

Figure 6. Interference with the binding of HP1γ and partial HP1γ domains.

2-6-3 clone (U2OS-derived clone containing a 200 copy chromosomal array of 256 lacO repeats and a reporter gene harboring 24 repeats of the MS2 bacteriophage) were co-transfected with YFP-tagged HP1γ, HP1γ CD (1-75) or HP1γ CSD (92-173) (green signal) and mCherry-tagged lacR, lacR-MeCP2 or lacR-VP16 (red signal).

A-C) Pictures show 3D images that were recorded of living cells (A-C). The images represent individual optical sections and nuclei have the same scale. Bar = 5 μm.

D) The graphs show FLIP (Fluorescent loss after photobleaching) curves of YFP-HP1γ in the presence of mCherry-lacR (control, blue line), mCherry-lacR-MeCP2 (green line) or mCherry-lacR-VP16 (red line). (E) The graphs show FLIP curves of YFP-HPγ CSD in the presence of mCherry-lacR (control, blue line) or mCherry-lacR-MeCP2 (red line).

Labeling	control	MeCP2	Transfection	control	MeCP2
H3K9me2	+/-	+/-	H1	+/-	+/-
H3K9me3	+/-	+/-	RNAPII	-	-
H1	+/-	+/-	TFIIB	-	-
EZH2	+/-	+/-	CREB	-	-
EED	-	-	Dnmt1	+	+
TFIIHp62	-	-	Dnmt3b	-	-
hBrahma	-	-	HP1α	+	+
H3K4me2	-	-	HP1β	+	+
H4K16ac	-	-	HP1γ	+	-
H3K27me2	-	-			
SC35	-	-			
SETDB1	-	-			
mCpG	+	+			

Table 2. The presence of MeCP2 associated factors at the amplified chromosomal array upon MeCP2 targeting.

Various factors were assayed at light microscopical level for their presence at the amplified chromosomal array in the AO3_1 clone (CHO derived clone containing an amplified chromosomal region consisting of the DHFR cDNA transgene and 256 lac operator repeats). Immunolabeling or co-transfection were performed upon expressing EGFP-lacR (control) or EGFP-lacR-MeCP2. Localization at the array is scored as (+) present, (+/-) infrequently present or (-) absent.

MeCP2 targeting does not change the genomic transcriptional state

To test whether lacR-tagged MeCP2 and MeCP2 subdomains modulate gene activity at the promoter level, we measured gene expression levels of a transfected plasmid containing a luciferase reporter gene fused to 8 lacO copies (Verschure et al., 2005). Targeting LacR-tagged MeCP2, MeCP2^{R133C} and ΔC-terminus to a transiently expressed lacO containing luciferase reporter gene in U2OS cells significantly repressed luciferase

expression (60-70%) compared to targeting only lacR (Figure 7A). In contrast, targeting the C-terminal domain of MeCP2 caused repression to a moderate extent (~25%) (Figure 7A). Taken together, these results demonstrate that the lacR-tagged MeCP2 protein is able to repress gene activity of a transiently expressed luciferase reporter gene plasmid. To address the effect of MeCP2 on gene activity at an integrated genomic locus, we assessed whether MeCP2 influences transcription of genes embedded in the lacO array integrated in the genome of AO3_1 cells. The MeCP2-induced unfolded chromatin structure in AO3_1 cells did not show enrichment of BrUTP-labeled transcripts from the DHFR selection gene compared to lacR-targeted control cells (Figure 7B). In contrast, a considerable increase in BrUTP-labeled transcripts was observed at the VP16-induced unfolded chromatin structure of the lacO chromosomal domain (Tsukamoto et al., 2000; Tumbar et al., 1999) (Figure 7B). Corroborating these findings, we performed RT-qPCR analysis of the DHFR reporter gene upon MeCP2 targeting and subsequent FACS sorting of the transfected AO3_1 cells. Our results show that the DHFR reporter gene expression was not significantly altered compared to lacR-targeted control cells, whereas VP16 targeting resulted in significantly enhanced expression levels of the reporter gene (Figure 7C). In addition, we employed the 2-6-3 clone to visualize MeCP2-induced changes in transcript levels (Janicki et al., 2004). Expression of MS2-YFP to visualize nascent transcripts showed that MeCP2 targeting did not activate transcription at the locus although significant unfolding of the chromosomal array was observed. Conversely, VP16 targeting induced significant accumulation of MS2-YFP-bound transcripts at the chromosomal array compared with MeCP2 targeting or lacR control targeting (Figure 7D). Taken together, we show that decondensation of the amplified chromosomal array upon MeCP2 targeting does not correlate with a change in gene activation.

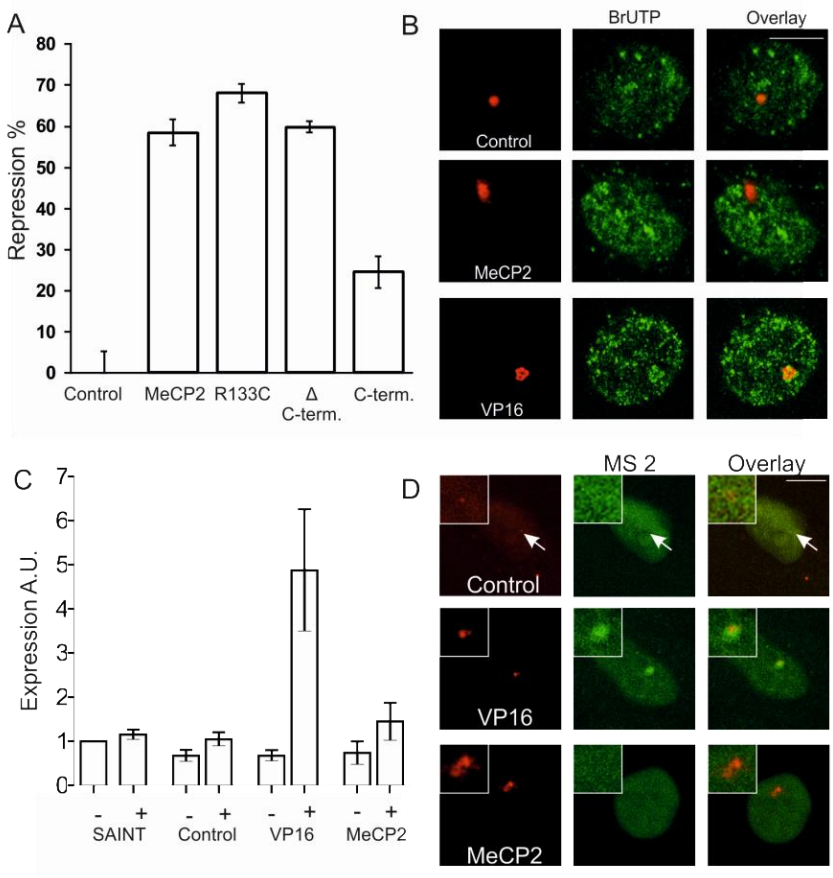

Figure 7. Reporter gene activity upon MeCP2-induced chromatin unfolding.

A) The histogram shows luciferase activity that was measured 48h after transfecting U2OS cells with β-Gal plasmid, an 8x lacO luciferase construct and the plasmids EGFP-lacR (control) and EGFP-lacR-tagged full length MeCP2 and partial MeCP2 domains (i.e. R133C Rett syndrome mutation, C-terminus and ΔC-terminus). Values are the mean ± standard error of 3 independent measurements.

B) AO3_1 cells (CHO-derived clone containing an amplified chromosomal region consisting of the DHFR cDNA transgene and 256 lac operator repeats) were transfected with mCherry-lacR, mCherry-lacR-MeCP2 or mCherry-lacR-VP16 (red signal) and nascent RNA was labeled by incorporation of BrUTP in permeabilized cells (green signal). Bar = 5 μm.

C) The histogram shows DHFR transcriptional activity of AO3_1 cells that were transfected with EGFP-lacR (control), EGFP-lacR-MeCP2 or EGFP-lacR-VP16. Cells were sorted with the FACS and RT-qPCR was performed on both the EGFP-positive (+) as well as on the negative (-) cell population. Data was normalized to non-transfected samples and a transfection control was included (SAINT mix), which were both not FACS sorted.

D) The images show the 2-6-3 clone (U2OS-derived clone containing a 200 copy chromosomal array of 256 lacO repeats and a reporter gene harboring 24 repeats of the MS2 bacteriophage) that was transfected with MS2-YFP to visualize transcribed RNA (green signal) together with mCherry-LacR-tagged MeCP2 or VP16 (red signal detecting the lacO array). The images represent individual optical sections and nuclei are on the same scale. Bar = 5 μm.

Discussion

Regulation of mammalian gene expression is a tightly controlled process. Mistakes in gene expression control can have far-reaching consequences, such as the manifestation of various developmental disorders or cancer. Mutations in the epigenetic regulatory protein MeCP2 underlies the developmental disorder known as Rett Syndrome (de Leon-Guerrero et al., 2011). Still, the molecular mechanisms underlying MeCP2-induced context-dependent functioning are largely unresolved. Post-translational MeCP2 modifications, changes in the MeCP2 genomic binding sites or regulation through MeCP2 co-factors likely influences whether MeCP2 acts as a transcriptional repressor or activator (de Leon-Guerrero et al., 2011).

Here we provide evidence that direct targeting of MeCP2 as an EGFP-lacR tagged protein to a lacO-containing chromosomal domain induces extensive chromatin unfolding. Previous studies have shown that the lacR-lacO targeting system is a very powerful method to define the causal effect of (epigenetic) regulatory proteins on genomic behavior (Janicki et al., 2004; Robinett et al., 1996; van Royen et al., 2007; Verschure et al., 2005) also since fluctuations in endogenous binding conditions might hamper to reveal a clear effect of the studied regulatory proteins. Engineered targeting systems allow to systematically unravel the cause-effect chain of the epigenetic state, chromatin folding, nuclear location and gene activity advancing our understanding of principles in functional genome biology. We show that MeCP2 binding to native chromatin in intact cells triggers extensive chromatin unfolding and that the MBD is not required for this effect. In contrast to our findings, previous *in vitro* studies showed that binding of the C-terminal domain of MeCP2 to reconstituted nucleosomal arrays results in chromatin compaction (Georgel et al., 2003; Nikitina et al., 2007a). It should be noted that reconstituted nucleosomal arrays lack higher-order chromatin structure and could therefore respond differently to MeCP2 binding than chromatin embedded in the nucleus. In intact mouse myoblasts, overexpression of MeCP2 is shown to induce the MBD-dependent clustering of chromo enters during myogenic differentiation (Brero et al., 2005). MeCP2 is a striking example of an intrinsically unstructured protein having a large number of regions predicted to acquire structure when complexed with binding

partners (Adams et al., 2007). The C-terminal portion of MeCP2 is known to be required for chromatin interactions, it harbors the Group II WW domain-binding motif required for splicing factor binding and the SPxK DNA-binding motif found in histone H1 (Ghosh et al., 2010b). Most likely, MeCP2 functioning depends on the type of chromatin and the MeCP2 domain involved. MeCP2 and histone H1 have been shown to compete for chromatin binding sites in vitro and in vivo (Ghosh et al., 2010b; Nikitina et al., 2007b). It has been suggested that a complex competitive equilibrium between MeCP2 and histone H1 for nucleosome and chromatin binding exists and that other competing chromatin binding proteins can affect this histone H1-MeCP2 binding equilibrium (Ghosh et al., 2010a). Such context-dependent *in vivo* functioning of MeCP2 is further underscored by a recent study demonstrating the unique physical properties and interaction domains of MeCP2(Ghosh et al., 2010a).

Several studies hint at a relationship between DNA methylation levels, the presence of methyl-CpG-binding proteins and changes in chromatin structure. For instance, a genome-wide loss of H3K9 di-methylation and a progressive increase in H3K9 acetylation, as well as increased chromocenter clustering was observed in mouse embryonic stem cells lacking DNA methyltransferases Dnmt3a and Dnmt3b. Moreover, during myogenic differentiation, overexpression of methyl-CpG-binding proteins induced increased DNA methylation levels and chromocenter clustering, independent of the H3K9 histone methylation pathway and requiring the MBD domain of MeCP2. We detected *in situ* CpG methylation both at the MeCP2-induced unfolded chromatin and the non-MeCP2 induced compact chromatin which is in line with our observations indicating that the chromatin unfolding is independent of the MeCP2 MBD domain.

Interestingly, we show that MeCP2 interferes with HP1γ chromatin binding. Our FRAP analysis shows similar kinetics of HP1γ at the lacO chromosomal domain as previously measured at mouse heterochromatic sites (Cheutin et al., 2003; Schmiedeberg et al., 2004). The MeCP2-binding-induced release of HP1γ is reflected by the loss of local HP1γ accumulation at the lacO chromosomal domain. This MeCP2-induced interference with HP1γ is also observed with the HP1γ CSD but not with the HP1γ CD, indicating that the

local (chromatin) protein composition influences the ability of MeCP2 to change the HP1γ binding kinetics. Moreover, we show that the transcriptional activator VP16 is also able to interfere with HP1γ binding upon chromatin unfolding and transcriptional activation, illustrating that the chromatin unfolding and HP1γ displacement is not restricted to the changes induced by MeCP2. However, while Janicki et al. showed that VP16-mediated unfolding triggered displacement of the HP1γ isoform (Janicki et al., 2004), we find MeCP2-induced chromatin unfolding to result in the selective removal of the HP1γ isoform. In breast cancer cells displacement of HP1γ is shown to precede transcriptional activation of an integrated luciferase reporter gene (Vicent et al., 2008). In this study, hormonal signaling triggered phosphorylation of H3S10, displacement of HP1γ and ATP-dependent chromatin remodeling resulting in an open, transcriptionally competent chromatin structure. It is tempting to speculate that the MeCP2-mediated chromatin unfolding and eviction of HP1γ are part of a similar mechanism to render chromatin amenable to subsequent transcriptional changes.

Our finding that MeCP2 mediates extensive chromatin unfolding, while maintaining transcriptional silencing of genes embedded within the unfolded chromatin structure, is quite surprising. Recent evidence suggests that proteins that typically accumulate at pericentromeric heterochromatin such as HP1 may function as transcriptional activators, in addition to their role as transcriptional silencer (Vakoc et al., 2005; de Wit et al., 2007; Yasui et al., 2007). Such findings would argue that the canonical view in which open chromatin is transcriptionally active and closed chromatin is transcriptionally inert is too simplistic. Our data might indicate that MeCP2-induced chromatin unfolding prepares chromatin for subsequent transcriptional regulation. Examples of changes in chromatin structure preceding transcriptional activation have been reported for the *HoxB* and *MHC* locus (Chambeyron and Bickmore, 2004; Volpi et al., 2000). Moreover, biochemical analyses revealed that transcriptionally inactive sites can occur both in compact and less compact chromatin (Gilbert et al., 2004). We propose that MeCP2-mediated chromatin unfolding reflects an indeterminate state that facilitates a switch in gene activity. In this scenario, the action of subsequent regulatory factors determines the transcriptional fate of genes embedded within chromatin that has been rendered permissive by MeCP2. Such

a role of MeCP2 fits well with recent observations in neuronal cells, where MeCP2 is abundantly present and proposed to act as a versatile global transcriptional regulator in concert with other regulatory proteins (Skene et al., 2010). Elucidating this global role of MeCP2 in restructuring chromatin *in vivo* is intriguing and may aid in understanding the pathophysiology of neurodevelopmental disorders, such as Rett syndrome.

Materials and methods

CONSTRUCTION OF PLASMIDS

The full-length rat MeCP2e2 isoform and MeCP2 containing point mutation R133C (Yusufzai and Wolffe, 2000) were PCR-amplified and cloned into the AscI site of p3'SS-EGFP-dimer *lac* repressor (Robinett et al., 1996) resulting in C-terminally-tagged EGFP-lacR. Full-length MeCP2 or MBD, TRD or MBD-TRD domains were PCR-amplified and cloned into the XbaI and XhoI site of p3'SS-EGFP-dimer *lac* repressor, resulting in N-terminally-tagged EGFP-lacR. mCherry-lacR and mCherry-lacR-MeCP2 were created by excising EGFP from EGFP-lacR or EGFP-lacR-MeCP2 with XbaI and BsrGI followed by insertion of mCherry.

CELL CULTURE, TRANSFECTION AND LUCIFERASE REPORTER ASSAY

Human osteosarcoma cells (U2OS) (ATCC 40342), NIH/3T3 mouse fibroblasts (ATCC, CRL-1658), AO3_1 and RRE_B1 clones (Andrew Belmont, University of Illinois. Urbana-Champaign (USA) (Belmont et al., 1999)) and the U2OS 2-6-3 clone (David Spector, Cold Spring Harbor Laboratory, New York (USA) (Janicki et al., 2004; Verschure et al., 2005)) were used. The AO3_1 and RRE_B1 clone are derivatives of CHO DG44 cells and contain an integrated amplified chromosomal region consisting of the dihydrofolate reductase (DHFR) cDNA transgene, 256 lac operator repeats and flanking DNA, representing a compact chromatin structure and an unusually extended fibrillar chromatin conformation, respectively. The 2-6-3 clone is a U2OS-derived clone containing a multicopy inducible transgene consisting of 256 lac operator repeats, a tetracycline-inducible reporter gene encoding cyano fluorescent protein with a peroxisomal targeting

signal, 24 repeats of the MS2 bacteriophage translational operator, a splicing cassette and the 3' UTR from the rabbit αglobin gene (Janicki et al., 2004; Verschure et al., 2005). U2OS and NIH/3T3 cells were cultured in Dulbecco minimal essential medium containing 10% fetal bovine serum, 1% pen/strep. (Gibco) The AO3_1 and RRE_B1 clone were cultured in Ham's F-12 medium without hypoxanthine or thymidine supplemented with 10% dialyzed fetal bovine serum (HyClone Labs, Logan, Utah), 1% pen/strep and methotrexate up to a final concentration of 0.03 μM or 10 μM, respectively. The 2-6-3 clone was cultured in high glucose Glutamax (Gibco) with 10% tetracycline free FBS (Clontech), 1% pen/strep and 100 μg/ml hygromycinB (Gibco). All cells were cultured at 37°C in a 5% CO_2 atmosphere.

Transfection was performed with Lipofectamine 2000 (Invitrogen) or SAINT mix (Synvolux Therapeutics, Groningen, The Netherlands) in their respective media without Pen/Strep. For microscopy experiments cells were seeded on cover slips coated with Alcian Blue or 35 mm glass bottom dishes. After 24-48 hours, cells were imaged directly or fixed in 4% paraformaldehyde for 15 minutes at 4°C and embedded in Vectashield (Brunschwig, Burlingame, CA) with DAPI (Vector Laboratories, Burlingame, CA).

Transfections for luciferase reporter assays were done with 8x lacO pGL3 luciferase vector, lacZ construct as an internal reference reporter and EGFP-lacR-tagged effector plasmids. Cells were harvested and lysed at 48 hours post-transfection. Luciferase reporter gene-targeted repression assay was performed as described previously (Verschure et al., 2005). Briefly, luciferase reporter assay transfections were done with 500 ng of the 8x lac operator containing pGL3 luciferase vector, 500 ng of pSV/β-Gal construct (Promega) as an internal reference reporter, and 500 ng of effector plasmid (i.e. EGFP-lacR, EGFP-lacR tagged full length MeCP2, C-terminus, ΔC-terminus and R133C) combined with 48 μl of FuGENE6 reagent per 25-cm^2 culture flask. Cells were harvested and lysed at 48 h post-transfection and luciferase and β-Gal were detected.

FACS SORTING AND QUANTITATIVE PCR

Expressing cells were sorted by flow cytometry (Mo Flo XPD Cell sorter Beckman Coulter, Woerden, The Netherlands). Extracted mRNA was converted to cDNA using the

Fermentas RevertAid™ First strand cDNA synthesis kit. Quantitative PCR amplifications were performed on an ABI Prism 7900HT Sequence Detection System. All PCR reactions were carried out in triplicate using Taqman® gene expression assay Mm00515662_m1 for DHFR and Mm99999915_g1 for GapdH (Applied biosystems). Relative quantification of gene expression was calculated based on the comparative cycle threshold (Ct) method.

BRUTP LABELING, IMMUNOLABELING AND FLUORESCENT IN SITU HYBRIDIZATION

Nascent RNA run-on immunolabeling was performed as described previously (van Royen et al., 2007; Wansink et al., 1993). Briefly, cells were detergent permeabilized with 0.05% TritonX-100 (Sigma, Chemical Co.), and 10U/ml RNAsin in 20mM Tris HCl, 0.5mM MgCl2, 0.5mM EGTA, 25% glycerin. For run-on transcription, the cells were incubated for 10 minutes in synthesis buffer, containing 0.5mM BrUTP ATP, CTP and GTP. Subsequently, the cells were treated with 1mM PMSF and 5U/ml RNAsin, fixed in 2% formaldehyde diluted in PBS and immunolabeled with rat anti BrdU (Seralab) diluted 1:500.

For immunolabeling 2% formaldehyde-fixed cells were treated with 0.5% TritonX-100 for 5 min, 100 mM Glycin for 10 minutes and blocked in 0.5% BSA. All treatments were buffered in 1xPBS. The primary antibodies were diluted in 1xPBS with 0.5% BSA and 0.05% Tween20. Primary antibodies include: rabbit anti-H3K9me2 (1:100) (Upstate, Milton Keynes, United Kingdom), rabbit anti-H3K9me3 (1:300) (Cowell et al., 2002), rabbit anti-SETDB1 (1:200) (Schultz et al., 2002), anti-EZH2 (1:1) and anti-EED(1:100) (Hamer et al., 2002), rabbit anti-TFIIH p62 subunit (1:100) (SantaCruz Biotech), mouse anti-SC35 (1:1000) (Abcam), mouse anti-histone H1 (1:500) (Imgen), goat anti-hBrahma (N-19) (1:100) (Santa Cruz Biotechnology), rabbit anti-H3K4me2 (1:100) (Upstate), rabbit anti-H4K16ac (1:200), rabbit anti-H3K27me2 (Upstate), rat anti-PCNA (1:200) (Leonhardt et al., 2000; Rottach et al., 2008), and rabbit anti-lacR (1:200) (Robinett et al., 1996) and rabbit anti-MeCP2 (1: 500) (Jost et al., 2011). For 5-methyl-cytosine labeling cells were fixed in 4% formaldehyde and treated as for regular immunolabeling in PBS, but also denatured in 2N HCl for 30 min at 37°C and blocked in 10% BSA prior to immunolabeling with mouse

anti-5mC (1:50) (Eurogentec) in 0.5% BSA and 0.05% Tween20, buffered in phosphate buffer pH7.4,

For fluorescence *in situ* hybridization, cells were fixed in 4% formaldehyde on ice, treated with 100 mM Glycin and 0.1N HCl, permeabilized with 0.5% Triton X-100 and 0.5% Saponin, buffered in 1xPBS (Verschure et al., 2002). Denaturation was buffered in SSC (0.15 M NaCl, 0.015 M sodium citrate) and carried out at 78°C in 2xSSC containing 50% formamide and 10% dextran sulfate. The probe was labeled following manufactures instruction by nick translation with a DIG and biotine tag (Roche) Hybridization of the lac operator octamer probe occurred overnight at 37°C in deionized formamide with 0.1x COT DNA and 0.05x Sonicated Salmon sperm (Roche). The cells and probe (25 ng) were denatured and hybridized in 50% formamide and 10% dextran sulfate. Posthybridization washes were carried out with 2× SSC-50% formamide at 45°C. Probe detection proceeded at room temperature in 4× SSC containing 5% (w/v) non-fat dried milk. Antibodies used to detect DIG and biotine tagged probes are FITC-conjugated streptavidin, mouse anti-DIG. Donkey anti-rabbit and donkey anti-mouse labeled with Cy3 or Cy5. All slides were stained with DAPI and embedded in vectashield.

IMAGE ACQUISITION

Cells were imaged using a Zeiss LSM 510 (Zeiss, Jena, Germany) confocal laser scanning microscope equipped with a Zeiss Plan-Apochromat 63x/1.4 oil immersion objective or a Zeiss plan neofluar 63x/1.25 NA oil objective. We used multitrack scanning, employing a UV laser (364 nm), an argon laser (488 and 514 nm) and a helium-neon laser (543 nm) to excite DAPI staining and green/yellow and red fluorochromes. Emitted fluorescence was detected with BP 385-470, BP 505-550 and 560 LP filters. Three-dimensional (3D) images were scanned at 512 by 512 pixels averaging 4 times using a voxel size of 200 nm axial and 60 nm lateral.

To detect the fluorescence intensity levels of the endogenously immunolabeled MeCP2 and exogenous transfected fluorescently tagged MeCP2, a tile scan was made of 64 tiles of 512 by 512 pixels/tile.

IMAGE ANALYSIS

For quantitative analyses approximately 30 nuclei were imaged with comparable microscopical set-up. To quantitatively analyze changes in large-scale chromatin structure, we applied 3D image analysis tools (the Huygens system 2 software package; Scientific Volume Imaging, Hilversum, The Netherlands) as described previously (de Leeuw et al., 2006; Verschure et al., 2005). Briefly, 3D images of the amplified chromosome region are acquired after which the EGFP-lacR- labeled chromosome region is automatically identified. Specific features of the LacO array (3D structure, volume and intensity) are subsequently calculated using Huygens software. To assess the 3D chromatin structure, we used a parameter termed the surface factor, which represents the surface of a given chromosomal domain/object normalized to the surface of a sphere with an equal volume (Rottach et al., 2008). A surface factor of 1 therefore represents a perfectly spherical structure, whereas a lower value represents a more furrowed structure, such as a decondensed chromatin domain. The distribution of the calculated surface factors (~30 nuclei per variable) is plotted in a box-plot. The second and third quartiles of the surface factor values are within the box, the median value is shown by the thick horizontal line, the vertical small lines show the first and fourth quartiles of the observed values. Since our surface factor data is not normally distributed (as tested with Shapiro Wilktest rejecting the null hypothesis that the data are normally distributed with $p < 0.05$, p values see S1) and exhibits an unequal variance (Variance Equivalence test), we used the Wilcoxon nonparametric test (Sokal and Rohlf, 2011) corrected for multiple testing (Bonferroni, $p = 0.07$) to calculate the P-value giving the probability that the control population (cells expressing EGFP-lacR) and the test population (cells expressing EGFP-lacR tagged MeCP2, MeCP2 partial domains or VP16 protein) are significantly different from each other. For the expression level measurements, the intensity of the transfected constructs at the lacO array was detected and normalized to the gain and offset settings of the PMT using a standard curve for the used parameters. The Pearson correlation coefficient was calculated to detect the correlation between the surface factor and the relative normalized intensities.

To depict variable expression levels of fluorescently tagged MeCP2, expression levels were measured using imageJ on both single scanned cells as well as tile-scanned images. Cells were masked and the nuclear counterstain intensities normalized.

PHOTO BLEACHING EXPERIMENTS

For FLIP and FRAP experiments, microscopes were equipped with an objective heater and cells were examined in microscopy medium (137 mM NaCl, 5.4 mM KCl, 1,8 mM $CaCl_2$, 0.8 mM $MgSO_4$, 20 mM D-glucose and 20 mM HEPES) at 37°C. FRAP and FLIP analysis was performed as described previously (Luijsterburg et al., 2007). FRAP was used to measure the mobility of GFP-HP1γ in- and outside of the array visualized by mCherry-LacR. Briefly, images were taken at 512x512 pixels (0.04x0.04 μm), 1.60 μs per frame, zoom 7. After 10 images, a square of 56x56 pixels was bleached for 10 scans (total time = 1.1 s) and recovery was measured for at least 60 images at a 2-second time interval. The data was normalized to the original intensity before the bleach pulse by using the equation: $I_{FRAP} = (I_{strip\ t=t} - I_{background\ t=t}) / (I_{strip\ t=0} - I_{background\ t=0})$, where $I_{strip\ t=t}$ and $I_{strip\ t=0}$ represent the intensity within the strip at t=t and the intensity before the bleach pulse (t=0), respectively. For graphical representation, recovery plots were normalized between 0 and 1. FLIP analysis was used to measure the residence times of GFP-HP1γ on chromatin. Briefly, images of 512x512 pixels were acquired with a scan time of 1.60 μs (1x average/frame) at zoom 7 (1 pixel is 0.04x0.04 μm). After 10 images, a region of 275x150 pixels, occupying an area of 1/3 of the nucleus (excluding the lac operator array), was continuously bleached with maximal 488 nm and 514 nm laser intensity (AOTF 100%). EGFP-HP1γ fluorescence was monitored with low laser intensity for at least 80 images with a 2-second time interval between images. The loss of fluorescence in the unbleached part of the nucleus was quantified. All values were background corrected and normalized to 1 by using the equation: $I_{FLIP} = (I_{spot\ t=t} - I_{background\ t=t}) / (I_{spot\ t=0} - I_{background\ t=0})$. Curve fitting was performed according to $N_1 * e^{(\lambda 1 * t)} + N_2 * e^{(\lambda 2 * t)}$.

Acknowledgements

We thank W. de Leeuw and S. Kooistra for experimental assistance and P. Hemmerich (Jena, Germany), Y. Hiraoka (Osaka, Japan), D. Chen (Sui Huang Lab, Chicago, USA), W.

Vermeulen (Rotterdam, The Netherlands), H. Eldar-Finkelman (Tel Aviv, Israel), N.P. Dantuma (Karolinska Institutet, Stockholm), D. Spector (New York, USA) and A.S. Belmont (Illinois, USA) for providing us with constructs and cell clones used in this study.

Supporting information

Table S1. Quantitative data MeCP2-induced chromatin unfolding.

Table S1 (11 pages) can be found on the plosone website:

http://journals.plos.org/plosone/article?id=10.1371/journal.pone.0069347#s5

Our measurements of the surface factor and the testing for a normal distribution of the surface factor data (Shapiro Wilktest), the microscopical gain and offset settings and the measurements of volume and intensity of the lacO chromosomal array are provided.

AO3_1 cells (CHO-derived clone containing an amplified chromosomal region consisting of the DHFR cDNA transgene and 256 lac operator repeats) were transfected with EGFP-lacR (control) or EGFP-lacR-tagged full-length MeCP2, -VP16 and -MeCP2 partial domains (i.e. MBD, ΔC-terminus, TRD, C-terminus and R133C Rett syndrome mutation) and 30 nuclei per transfected construct were measured with comparable microscopical set-up. We applied a 3D image analysis tools (the Huygens system 2 software package; Scientific Volume Imaging, Hilversum, The Netherlands) as described previously (de Leeuw et al., 2006; Verschure et al., 2005). Specific features of the LacO array (3D structure, volume and intensity) are calculated using Huygens software. The EGFP-lacR- labeled chromosome region is automatically identified in the acquired 3D images, given as the volume. Changes in lacO array large-scale chromatin structure are measured with a 3D image analysis tool, i.e. the surface factor. The surface factor determines the surface of a given chromosomal domain/object normalized to the surface of a sphere with an equal volume (Rottach et al., 2008). We tested with Shapiro Wilktest whether the surface factor data is normally distributed. The intensity of the transfected constructs at the lacO array is detected, i.e. total array intensity and normalized to the gain and offset settings of the PMT using a standard curve for the used parameters thereby providing the relative normalized intensity of the transfected constructs.

Bibliography

Adams, V.H., McBryant, S.J., Wade, P.A., Woodcock, C.L., and Hansen, J.C. (2007). Intrinsic disorder and autonomous domain function in the multifunctional nuclear protein, MeCP2. J. Biol. Chem. *282*, 15057–15064.

Agarwal, N., Hardt, T., Brero, A., Nowak, D., Rothbauer, U., Becker, A., Leonhardt, H., and Cardoso, M.C. (2007). MeCP2 interacts with HP1 and modulates its heterochromatin association during myogenic differentiation. Nucleic Acids Res *35*, 5402–5408.

Akhtar, W., de Jong, J., Pindyurin, A. V, Pagie, L., Meuleman, W., de Ridder, J., Berns, A., Wessels, L.F. a, van Lohuizen, M., and van Steensel, B. (2013). Chromatin position effects assayed by thousands of reporters integrated in parallel. Cell *154*, 914–927.

Al-Allaf, F. a., Tolmachov, O.E., Zambetti, L.P., Tchetchelnitski, V., and Mehmet, H. (2012). Remarkable stability of an instability-prone lentiviral vector plasmid in Escherichia coli Stbl3. 3 Biotech 61–70.

Alvarez-Saavedra, M., Antoun, G., Yanagiya, A., Oliva-Hernandez, R., Cornejo-Palma, D., Perez-Iratxeta, C., Sonenberg, N., and Cheng, H.Y.M. (2011). miRNA-132 orchestrates chromatin remodeling and translational control of the circadian clock. Hum. Mol. Genet. *20*, 731–751.

Amir, R.E., Van den Veyver, I.B., Wan, M., Tran, C.Q., Francke, U., and Zoghbi, H.Y. (1999). Rett syndrome is caused by mutations in X-linked MECP2, encoding methyl-CpG-binding protein 2. Nat. Genet. *23*, 185–188.

Anderson, A., Wong, K., Jacoby, P., Downs, J., and Leonard, H. (2014). Twenty years of surveillance in Rett syndrome: what does this tell us? Orphanet J. Rare Dis. *9*, 87.

Babbio, F., Castiglioni, I., Cassina, C., Gariboldi, M., Pistore, C., Magnani, E., Badaracco, G., Monti, E., and Bonapace, I. (2012). Knock-down of methyl CpG-binding protein 2 (MeCP2) causes alterations in cell proliferation and nuclear lamins expression in mammalian cells. BMC Cell Biol. *13*, 19.

Baker, S.A., Chen, L., Wilkins, A.D., Yu, P., Lichtarge, O., and Zoghbi, H.Y. (2013). An AT-hook domain in MeCP2 determines the clinical course of Rett syndrome and related disorders. Cell *152*, 984–996.

Ballas, N., Lioy, D.T., Grunseich, C., and Mandel, G. (2009). Non-cell autonomous influence of MeCP2-deficient glia on neuronal dendritic morphology. Nat. Neurosci. *12*, 311–317.

Ballestar, E., Yusufzai, T.M., and Wolffe, A.P. (2000). Effects of Rett syndrome mutations of the methyl-CpG binding domain of the transcriptional repressor MeCP2 on selectivity for association with methylated DNA. Biochemistry *39*, 7100–7106.

Barth, T.K., and Imhof, A. (2010). Fast signals and slow marks: the dynamics of histone modifications. Trends Biochem. Sci. *35*, 618–626.

Battich, N., Stoeger, T., and Pelkmans, L. (2013). Image-based transcriptomics in thousands of single human cells at single-molecule resolution. Nat. Methods *10*, 1127–1133.

Bellini, E., Pavesi, G., Barbiero, I., Bergo, A., Chandola, C., Nawaz, M.S., Rusconi, L., Stefanelli, G., Strollo, M., Valente, M.M., et al. (2014). MeCP2 post-translational modifications: a mechanism to control its involvement in synaptic plasticity and homeostasis? Front. Cell. Neurosci. *8*, 1–15.

Belmont, A.S., Li, G., Sudlow, G., and Robinett, C. (1999). Visualization of large-scale chromatin structure and dynamics using the lac operator/lac repressor reporter system. Methods Cell Biol *58*, 203–222.

Ben-Ari, Y., Brody, Y., Kinor, N., Mor, A., Tsukamoto, T., Spector, D.L., Singer, R.H., and Shav-Tal, Y. (2010). The life of an mRNA in space and time. J. Cell Sci. *123*, 1761–1774.

Ben-Shachar, S., Chahrour, M., Thaller, C., Shaw, C.A., and Zoghbi, H.Y. (2009). Mouse models of MeCP2 disorders share gene expression changes in the cerebellum and hypothalamus. Hum Mol Genet *18*, 2431–2442.

Bergo, A., Strollo, M., Gai, M., Barbiero, I., Stefanelli, G., Gigli, C.C., Cunto, F. Di, and Kilstrup-nielsen, C. (2014). Novel and unexpected centrosome-related functions of MeCP2. *2*.

Bertrand, E., Chartrand, P., Schaefer, M., Shenoy, S.M., Singer, R.H., and Long, R.M. (1998). Localization of ASH1 mRNA particles in living yeast. Mol. Cell *2*, 437–445.

Bienvenu, T., and Chelly, J. (2006). Molecular genetics of Rett syndrome: when DNA methylation goes unrecognized. Nat. Rev. Genet. *7*, 415–426.

Bodnar, M.S., and Spector, D.L. (2013). Chromatin Meets Its Organizers. Cell *153*, 1187–1189.

Boettcher, M., and McManus, M.T. (2015). Choosing the Right Tool for the Job: RNAi, TALEN, or CRISPR. Mol. Cell *58*, 575–585.

Brero, A., Easwaran, H.P., Nowak, D., Grunewald, I., Cremer, T., Leonhardt, H., and Cardoso, M.C. (2005). Methyl CpG-binding proteins induce large-scale chromatin reorganization during terminal differentiation. J Cell Biol *169*, 733–743.

Brink, M.C., Piebes, D.G.E., de Groote, M.L., Luijsterburg, M.S., Casas-Delucchi, C.S., van Driel, R., Rots, M.G., Cardoso, M.C., and Verschure, P.J. (2013). A role for MeCP2 in switching gene activity via chromatin unfolding and HP1γ displacement. PLoS One *8*, e69347.

Brody, Y., and Shav-Tal, Y. (2011). Measuring the kinetics of mRNA transcription in single living cells. J. Vis. Exp. 1–6.

Buschdorf, J.P., and Strätling, W.H. (2004). A WW domain binding region in methyl-CpG-binding protein MeCP2: Impact on Rett syndrome. J. Mol. Med. *82*, 135–143.

Buyse, I.M., Fang, P., Hoon, K.T., Amir, R.E., Zoghbi, H.Y., and Roa, B.B. (2000). Diagnostic testing for Rett syndrome by DHPLC and direct sequencing analysis of the MECP2 gene: identification of several novel mutations and polymorphisms. Am. J. Hum. Genet. *67*, 1428–1436.

Chahrour, M., Jung, S.Y., Shaw, C., Zhou, X., Wong, S.T.C., Qin, J., and Zoghbi, H.Y. (2008). MeCP2, a key contributor to neurological disease, activates and represses transcription. Science *320*, 1224–1229.

Chambeyron, S., and Bickmore, W.A. (2004). Chromatin decondensation and nuclear reorganization of the HoxB locus upon induction of transcription. Genes Dev *18*, 1119–1130.

Chao, H.-T., and Zoghbi, H.Y. (2009). The yin and yang of MeCP2 phosphorylation. Proc. Natl. Acad. Sci. U. S. A. *106*, 4577–4578.

Chen, K.H., Boettiger, A.N., Moffitt, J.R., Wang, S., and Zhuang, X. (2015). Spatially resolved, highly multiplexed RNA profiling in single cells. Science *348*, aaa6090.

Cheutin, T., McNairn, A.J., Jenuwein, T., Gilbert, D.M., Singh, P.B., and Misteli, T. (2003). Maintenance of stable heterochromatin domains by dynamic HP1 binding. Science (80-.). *299*, 721–725.

Chiang, K., Liu, H., and Rice, A.P. (2013). MiR-132 enhances HIV-1 replication. Virology *438*, 1–4.

Christodoulou, J., Grimm, A., Maher, T., and Bennetts, B. (2003). RettBASE: The IRSA MECP2 variation database-a new mutation database in evolution. Hum. Mutat. *21*, 466–472.

Colantuoni, C., Jeon, O.H., Hyder, K., Chenchik, A., Khimani, A.H., Narayanan, V., Hoffman, E.P., Kaufmann, W.E., Naidu, S., and Pevsner, J. (2001). Gene expression profiling in postmortem Rett Syndrome brain: differential gene expression and patient classification. Neurobiol. Dis. *8*, 847–865.

Collins, A.L., Levenson, J.M., Vilaythong, A.P., Richman, R., Armstrong, D.L., Noebels, J.L., Sweatt, J.D., and Zoghbi, H.Y. (2004). Mild overexpression of MeCP2 causes a progressive neurological disorder in mice. Hum. Mol. Genet. *13*, 2679–2689.

Coulon, A., Chow, C.C., Singer, R.H., and Larson, D.R. (2013). Eukaryotic transcriptional dynamics: from single molecules to cell populations. Nat. Rev. Genet. *14*, 572–584.

Cowell, I.G., Aucott, R., Mahadevaiah, S.K., Burgoyne, P.S., Huskisson, N., Bongiorni, S., Prantera, G., Fanti, L., Pimpinelli, S., Wu, R., et al. (2002). Heterochromatin, HP1 and methylation at lysine 9 of histone H3 in animals. Chromosoma *111*, 22–36.

Cutter, A.R., and Hayes, J.J. (2015). A brief review of nucleosome structure. FEBS Lett. 1–9.

Darzacq, X., Shav-Tal, Y., de Turris, V., Brody, Y., Shenoy, S.M., Phair, R.D., and Singer, R.H. (2007). In vivo dynamics of RNA polymerase II transcription. Nat. Struct. Mol. Biol. *14*, 796–806.

Deng, W., and Blobel, G. a. (2014). Manipulating nuclear architecture. Curr. Opin. Genet. Dev. *25*, 1–7.

Dintilhac, A., and Bernués, J. (2002). HMGB1 interacts with many apparently unrelated proteins by recognizing short amino acid sequences. J. Biol. Chem. *277*, 7021–7028.

Dion, M.F., Kaplan, T., Kim, M., Buratowski, S., Friedman, N., and Rando, O.J. (2007). Dynamics of replication-independent histone turnover in budding yeast. Science (80-.). *315*, 1405–1408.

Dobrzynski, M., and Bruggeman, F.J. (2009). Elongation dynamics shape bursty transcription and translation. Proc. Natl. Acad. Sci. U. S. A. *106*, 2583–2588.

Ego, T., Tanaka, Y., and Shimotohno, K. (2005). Interaction of HTLV-1 Tax and methyl-CpG-binding domain 2 positively regulates the gene expression from the hypermethylated LTR. Oncogene *24*, 1914–1923.

Eivazova, E.R., Gavrilov, A., Pirozhkova, I., Petrov, A., Iarovaia, O. V., Razin, S. V., Lipinski, M., and Vassetzky, Y.S. (2009). Interaction in vivo between the two matrix attachment regions flanking a single chromatin loop. J Mol Biol *386*, 929–937.

Ernst, J., and Kellis, M. (2010). Discovery and characterization of chromatin states for systematic annotation of the human genome. Nat. Biotechnol. *28*, 817–825.

Van Esch, H. (2012). MECP2 duplication syndrome. Mol. Syndromol. *2*, 128–136.

Fuks, F., Hurd, P.J., Wolf, D., Nan, X., Bird, A.P., and Kouzarides, T. (2003). The methyl-CpG-binding protein MeCP2 links DNA methylation to histone methylation. J Biol Chem *278*, 4035–4040.

Fyfe, S., Cream, A., de Klerk, N., Christodoulou, J., and Leonard, H. (2003). InterRett and RettBASE: International Rett Syndrome Association databases for Rett syndrome. J. Child Neurol. *18*, 709–713.

Gadalla, K.K.E., Bailey, M.E.S., and Cobb, S.R. (2011). MeCP2 and Rett syndrome: reversibility and potential avenues for therapy. Biochem. J. *439*, 1–14.

Gandhi, S.J., Zenklusen, D., Lionnet, T., and Singer, R.H. (2011). Transcription of functionally related constitutive genes is not coordinated. Nat. Struct. Mol. Biol. *18*, 27–34.

Garg, S.K., Lioy, D.T., Cheval, H., McGann, J.C., Bissonnette, J.M., Murtha, M.J., Foust, K.D., Kaspar, B.K., Bird, A., and Mandel, G. (2013). Systemic delivery of MeCP2 rescues behavioral and cellular deficits in female mouse models of Rett syndrome. J. Neurosci. *33*, 13612–13620.

Georgel, P.T., Horowitz-Scherer, R.A., Adkins, N., Woodcock, C.L., Wade, P.A., and Hansen, J.C. (2003). Chromatin compaction by human MeCP2. Assembly of novel secondary chromatin structures in the absence of DNA methylation. J Biol Chem *278*, 32181–32188.

Ghosh, R.P., Horowitz-Scherer, R.A., Nikitina, T., Shlyakhtenko, L.S., and Woodcock, C.L. (2010a). MeCP2 binds cooperatively to its substrate and competes with histone H1 for chromatin binding sites. Mol Cell Biol *30*, 4656–4670.

Ghosh, R.P., Nikitina, T., Horowitz-Scherer, R. a, Gierasch, L.M., Uversky, V.N., Hite, K., Hansen, J.C., and Woodcock, C.L. (2010b). Unique physical properties and interactions of the domains of methylated DNA binding protein 2. Biochemistry *49*, 4395–4410.

Gibson, D.G., Young, L., Chuang, R.-Y., Venter, J.C., Hutchison, C.A., and Smith, H.O. (2009). Enzymatic assembly of DNA molecules up to several hundred kilobases. Nat. Methods *6*, 343–345.

Gierman, H.J., Indemans, M.H.G., Koster, J., Goetze, S., Seppen, J., Geerts, D., van Driel, R., and Versteeg, R. (2007). Domain-wide regulation of gene expression in the human genome. Genome Res. *17*, 1286–1295.

Gilbert, N., Boyle, S., Fiegler, H., Woodfine, K., Carter, N.P., and Bickmore, W.A. (2004). Chromatin architecture of the human genome: gene-rich domains are enriched in open chromatin fibers. Cell *118*, 555–566.

Goedhart, J., van Weeren, L., Hink, M.A., Vischer, N.O.E., Jalink, K., and Gadella, T.W.J. (2010). Bright cyan fluorescent protein variants identified by fluorescence lifetime screening. Nat. Methods *7*, 137–139.

Gossen, M., and Bujard, H. (1992). Tight control of gene expression in mammalian cells by tetracycline-responsive promoters. Proc. Natl. Acad. Sci. U. S. A. *89*, 5547–5551.

Groner, A.C., Meylan, S., Ciuffi, A., Zangger, N., Ambrosini, G., Denervaud, N., Bucher, P., and Trono, D. (2010). KRAB-zinc finger proteins and KAP1 can mediate long-range transcriptional repression through heterochromatin spreading. PLoS Genet *6*, e1000869.

Guarda, A., Bolognese, F., Bonapace, I.M., and Badaracco, G. (2009). Interaction between the inner nuclear membrane lamin B receptor and the heterochromatic methyl binding protein, MeCP2. Exp. Cell Res. *315*, 1895–1903.

Guo, J.U., Su, Y., Zhong, C., Ming, G.-L., and Song, H. (2011). Hydroxylation of 5-Methylcytosine by TET1 Promotes Active DNA Demethylation in the Adult Brain. Cell *145*, 423–434.

Gurard-Levin, Z. a, and Almouzni, G. (2014). Histone modifications and a choice of variant: a language that helps the genome express itself. F1000Prime Rep *6*, 76.

Guy, J., Hendrich, B., Holmes, M., Martin, J.E., and Bird, A. (2001). A mouse Mecp2-null mutation causes neurological symptoms that mimic Rett syndrome. Nat. Genet. *27*, 322–326.

Guy, J., Gan, J., Selfridge, J., Cobb, S., and Bird, A. (2007). Reversal of neurological defects in a mouse model of Rett syndrome. Science *315*, 1143–1147.

Hager, G.L., Fletcher, T.M., Xiao, N., Baumann, C.T., Müller, W.G., and McNally, J.G. (2000). Dynamics of gene targeting and chromatin remodelling by nuclear receptors. Biochem. Soc. Trans. *28*, 405–410.

Hager, G.L., McNally, J.G., and Misteli, T. (2009). Transcription dynamics. Mol. Cell *35*, 741–753.

Hamer, K.M., Sewalt, R.G., den Blaauwen, J.L., Hendrix, T., Satijn, D.P., and Otte, A.P. (2002). A panel of monoclonal antibodies against human polycomb group proteins. Hybrid Hybridomics *21*, 245–252.

Harikrishnan, K.N., Chow, M.Z., Baker, E.K., Pal, S., Bassal, S., Brasacchio, D., Wang, L., Craig, J.M., Jones, P.L., Sif, S., et al. (2005). Brahma links the SWI/SNF chromatin-remodeling complex with MeCP2-dependent transcriptional silencing. Nat Genet *37*, 254–264.

Harper, C. V, Finkenstädt, B., Woodcock, D.J., Friedrichsen, S., Semprini, S., Ashall, L., Spiller, D.G., Mullins, J.J., Rand, D.A., Davis, J.R.E., et al. (2011). Dynamic analysis of stochastic transcription cycles. PLoS Biol. *9*, e1000607.

Hassan, A.H., Prochasson, P., Neely, K.E., Galasinski, S.C., Chandy, M., Carrozza, M.J., and Workman, J.L. (2002). Function and selectivity of bromodomains in anchoring chromatin-modifying complexes to promoter nucleosomes. Cell *111*, 369–379.

Hayakawa, T., Haraguchi, T., Masumoto, H., and Hiraoka, Y. (2003). Cell cycle behavior of human HP1 subtypes: distinct molecular domains of HP1 are required for their centromeric localization during interphase and metaphase. J Cell Sci *116*, 3327–3338.

Hemmerich, P., Schmiedeberg, L., and Diekmann, S. (2011). Dynamic as well as stable protein interactions contribute to genome function and maintenance. Chromosom. Res *19*, 131–151.

Hines, K.A., Cryderman, D.E., Flannery, K.M., Yang, H., Vitalini, M.W., Hazelrigg, T., Mizzen, C.A., and Wallrath, L.L. (2009). Domains of heterochromatin protein 1 required for Drosophila melanogaster heterochromatin spreading. Genetics *182*, 967–977.

Hocine, S., Raymond, P., Zenklusen, D., Chao, J. a, and Singer, R.H. (2013). Single-molecule analysis of gene expression using two-color RNA labeling in live yeast. Nat. Methods *10*, 119–121.

Hoppe, P.S., Coutu, D.L., and Schroeder, T. (2014). Single-cell technologies sharpen up mammalian stem cell research. Nat. Cell Biol. *16*, 919–927.

Horike, S., Cai, S., Miyano, M., Cheng, J.F., and Kohwi-Shigematsu, T. (2005). Loss of silent-chromatin looping and impaired imprinting of DLX5 in Rett syndrome. Nat Genet *37*, 31–40.

Hsu, P.D., Lander, E.S., and Zhang, F. (2014). Development and Applications of CRISPR-Cas9 for Genome Engineering. Cell *157*, 1262–1278.

Hu, K., Nan, X., Bird, A., and Wang, W. (2006). Testing for association between MeCP2 and the brahma-associated SWI/SNF chromatin-remodeling complex. Nat Genet *38*, 962–967.

Huranová, M., Ivani, I., Benda, A., Poser, I., Brody, Y., Hof, M., Shav-Tal, Y., Neugebauer, K.M., and Staněk, D. (2010). The differential interaction of snRNPs with pre-mRNA reveals splicing kinetics in living cells. J. Cell Biol. *191*, 75–86.

Iizuka, M., and Smith, M.M. (2003). Functional consequences of histone modifications. Curr. Opin. Genet. Dev. *13*, 154–160.

Janicki, S.M., Tsukamoto, T., Salghetti, S.E., Tansey, W.P., Sachidanandam, R., Prasanth, K. V, Ried, T., Shav-Tal, Y., Bertrand, E., Singer, R.H., et al. (2004). From silencing to gene expression: real-time analysis in single cells. Cell *116*, 683–698.

Jiang, M., Ash, R.T., Baker, S.A., Suter, B., Ferguson, A., Park, J., Rudy, J., Torsky, S.P., Chao, H.-T., Zoghbi, H.Y., et al. (2013). Dendritic arborization and spine dynamics are abnormal in the mouse model of MECP2 duplication syndrome. J. Neurosci. *33*, 19518–19533.

Johnston, I.G., Gaal, B., das Neves, R.P., Enver, T., Iborra, F.J., and Jones, N.S. (2012). Mitochondrial variability as a source of extrinsic cellular noise. PLoS Comput. Biol. *8*.

Jones, P.L., Veenstra, G.J., Wade, P.A., Vermaak, D., Kass, S.U., Landsberger, N., Strouboulis, J., and Wolffe, A.P. (1998). Methylated DNA and MeCP2 recruit histone deacetylase to repress transcription. Nat Genet *19*, 187–191.

Jost, K.L., Rottach, A., Milden, M., Bertulat, B., Becker, A., Wolf, P., Sandoval, J., Petazzi, P., Huertas, D., Esteller, M., et al. (2011). Generation and characterization of rat and mouse monoclonal antibodies specific for MeCP2 and their use in X-inactivation studies. PLoS One *6*, e26499.

Kaludov, N.K., and Wolffe, A.P. (2000). MeCP2 driven transcriptional repression in vitro: selectivity for methylated DNA, action at a distance and contacts with the basal transcription machinery. Nucleic Acids Res *28*, 1921–1928.

Van Kampen, N.G. (1992). Stochastic processes in physics and chemistry.

Kang, M., Day, C.A., Kenworthy, A.K., and DiBenedetto, E. (2012). Simplified equation to extract diffusion coefficients from confocal FRAP data. Traffic *13*, 1589–1600.

Kato, M. (2006). A new paradigm for West syndrome based on molecular and cell biology. Epilepsy Res. *70*, 87–95.

Kernohan, K.D., Jiang, Y., Tremblay, D.C., Bonvissuto, A.C., Eubanks, J.H., Mann, M.R.W., Berube, N.G., and Bérubé, N.G. (2010). ATRX partners with cohesin and MeCP2 and contributes to developmental silencing of imprinted genes in the brain. Dev Cell *18*, 191–202.

Kernohan, K.D., Vernimmen, D., Gloor, G.B., and B??rub??, N.G. (2014). Analysis of neonatal brain lacking ATRX or MeCP2 reveals changes in nucleosome density, CTCF binding and chromatin looping. Nucleic Acids Res. *42*, 8356–8368.

Khrapunov, S., Warren, C., Cheng, H., Berko, E.R., Greally, J.M., and Brenowitz, M. (2014). Unusual characteristics of the DNA binding domain of epigenetic regulatory protein MeCP2 determine its binding specificity. Biochemistry *53*, 3379–3391.

Kimura, H., and Shiota, K. (2003). Methyl-CpG-binding protein, MeCP2, is a target molecule for maintenance DNA methyltransferase, Dnmt1. J. Biol. Chem. *278*, 4806–4812.

Kinde, B., Gabel, H.W., Gilbert, C.S., Griffith, E.C., and Greenberg, M.E. (2015). Reading the unique DNA methylation landscape of the brain: Non-CpG methylation, hydroxymethylation, and MeCP2. Proc. Natl. Acad. Sci. U. S. A. 1–7.

Klose, R.J., Sarraf, S.A., Schmiedeberg, L., McDermott, S.M., Stancheva, I., and Bird, A.P. (2005). DNA binding selectivity of MeCP2 due to a requirement for A/T sequences adjacent to methyl-CpG. Mol Cell *19*, 667–678.

Kouzarides, T. (2007a). SnapShot: Histone-Modifying Enzymes. Cell *131*.

Kouzarides, T. (2007b). Chromatin Modifications and Their Function. Cell *128*, 693–705.

Kriaucionis, S., and Bird, A. (2004). The major form of MeCP2 has a novel N-terminus generated by alternative splicing. Nucleic Acids Res. *32*, 1818–1823.

Kucukkal, T.G., and Alexov, E. (2015). Structural, Dynamical, and Energetical Consequences of Rett Syndrome Mutation R133C in MeCP2. Comput. Math. Methods Med. *2015*, 746157.

Kwak, H., and Lis, J.T. (2013). Control of transcriptional elongation. Annu. Rev. Genet. *47*, 483–508.

Lam, C.W., Yeung, W.L., Ko, C.H., Poon, P.M., Tong, S.F., Chan, K.Y., Lo, I.F., Chan, L.Y., Hui, J., Wong, V., et al. (2000). Spectrum of mutations in the MECP2 gene in patients with infantile autism and Rett syndrome. J Med Genet *37*, E41.

Lange, S., Katayama, Y., Schmid, M., Burkacky, O., Brauchle, C., Lamb D.C., D.C., and Jansen, R.P. (2008). Simultaneous transport of different localized mRNA species revealed by live-cell imaging. Traffic *9*, 1256–1267.

Larson, D.R., Singer, R.H., and Zenklusen, D. (2009). A single molecule view of gene expression. Trends Cell Biol. *19*, 630–637.

Larson, D.R., Zenklusen, D., Wu, B., Chao, J. a, and Singer, R.H. (2011). Real-time observation of transcription initiation and elongation on an endogenous yeast gene. Science *332*, 475–478.

LaSalle, J.M. (2007). The odyssey of MeCP2 and parental imprinting. Epigenetics *2*, 5–10.

Lee, J.H., Daugharthy, E.R., Scheiman, J., Kalhor, R., Yang, J.L., Ferrante, T.C., Terry, R., Jeanty, S.S.F., Li, C., Amamoto, R., et al. (2014). Highly Multiplexed Subcellular RNA Sequencing in Situ. Science (80-.). *343*, 1360–1363.

de Leeuw, W., Verschure, P.J., and van Liere, R. (2006). Isualization and analysis of large data collections: a case study applied to confocal microscopy data. IEEE Trans Vis Comput Graph *12*, 1251–1258.

de Leon-Guerrero, S.D., Pedraza-Alva, G., and Perez-Martinez, L. (2011). In sickness and in health: the role of methyl-CpG binding protein 2 in the central nervous system. Eur J Neurosci *33*, 1563–1574.

Leonhardt, H., Rahn, H.P., Weinzierl, P., Sporbert, A., Cremer, T., Zink, D., and Cardoso, M.C. (2000). Dynamics of DNA replication factories in living cells. J Cell Biol *149*, 271–280.

Lev Maor, G., Yearim, A., and Ast, G. (2015). The alternative role of DNA methylation in splicing regulation. Trends Genet. *31*, 274–280.

Lewis, J.D., Meehan, R.R., Henzel, W.J., Maurer-Fogy, I., Jeppesen, P., Klein, F., and Bird, A. (1992). Purification, sequence, and cellular localization of a novel chromosomal protein that binds to methylated DNA. Cell *69*, 905–914.

Li, X. (1998). Generation of Destabilized Green Fluorescent Protein as a Transcription Reporter. J. Biol. Chem. *273*, 34970–34975.

Li, G., and Zhu, P. (2015). Structure and organization of chromatin fiber in the nucleus. FEBS Lett.

Li, B., Carey, M., and Workman, J.L. (2007). The Role of Chromatin during Transcription. Cell *128*, 707–719.

Linhoff, M.W., Garg, S.K., and Mandel, G. (2015). A High-Resolution Imaging Approach to Investigate Chromatin Architecture in Complex Tissues. Cell *163*, 246–255.

Lionnet, T., Czaplinski, K., Darzacq, X., Shav-Tal, Y., Wells, A.L., Chao, J.A., Park, H.Y., de Turris, V., Lopez-Jones, M., and Singer, R.H. (2011). A transgenic mouse for in vivo detection of endogenous labeled mRNA. Nat. Methods *8*, 165–170.

Lioy, D.T., Garg, S.K., Monaghan, C.E., Raber, J., Foust, K.D., Kaspar, B.K., Hirrlinger, P.G., Kirchhoff, F., Bissonnette, J.M., Ballas, N., et al. (2011). A role for glia in the progression of Rett's syndrome. Nature *475*, 497–500.

Lister, R., Mukamel, E.A., Nery, J.R., Urich, M., Puddifoot, C.A., Johnson, N.D., Lucero, J., Huang, Y., Dwork, A.J., Schultz, M.D., et al. (2013). Global epigenomic reconfiguration during mammalian brain development. Science *341*, 1237905.

Liu, B., Xu, H., Miao, J., Zhang, A., Kou, X., Li, W., Zhou, L., Xie, H.-G., Sirois, P., and Li, K. (2015). CRISPR/Cas: A Faster and More Efficient Gene Editing System. J. Nanosci. Nanotechnol. *15*, 1946–1959.

Lubs, H., Abidi, F., Bier, J.A.B., Abuelo, D., Ouzts, L., Voeller, K., Fennell, E., Stevenson, R.E., Schwartz, C.E., and Arena, F. (1999). XLMR syndrome characterized by multiple respiratory infections, hypertelorism, severe CNS deterioration and early death localizes to distal Xq28. Am. J. Med. Genet. *85*, 243–248.

Luger, K., and Hansen, J.C. (2005). Nucleosome and chromatin fiber dynamics. Curr. Opin. Struct. Biol. *15*, 188–196.

Luijsterburg, M.S., Goedhart, J., Moser, J., Kool, H., Geverts, B., Houtsmuller, A.B., Mullenders, L.H., Vermeulen, W., and van Driel, R. (2007). Dynamic in vivo interaction of DDB2 E3 ubiquitin ligase with UV-damaged DNA is independent of damage-recognition protein XPC. J Cell Sci *120*, 2706–2716.

Luikenhuis, S., Giacometti, E., Beard, C.F., and Jaenisch, R. (2004). Expression of MeCP2 in postmitotic neurons rescues Rett syndrome in mice. Proc. Natl. Acad. Sci. U. S. A. *101*, 6033–6038.

Lunyak, V. V, Burgess, R., Prefontaine, G.G., Nelson, C., Sze, S.-H., Chenoweth, J., Schwartz, P., Pevzner, P.A., Glass, C., Mandel, G., et al. (2002). Corepressor-dependent silencing of chromosomal regions encoding neuronal genes. Science *298*, 1747–1752.

Lv, J., Xin, Y., Zhou, W., and Qiu, Z. (2013). The epigenetic switches for neural development and psychiatric disorders. J. Genet. Genomics *40*, 339–346.

Lyst, M.J., Ekiert, R., Ebert, D.H., Merusi, C., Nowak, J., Selfridge, J., Guy, J., Kastan, N.R.,

Robinson, N.D., de Lima Alves, F., et al. (2013). Rett syndrome mutations abolish the interaction of MeCP2 with the NCoR/SMRT co-repressor. Nat. Neurosci. *16*, 898–902.

MacQuarrie, K.L., Fong, A.P., Morse, R.H., and Tapscott, S.J. (2011). Genome-wide transcription factor binding: Beyond direct target regulation. Trends Genet. *27*, 141–148.

Maheshri, N., and O'Shea, E.K. (2007). Living with noisy genes: how cells function reliably with inherent variability in gene expression. Annu. Rev. Biophys. Biomol. Struct. *36*, 413–434.

Mari, F., Azimonti, S., Bertani, I., Bolognese, F., Colombo, E., Caselli, R., Scala, E., Longo, I., Grosso, S., Pescucci, C., et al. (2005). CDKL5 belongs to the same molecular pathway of MeCP2 and it is responsible for the early-onset seizure variant of Rett syndrome. Hum. Mol. Genet. *14*, 1935–1946.

Martı, A., Paz, D., Esteller, M., and Ausio, J. (2014). MeCP2 : the long trip from a chromatin protein to neurological disorders. 1–12.

Martínez de Paz, A., Vicente Sanchez-Mut, J., Samitier-Martí, M., Petazzi, P., Sáez, M., Szczesna, K., Huertas, D., Esteller, M., and Ausió, J. (2015). Circadian Cycle-Dependent MeCP2 and Brain Chromatin Changes. PLoS One *10*, e0123693.

Martins, S.B., Rino, J., Carvalho, T., Carvalho, C., Yoshida, M., Klose, J.M., de Almeida, S.F., and Carmo-Fonseca, M. (2011). Spliceosome assembly is coupled to RNA polymerase II dynamics at the 3′ end of human genes. Nat. Struct. Mol. Biol. *18*, 1115–1123.

Mason, P.B., and Struhl, K. (2005). Distinction and relationship between elongation rate and processivity of RNA polymerase II in vivo. Mol. Cell *17*, 831–840.

Matsumura, S., Persson, L.M., Wong, L., and Wilson, A.C. (2010). The latency-associated nuclear antigen interacts with MeCP2 and nucleosomes through separate domains. J Virol *84*, 2318–2330.

McBurney, M.W., Staines, W.A., Boekelheide, K., Parry, D., Jardine, K., and Pickavance, L. (1994). Murine PGK-1 promoter drives widespread but not uniform expression in transgenic mice. Dev. Dyn. *200*, 278–293.

McFarland, K.N., Huizenga, M.N., Darnell, S.B., Sangrey, G.R., Berezovska, O., Cha, J.-H.J.H.J., Outeiro, T.F., and Sadri-Vakili, G. (2014). MeCP2: a novel Huntingtin interactor. Hum. Mol. Genet. *23*, 1036–1044.

McNally, J.G., Müller, W.G., Walker, D., Wolford, R., and Hager, G.L. (2000). The glucocorticoid receptor: rapid exchange with regulatory sites in living cells. Science *287*, 1262–1265.

Meehan, R.R., Lewis, J.D., and Bird, A.P. (1992). Characterization of MeCP2, a vertebrate DNA binding protein with affinity for methylated DNA. Nucleic Acids Res. *20*, 5085–5092.

Meins, M., Lehmann, J., Gerresheim, F., Herchenbach, J., Hagedorn, M., Hameister, K., and Epplen, J.T. (2005). Submicroscopic duplication in Xq28 causes increased expression of the MECP2 gene in a boy with severe mental retardation and features of Rett syndrome. J. Med. Genet. *42*, e12.

Mellén, M., Ayata, P., Dewell, S., Kriaucionis, S., and Heintz, N. (2012). MeCP2 binds to 5hmC enriched within active genes and accessible chromatin in the nervous system. Cell *151*, 1417–1430.

Mnatzakanian, G.N., Lohi, H., Munteanu, I., Alfred, S.E., Yamada, T., MacLeod, P.J.M., Jones, J.R., Scherer, S.W., Schanen, N.C., Friez, M.J., et al. (2004). A previously unidentified MECP2 open reading frame defines a new protein isoform relevant to Rett syndrome. Nat. Genet. *36*, 339–341.

Mor, A., Suliman, S., Ben-Yishay, R., Yunger, S., Brody, Y., and Shav-Tal, Y. (2010). Dynamics of single mRNP nucleocytoplasmic transport and export through the nuclear pore in living cells. Nat. Cell Biol. *12*, 543–552.

Muotri, A.R., Marchetto, M.C.N., Coufal, N.G., Oefner, R., Yeo, G., Nakashima, K., and Gage, F.H. (2010). L1 retrotransposition in neurons is modulated by MeCP2. Nature *468*, 443–446.

Murtaza, M., Dawson, S.-J., Tsui, D.W.Y., Gale, D., Forshew, T., Piskorz, A.M., Parkinson, C., Chin, S.-F., Kingsbury, Z., Wong, A.S.C., et al. (2013). Non-invasive analysis of acquired resistance to cancer therapy by sequencing of plasma DNA. Nature *497*, 108–112.

Na, E.S., Nelson, E.D., Kavalali, E.T., and Monteggia, L.M. (2013). The impact of MeCP2 loss- or gain-of-function on synaptic plasticity. Neuropsychopharmacology *38*, 212–219.

Nan, X., Meehan, R.R., and Bird, A. (1993). Dissection of the methyl-CpG binding domain from the chromosomal protein MeCP2. Nucleic Acids Res. *21*, 4886–4892.

Nan, X., Campoy, F.J., and Bird, A. (1997). MeCP2 is a transcriptional repressor with abundant binding sites in genomic chromatin. Cell *88*, 471–481.

Nan, X., Cross, S., and Bird, A. (1998a). Gene silencing by methyl-CpG-binding proteins. Novartis Found Symp *214*, 6–21,46–50.

Nan, X., Ng, H.H., Johnson, C.A., Laherty, C.D., Turner, B.M., Eisenman, R.N., and Bird, A. (1998b). Transcriptional repression by the methyl-CpG-binding protein MeCP2 involves a histone deacetylase complex. Nature *393*, 386–389.

Nan, X., Hou, J., Maclean, A., Nasir, J., Lafuente, M.J., Shu, X., Kriaucionis, S., and Bird, A. (2007). Interaction between chromatin proteins MECP2 and ATRX is disrupted by mutations that cause inherited mental retardation. Proc Natl Acad Sci U S A *104*, 2709–2714.

Navin, N., Kendall, J., Troge, J., Andrews, P., Rodgers, L., McIndoo, J., Cook, K., Stepansky, A., Levy, D., Esposito, D., et al. (2011). Tumour evolution inferred by single-cell sequencing. Nature *472*, 90–94.

Neul, J.L., and Zoghbi, H.Y. (2004). Rett syndrome: a prototypical neurodevelopmental disorder. Neuroscientist *10*, 118–128.

Nikitina, T., Ghosh, R.P., Horowitz-Scherer, R.A., Hansen, J.C., Grigoryev, S.A., and Woodcock, C.L. (2007a). MeCP2-chromatin interactions include the formation of chromatosome-like structures and are altered in mutations causing Rett syndrome. J Biol Chem *282*, 28237–28245.

Nikitina, T., Shi, X., Ghosh, R.P., Horowitz-Scherer, R.A., Hansen, J.C., and Woodcock, C.L. (2007b). Multiple modes of interaction between the methylated DNA binding protein MeCP2 and chromatin. Mol Cell Biol *27*, 864–877.

Nomura, J., and Takumi, T. (2012). Animal models of psychiatric disorDers that reflect human copy number variation. Neural Plast. *2012*.

Noordermeer, D., and Duboule, D. (2013). Chromatin looping and organization at developmentally regulated gene loci. Wiley Interdiscip. Rev. Dev. Biol. *2*, 615–630.

Peccoud, J., and Ycart, B. (1995). Markovian Modeling of Gene-Product Synthesis. Theor. Popul. Biol. *48*, 222–234.

Rafalska-Metcalf, I.U., and Janicki, S.M. (2007). Show and tell: visualizing gene expression in living cells. J. Cell Sci. *120*, 2301–2307.

Rafalska-Metcalf, I.U., Powers, S.L., Joo, L.M., LeRoy, G., and Janicki, S.M. (2010). Single cell analysis of transcriptional activation dynamics. PLoS One *5*, e10272.

Raj, A., Peskin, C.S., Tranchina, D., Vargas, D.Y., and Tyagi, S. (2006). Stochastic mRNA synthesis in mammalian cells. PLoS Biol. *4*, e309.

Raj, A., van den Bogaard, P., Rifkin, S.A., van Oudenaarden, A., and Tyagi, S. (2008). Imaging individual mRNA molecules using multiple singly labeled probes. Nat. Methods *5*, 877–879.

Ramocki, M.B., Tavyev, Y.J., and Peters, S.U. (2010). The MECP2 Duplication Syndrome.

Ratnakumar, K., and Bernstein, E. (2013). ATRX: The case of a peculiar chromatin remodeler. Epigenetics *8*, 3–9.

Reddy, K.L., Zullo, J.M., Bertolino, E., and Singh, H. (2008). Transcriptional repression mediated by repositioning of genes to the nuclear lamina. Nature *452*, 243–247.

Reid, G., Gallais, R., and Metivier, R. (2009). Marking time: the dynamic role of chromatin and covalent modification in transcription. Int. J. Biochem. Cell Biol. *41*, 155–163.

Rett, A. (1966). [On a unusual brain atrophy syndrome in hyperammonemia in childhood] [article in german]. Wien Med Wochenschr *116*, 723–726.

Revenkova, E., Focarelli, M.L., Susani, L., Paulis, M., Bassi, M.T., Mannini, L., Frattini, A., Delia, D., Krantz, I., Vezzoni, P., et al. (2009). Cornelia de Lange syndrome mutations in SMC1A or SMC3 affect binding to DNA. Hum. Mol. Genet. *18*, 418–427.

Robinett, C.C., Straight, A., Li, G., Willhelm, C., Sudlow, G., Murray, A., and Belmont, A.S. (1996). In vivo localization of DNA sequences and visualization of large-scale chromatin organization using lac operator/repressor recognition. J Cell Biol *135*, 1685–1700.

Rottach, A., Kremmer, E., Nowak, D., Boisguerin, P., Volkmer, R., Cardoso, M.C., Leonhardt, H., and Rothbauer, U. (2008). Generation and characterization of a rat monoclonal antibody specific for PCNA. Hybrid. *27*, 91–98.

van Royen, M.E., Cunha, S.M., Brink, M.C., Mattern, K.A., Nigg, A.L., Dubbink, H.J., Verschure, P.J., Trapman, J., and Houtsmuller, A.B. (2007). Compartmentalization of androgen receptor protein-protein interactions in living cells. J Cell Biol *177*, 63–72.

Rybakova, K.N., Bruggeman, F.J., Tomaszewska, A., Mone, M.J., Carlberg, C., and Westerhoff, H. V (2015). Multiplex Eukaryotic Transcription (In)activation: Timing, Bursting and Cycling of a Ratchet Clock Mechanism. PLoS Comput. Biol. *11*, e1004236.

Sage, D., Neumann, F.R., Hediger, F., Gasser, S.M., and Unser, M. (2005). Automatic tracking of individual fluorescence particles: Application to the study of chromosome dynamics. IEEE Trans. Image Process. *14*, 1372–1383.

Saunders, A., Core, L.J., and Lis, J.T. (2006). Breaking barriers to transcription elongation. Nat. Rev. Mol. Cell Biol. *7*, 557–567.

Schmidt, U., Basyuk, E., Robert, M.C., Yoshida, M., Villemin, J.P., Auboeuf, D., Aitken, S., and Bertrand, E. (2011). Real-time imaging of cotranscriptional splicing reveals a kinetic model that reduces noise: Implications for alternative splicing regulation. J. Cell Biol. *193*, 819–829.

Schmiedeberg, L., Weisshart, K., Diekmann, S., Meyer Zu Hoerste, G., and Hemmerich, P. (2004). High- and low-mobility populations of HP1 in heterochromatin of mammalian cells. Mol Biol Cell *15*, 2819–2833.

Schotta, G., Lachner, M., Sarma, K., Ebert, A., Sengupta, R., Reuter, G., Reinberg, D., and Jenuwein, T. (2004). A silencing pathway to induce H3-K9 and H4-K20 trimethylation at constitutive heterochromatin. Genes Dev. *18*, 1251–1262.

Schultz, D.C., Ayyanathan, K., Negorev, D., Maul, G.G., and Rauscher 3rd, F.J. (2002). SETDB1: a novel KAP-1-associated histone H3, lysine 9-specific methyltransferase that contributes to HP1-mediated silencing of euchromatic genes by KRAB zinc-finger proteins. Genes Dev *16*, 919–932.

Schwabe, A., Rybakova, K.N., and Bruggeman, F.J. (2012). Transcription stochasticity of complex gene regulation models. Biophys. J. *103*, 1152–1161.

Shahbazian, M.D., and Grunstein, M. (2007). Functions of site-specific histone acetylation and deacetylation. Annu. Rev. Biochem. *76*, 75–100.

Shahbazian, M.D., Young, J.I., Yuva-Paylor, L.A., Spencer, C.M., Antalffy, B.A., Noebels, J.L., Armstrong, D.L., Paylor, R., and Zoghbi, H.Y. (2002a). Mice with truncated MeCP2 recapitulate many Rett syndrome features and display hyperacetylation of histone H3. Neuron *35*, 243–254.

Shahbazian, M.D., Antalffy, B., Armstrong, D.L., and Zoghbi, H.Y. (2002b). Insight into Rett syndrome: MeCP2 levels display tissue- and cell-specific differences and correlate with neuronal maturation. Hum Mol Genet *11*, 115–124.

Shav-Tal, Y., Darzacq, X., Shenoy, S.M., Fusco, D., Janicki, S.M., Spector, D.L., and Singer, R.H. (2004). Dynamics of single mRNPs in nuclei of living cells. Science *304*, 1797–1800.

Shirai, S., Takahashi, K., Kohsaka, S., Tsukamoto, T., Isogai, H., Kudo, S., Sawa, H., Nagashima, K., and Tanaka, S. (2011). Or i gi na l Ar t i c l e High expression of MeCP2 in JC virus-infected cells of progressive multifocal leukoencephalopathy brains. 38–41.

Singleton, M.K., Gonzales, M.L., Leung, K.N., Yasui, D.H., Schroeder, D.I., Dunaway, K., and LaSalle, J.M. (2011). MeCP2 is required for global heterochromatic and nucleolar changes during activity-dependent neuronal maturation. Neurobiol Dis *43*, 190–200.

Skene, P.J., Illingworth, R.S., Webb, S., Kerr, A.R.W., James, K.D., Turner, D.J., Andrews, R., and Bird, A.P. (2010). Neuronal MeCP2 Is Expressed at Near Histone-Octamer Levels and Globally Alters the Chromatin State. Mol. Cell *37*, 457–468.

Sokal, R., and Rohlf, F. (2011). Biometry: The principles and practice of statistics in biological research (New York: WH Freeman and co).

Song, C., Feodorova, Y., Guy, J., Peichl, L., Jost, K.L., Kimura, H., Cardoso, M.C., Bird, A., Leonhardt, H., Joffe, B., et al. (2014). DNA methylation reader MECP2: cell type- and differentiation stage-specific protein distribution. Epigenetics Chromatin *7*, 17.

Stafford, G. a, and Morse, R.H. (2001). GCN5 dependence of chromatin remodeling and transcriptional activation by the GAL4 and VP16 activation domains in budding yeast. Mol. Cell. Biol. *21*, 4568–4578.

van Steensel, B. (2011). Chromatin: constructing the big picture. EMBO J. *30*, 1885–1895.

Stegle, O., Teichman, S.A., and Marioni, J.C. (2015). Computational and analytical challenges in single-cell transcriptomics. Nat. Publ. Gr. *16*, 133–145.

Suter, D.M., Molina, N., Gatfield, D., Schneider, K., Schibler, U., and Naef, F. (2011). Mammalian genes are transcribed with widely different bursting kinetics. Science *332*, 472–474.

Svejstrup, J.Q. (2004). The RNA polymerase II transcription cycle: Cycling through chromatin. Biochim. Biophys. Acta - Gene Struct. Expr. *1677*, 64–73.

Tao, J., Hu, K., Chang, Q., Wu, H., Sherman, N.E., Martinowich, K., Klose, R.J., Schanen, C., Jaenisch, R., Wang, W., et al. (2009). Phosphorylation of MeCP2 at Serine 80 regulates its chromatin association and neurological function. Proc. Natl. Acad. Sci. U. S. A. *106*, 4882–4887.

Thatcher, K.N., and Lasalle, J.M. (2006). Dynamic Changes in Histone H3 Lysine 9 Acetylation Localization ND ES SC ABBREVIATIONS. 24–31.

Tsukamoto, T., Hashiguchi, N., Janicki, S.M., Tumbar, T., Belmont, a S., and Spector, D.L. (2000). Visualization of gene activity in living cells. Nat. Cell Biol. *2*, 871–878.

Tudor, M., Akbarian, S., Chen, R.Z., and Jaenisch, R. (2002). Transcriptional profiling of a mouse model for Rett syndrome reveals subtle transcriptional changes in the brain. Proc. Natl. Acad. Sci. U. S. A. *99*, 15536–15541.

Tumbar, T., Sudlow, G., and Belmont, A.S. (1999). Large-scale chromatin unfolding and remodeling induced by VP16 acidic activation domain. J Cell Biol *145*, 1341–1354.

Vakoc, C.R., Letting, D.L., Gheldof, N., Sawado, T., Bender, M.A., Groudine, M., Weiss, M.J., Dekker, J., and Blobel, G.A. (2005). Proximity among distant regulatory elements at the beta-globin locus requires GATA-1 and FOG-1. Mol Cell *17*, 453–462.

Valinluck, V., Tsai, H.-H., Rogstad, D.K., Burdzy, A., Bird, A., and Sowers, L.C. (2004). Oxidative damage to methyl-CpG sequences inhibits the binding of the methyl-CpG binding domain (MBD) of methyl-CpG binding protein 2 (MeCP2). Nucleic Acids Res. *32*, 4100–4108.

Venkatesh, S., and Workman, J.L. (2015). Histone exchange, chromatin structure and the regulation of transcription. Nat. Rev. Mol. Cell Biol. *16*, 178–189.

Verschure, P.J., van Der Kraan, I., Manders, E.M., and van Driel, R. (1999). Spatial relationship between transcription sites and chromosome territories. J Cell Biol *147*, 13–24.

Verschure, P.J., Van Der Kraan, I., Enserink, J.M., Mone, M.J., Manders, E.M., and Van Driel, R. (2002). Large-scale chromatin organization and the localization of proteins involved in gene expression in human cells. J Histochem Cytochem *50*, 1303–1312.

Verschure, P.J., van der Kraan, I., de Leeuw, W., van der Vlag, J., Carpenter, A.E., Belmont, A.S., and van Driel, R. (2005). In vivo HP1 targeting causes large-scale chromatin condensation and enhanced histone lysine methylation. Mol. Cell. Biol. *25*, 4552–4564.

Vicent, G.P., Ballare, C., Nacht, A.S., Clausell, J., Subtil-Rodriguez, A., Quiles, I., Jordan, A., and Beato, M. (2008). Convergence on chromatin of non-genomic and genomic pathways of hormone signaling. J Steroid Biochem Mol Biol *109*, 344–349.

Viñuelas, J., Kaneko, G., Coulon, A., Vallin, E., Morin, V., Mejia-pous, C., Kupiec, J., Beslon, G., and Gandrillon, O. (2013). Quantifying the contribution of chromatin dynamics to stochastic gene expression reveals long, locus-dependent periods between transcriptional bursts. BMC Biol. *11*, 15.

Volpi, E. V, Chevret, E., Jones, T., Vatcheva, R., Williamson, J., Beck, S., Campbell, R.D., Goldsworthy, M., Powis, S.H., Ragoussis, J., et al. (2000). Large-scale chromatin organization of the major histocompatibility complex and other regions of human chromosome 6 and its response to interferon in interphase nuclei. J Cell Sci *113 (Pt 9*, 1565–1576.

Wang, W. (2003). The SWI/SNF family of ATP-dependent chromatin remodelers: similar mechanisms for diverse functions. Curr Top Microbiol Immunol *274*, 143–169.

Wansink, D.G., Schul, W., van der Kraan, I., van Steensel, B., van Driel, R., and de Jong, L. (1993). Fluorescent labeling of nascent RNA reveals transcription by RNA polymerase II in domains scattered throughout the nucleus. J Cell Biol *122*, 283–293.

Weaving, L.S., Christodoulou, J., Williamson, S.L., Friend, K.L., McKenzie, O.L.D., Archer, H., Evans, J., Clarke, A., Pelka, G.J., Tam, P.P.L., et al. (2004). Mutations of CDKL5 cause a severe neurodevelopmental disorder with infantile spasms and mental retardation. Am. J. Hum. Genet. *75*, 1079–1093.

Weil, T.T., Parton, R.M., and Davis, I. (2010). Making the message clear: visualizing mRNA localization. Trends Cell Biol *20*, 380–390.

Weitzel, J.M., Buhrmester, H., and Strätling, W.H. (1997). Chicken MAR-binding protein ARBP is homologous to rat methyl-CpG-binding protein MeCP2. Mol. Cell. Biol. *17*, 5656–5666.

Wendt, K.S., and Grosveld, F.G. (2014). Transcription in the context of the 3D nucleus. Curr. Opin. Genet. Dev. *25*, 62–67.

de Wit, E., Greil, F., and van Steensel, B. (2007). High-resolution mapping reveals links of HP1 with active and inactive chromatin components. PLoS Genet *3*, e38.

Xu, X., Miller, E.C., and Pozzo-Miller, L. (2014). Dendritic spine dysgenesis in Rett syndrome. Front. Neuroanat. *8*, 1–8.

Yadon, A.N., Singh, B.N., Hampsey, M., and Tsukiyama, T. (2013). DNA looping facilitates targeting of a chromatin remodeling enzyme. Mol. Cell *50*, 93–103.

Yang, T., Ramocki, M.B., Neul, J.L., Lu, W., Roberts, L., Knight, J., Ward, C.S., Zoghbi, H.Y., Kheradmand, F., and Corry, D.B. (2012). Overexpression of Methyl-CpG Binding Protein 2 Impairs TH1 Responses. Sci. Transl. Med. *4*, 163ra158.

Yasui, D.H., Peddada, S., Bieda, M.C., Vallero, R.O., Hogart, A., Nagarajan, R.P., Thatcher, K.N., Farnham, P.J., and Lasalle, J.M. (2007). Integrated epigenomic analyses of neuronal MeCP2 reveal a role for long-range interaction with active genes. Proc Natl Acad Sci U S A *104*, 19416–19421.

Yntema, H.G., Kleefstra, T., Oudakker, A.R., Romein, T., de Vries, B.B.A., Nillesen, W., Sistermans, E.A., Brunner, H.G., Hamel, B.C.J., and van Bokhoven, H. (2002). Low frequency of MECP2 mutations in mentally retarded males. Eur. J. Hum. Genet. *10*, 487–490.

Young, J.I., Hong, E.P., Castle, J.C., Crespo-Barreto, J., Bowman, A.B., Rose, M.F., Kang, D., Richman, R., Johnson, J.M., Berget, S., et al. (2005). Regulation of RNA splicing by the methylation-dependent transcriptional repressor methyl-CpG binding protein 2. Proc. Natl. Acad. Sci. U. S. A. *102*, 17551–17558.

Yunger, S., Rosenfeld, L., Garini, Y., and Shav-Tal, Y. (2010). Single-allele analysis of transcription kinetics in living mammalian cells. Nat. Methods *7*, 631–633.

Yusufzai, T.M., and Wolffe, A.P. (2000). Functional consequences of Rett syndrome mutations on human MeCP2. Nucleic Acids Res *28*, 4172–4179.

Zhao, R., Bodnar, M.S., and Spector, D.L. (2009). Nuclear neighborhoods and gene expression. Curr. Opin. Genet. Dev. *19*, 172–179.

Zhao, R., Nakamura, T., Fu, Y., Lazar, Z., and Spector, D.L. (2011). Gene bookmarking accelerates the kinetics of. *13*.

Zhou, Q., Li, T., and Price, D.H. (2012). RNA polymerase II elongation control. Annu. Rev. Biochem. *81*, 119–143.

Zhou, Z., Hong, E.J., Cohen, S., Zhao, W.N., Ho, H.Y.H., Schmidt, L., Chen, W.G., Lin, Y., Savner, E., Griffith, E.C., et al. (2006). Brain-Specific Phosphorylation of MeCP2 Regulates Activity-Dependent Bdnf Transcription, Dendritic Growth, and Spine Maturation. Neuron *52*, 255–269.

Summary

Summary

Summary

Transcription processing and chromatin structural changes are intertwined processes in the nucleus. In this thesis we focused on the dynamic interplay of chromatin and its widespread functions such as genome stability and transcription regulation. We studied the effect of targeting the epigenetic regulatory protein Methyl CpG binding protein2 (MeCP2) and measure alterations in chromatin structure and and transcription regulation in real-time, in order to unravel the causal relationship between the epigenetic chromatin state and transcriptional repression in time and space.

In **the introduction** we introduce transcription regulation, chromatin and epigenetics and describe the molecular interactions of transcription. We introduce MeCP2 and neurodegenerative diseases related to this protein. We conclude with an explanation of using engineered reporter gene arrays in cultured cells, a method used throughout this thesis in order to modify chromatin and subsequently determine cause and consequence of alterations in chromatin structure and/or transcriptional activity.

In **Chapter 1** we use an experimental set-up that allows us to modulate the chromatin context (lacO and tetO targeting) of a reporter gene array and to measure the decrease in MS2 tagged transcripts in real-time in single living cells. We modulate the chromatin context by targeting methyl-CpG binding protein 2 (MeCP2). Our data show that the measured transcription repression follows a biphasic behavior consisting of a time-delayed response and a subsequent exponential decrease in the transcripts at the reporter gene array that is rather time-consuming compared to the rapid decrease in transcriptional activator at the array. The delay time preceding the decrease in transcript levels is significantly shorter when MeCP2 is targeted to the reporter gene array. We simulated the diffusion rate of MS2 tagged transcripts with a 2 dimensional finite difference diffusion model. These data estimate that mRNA diffusion from the reporter gene is much faster than the measured decrease in transcripts at the array. Our data indicate that transcription initiation is still ongoing beyond the point that the transcriptional activator is removed from the reporter gene array with a delayed response. The MeCP2-targeted chromatin context only affects the response time and not the actual decrease in transcripts, suggesting that the local chromatin context determines

whether new transcription initiation events are allowed thereby regulating the delay time of transcription repression.

In **Chapter 2** we describe the design and construction of a cell line harboring a novel reporter gene cassette. We designed this reporter gene cassette such that it can be integrated via homologous integration as a single known genomic integration site. The cassette is equipped with a readout to measure mRNA and protein kinetics of a reporter gene in real-time upon modulating the epigenetic chromatin state. The bacteriophage MS2 hairpin repeats are used to detect RNA transcripts via fluorescently tagged MS2 protein binding. We used a fluorescent protein consisting of a degradation signal coding for a short-lived fluorescent protein allowing to measure changes in protein level of the reporter gene upon inducing transcriptional repression in time. The integration of a 84x tetO tandem repeat upstream of the reporter gene enables modulation of the epigenetic chromatin state via tetR targeting. We created tetR-tagged epigenetic regulatory proteins MeCP2 and HP1 to study reporter gene transcript and protein levels at single gene level in real-time in living cells upon inducing a repressive chromatin context. We show that the reporter gene cassette is being expressed when transfected in human cells and that the target constructs bind to their tet operator repeat binding sequences. In future studies will integrate the cassette via homologous integration in the human genome and measure single gene, single cell real-time transcription upon modulating a defined chromatin structure.

In **Chapter 3** we provide an overview of the numerous functions of MeCP2 contributing to transcriptional regulation and chromatin organization. The disordered protein structure of MeCP2 allows MeCP2 to bind with its MBD, TRD or C-terminal domain to various DNA sites and regulatory proteins. Dependent on the posttranslational modification state of MeCP2 and on its binding partners, MeCP2 is able to perform opposing tasks such as transcriptional repression or activation. We highlight the molecular effects of MeCP2 (dys)regulation at the cellular level; Loss and gain of function of MeCP2 is catastrophic for the identity of brain cells and gives rise to neurodevelopmental diseases such as Rett and Xq28 duplication syndrome. We provide a model-representation showing how the

delicate balance of the affinity of MeCP2 binding and the concentration of MeCP2 afffects the MeCP2 functional fraction. Our model-representation indicates that the molecular behavior of Rett syndrome and Xq28 duplication syndrome are strikingly different although their disease symptoms show quite some overlap.

In **Chapter 4** we provide evidence that targeting MeCP2 to a large amplified chromosomal lacO array elicits an as yet undiscovered extensive chromatin unfolding. This chromatin unfolding is also observed, but to a lesser extent, when untargeted MeCP2 is overexpressed. We quantified the MeCP2-induced chromatin unfolding of full length MeCP2 versus its partial domains, i.e. MBD, TRD, C-terminus, MeCP2 lacking its C-terminus, or the Rett mutant MeCP2. For chromatin structure measurements, 3D confocal microscopy images of the large amplified chromosomal lacO array were used to determine changes in 3D image analysis parameters of the chromosomal array, i.e. the surface factor which represents the surface of a given chromosomal domain or object normalized to the surface of a sphere with an equal volume. We noted that none of the partial MeCP2 domains alone were capable of inducing the extensive chromatin unfolding produced by full-length MeCP2. FLIP analysis showed that MeCP2 binding triggers the loss of HP1γ from the chromosomal domain and an increased HP1γ mobility in the cell nucleus, which is not observed for other HP1 isoforms HP1α and HP1β. MeCP2-induced chromatin unfolding is not associated with transcriptional activation. In relation with these observations, we describe in chapter 2 that MeCP2 targeting to a reporter gene array diminished the delay in transcription repression response while the subsequent decrease in transcripts at the reporter gene array appeared unaffected. Based on these findings we proposed that the local chromatin context determines whether new transcription initiation events are allowed thereby regulating the delay time of transcription repression. Our findings in chapter 5 might indicate that MeCP2-induced chromatin unfolding prepares chromatin for subsequent transcriptional regulation, facilitating a switch in gene activity.

The causal relationship between the molecular interactions underlying protein kinetics, chromatin structural alterations and transcriptional activity is a central challenge in the field and biochemically difficult to determine. The use of engineered cell systems allows us to focus on a defined set of involved molecular interactions within the context of a living cell and modulate their actions in time and space. Such an engineered approach enables to test and demonstrate complex temporal regulation at single molecule, single cell and genome-wide levels enhancing our understanding of the concerted actions of transcription dynamics in vivo. In this thesis we designed a single cell, single gene set-up integrating the reporter gene cassette via homologous recombination.

Nowadays CRISPR/Cas9 molecular engineering provides many opportunities to create genomic changes and follow molecular interations of transcription regulation at endogenous genes and in a modified epigenetic context. CRISPR/Cas9 engieering opens-up a novel field with infinite potential for cell engineering. Another recent advance in the field is determining gene activity regulation biochemically in single cells at DNAsequence resolution level. Such single cell genome-wide analysis enables to robustly profile RNA, DNA methylation and chromatin folding but it does not give insight in temporal and spatial aspects of transcription regulation and the epigenetic chromatin state.

These biochemical population apporaches have been complemented with single cell imaging techniques. Despite tremendous advances in our understanding based on these biochemical and single cell microscopical studies, we still lack mechanistic insight of molecular concerted actions of transcription regulation in time and space.

In this thesis we focus on MeCP2, an epigenetic regulatory protein well known from MeCP2 related diseases caused by mutations in the MeCP2 coding region. We discuss the various different functionalities of MeCP2, i.e. to act as an activator as well as a repressor. Moreover, we conclude that determining molecular functioning of MeCP2 is essential to find ways to monitor or treat MeCP2 related disease development. In our reporter gene array studies we show that MeCP2 is able to alter chromatin structure and timing of transcription repression. These data suggest that MeCP2 acts as a 'facilitator' protein being able to either induce gene activity or silencing based on the facilitated sequence of

events. This facilitator functioning might be a general concept of the concerted action of epigenetic regulatory proteins to establish and maintain transcription patterns.

Samenvatting

Samenvatting

Transcriptie en de structuur veranderingen van chromatine zijn processen in de celkern die nauw verweven zijn met elkaar. In dit proefschift richten wij ons op de dynamische interactie en de veelzijdige functies van chromatine zoals genoomstabiliteit en transcriptieregulatie. We bestuderen epigenetisch regulatie-eiwit Methyl CpG Protein2 (MeCP2) om chromatine te moduleren en om daarbij de veranderingen in chromatine structuur en de transcriptieregulatie te meten in *real-time*. Dit om meer inzicht te verschaffen in het causale verband tussen de epigentische staat van het chromatine en transcriptierepressie in tijd en ruimte.

In **de introductie** introduceren we transcriptieregulatie, chromatine en epigenetica. We leggen de aandacht op de dynamische processen die besproken worden in dit proefschrift. We introduceren MeCP2 en neurodegeneratieve ziekten die gerelateerd zijn aan MeCP2. We eindigen met een korte omschrijving van het gebruik van gegenereerde chromatine-reeksen in het genoom van gekweekte cellen, een methode die we in dit proefschrift veelvuldig gebruiken voor het manipuleren van chromatine om vervolgens de oorzaak en het gevolg van veranderingen in chromatinestructuur en transcriptionele activiteit te bepalen.

In **hoofdstuk 1** gebruiken we een experimentele set-up die ons in staat stelt om de chromatinecontext te veranderen (lacO/lacR en tetO/tetR) van een 200x reportergenreeksen en om de afname van mRNA te meten, met behulp van MS2 gelabelde transcripten in levende cellen. We veranderen de chromatinecontext door Methyl CpG binding protein2 (MeCP2) te sturen naar het reportergenreeks. Onze data laten zien dat de gemeten transcriptierepressie een bifasisch gedrag vertoont, bestaande uit een vertraging en een daaropvolgende exponentiële afname van het aantal transcripten op de reportergenreeks, deze afname duurt tamelijk lang vergeleken met de afname van de transcriptieactivator op de reportergenreeks.

De vertragingstijd voorafgaand aan de exponentiele afname is significant korter wanneer MeCP2 naar de reportergenarray is gestuurd. We simuleren de diffusie van de transcripten met een 2 dimensionaal diffusie-model gebaseerd op de eindige differentiatiemethode. Deze data laten zien dat de mRNA diffusie van de

reportergenreeks veel sneller is dan de gemeten afname van mRNA van de reeks in onze experimentele set-up. Onze data lijken erop te wijzen dat er nog steeds transcriptieinitiatie plaatsvindt nadat de transcriptieactivator van de reportergenreeks verdwenen is.

De MeCP2 gemoduleerde chromatinecontext beïnvloedt alleen de vertragingstijd en niet de exponentiële afname van de transcripten. Dit wijst erop dat de chromatinecontext bepaalt of er nieuwe initiatie kan plaats vinden en of de reactietijd verandert.

In **hoofdstuk 2** beschrijven we het ontwerp en de constructie van een cellijn die een nieuw reportergencassette bevat. De ontworpen cassette kan worden geïntegreerd in een bekende chromatine-integratieplek in het genoom met behulp van homologe recombinatie. De cassette is zodanig geconstrueerd dat de kinetiek van mRNA transcripten en van eiwitten kan worden gemeten in real-time na modulering van de epigentische chromatine samenstelling. Met de bacteriofage MS2 haarpinreeks is het mogelijk fluorescent gelabelde MS2 eiwitbinding te meten als maat voor nieuw gesynthetiseerd mRNA. We gebruiken een reportergen met een signaalcode voor kortlevende eiwitten, dat ons in staat stelt om eiwitafname te meten van het reportereiwit in de tijd. De integratie van een 84x tetO tandemreeks *upstream* van het reportergen maakt het mogelijk om de chromatinesamenstelling te veranderen door het sturen van eiwitten in een fusieconstruct met tetR.

We hebben een aantal fusieconstructen gegenereerd met regulerende eiwitten MeCP2 en HP1β om het effect te meten van de geïnduceerde transcriptierepressiecontext op de dynamische hoeveelheid mRNA en de eiwitten in levende cellen in de tijd. Hier laten we zien dat het construct tot expressie komt in de cellijn waarin we het construct beogen te integreren en dat de fusieconstructen binden aan een tetO reeks. In toekomstige studies kan het construct geïntegreerd worden in het humane genoom door middel van homologe recombinatie en kan van een enkel gen, in een enkele levende cel de eiwit en mRNA hoeveelheid in de tijd gemeten worden.

In **hoofdstuk 3** geven we een overzicht van de talrijke functies van MeCP2 welke bijdragen aan transcriptieregulering en chromatine organisering. De ongeordende eiwit structuur van MeCP2 maakt dat het eiwit verschillende DNA doellocaties en verschillende regulatoire eiwitten kan binden met zijn domeinen: MBD, TRD en C-terminal. Afhankelijk van de bindingsparnters en de posttranslationele modificaties op MeCP2, kan MeCP2 tegengestelde functies uitvoeren zoals transcriptionele activering en repressie.

We geven aandacht aan de moleculaire effecten van (mis)regulatie op cel-niveau. Verlies en winst van functies van MeCP2 is catastrofaal voor de identiteit van hersencellen en leidt tot neurologische ontwikkelingsziekten zoals Rett Syndroom en Xq28 duplicatie Syndroom. We geven een modelrepresentatie waarmee we laten zien hoe delicaat de balans is tussen bindingsaffiniteit en concentratie is en hoe veranderingen in deze balans de functionaliteit van MeCP2 kan verstoren. Ons model geeft aan dat de oorzaak van Rett syndroom en Xq28 verschillend zijn, terwijl de phenotypes vele overeenkomsten vertonen.

In **hoofdstuk 4** geven we bewijs dat het sturen van MeCP2 naar een grote geamplificeerde chromosomale lacO reeks een tot nu toe onontdekte grootschalige chromatineontvouwing teweeg brengt. Deze ontvouwing wordt, in kleinere mate, ook geobserveerd wanneer MeCP2 niet specifiek gestuurd in de cellen tot expressie wordt gebracht. We hebben de mate van MeCP2 geïnduceerde chromatineontvouwing gequantificeerd zowel in de situatie waarbij het volledige MeCP2-eiwit tot expressie wordt gebracht alsmede de situatie waarbij gedeeltelijke MeCP2 domeinen tot expressie worden gebracht, te weten MBD, TRD en C-terminus, MeCP2 zonder C-terminus en een Rett-syndroom variant. Voor structuuranalyses van het chromatine werden 3D confocale microscopiebeelden van de grote geamplificeerde chromosomale lacO reeks gemaakt en met behulp van beeld analyses, waarbij de oppervlaktefactor wordt bepaald, die een quantificatie geeft van het verschil tussen de gevonden chromosomale structuur en een perfecte bol met hetzelfde volume.

We obseveerden dat geen van de MeCP2 domeinen op zichzelf dezelfde grootschalige ontvouwing kan veroorzaken als het volledige MeCP2 eiwit. Microscopische *Fluorescence*

Loss in Photobleaching (FLIP) analyses laten zien dat MeCP2 binding het verlies van HP1γ van het chromosomaal domein veroorzaakt. We observeren een verhoogde mobiliteit van HP1γ in de celkern die niet wordt gemeten bij de andere isoformen HP1α en β. De MeCP2 geïnduceerde ontvouwing gaat niet gepaard met activering van transcriptie. In relatie met deze observering laten we in hoofdstuk 2 zien dat MeCP2 inductie van het chromatine naar een reporterreeks de vertragingstijd tot de transcriptierepressie vrijwel teniet doet. Gebasseerd op deze bevindingen stellen wij dat locale chromatine context bepaalt of nieuwe initiatie evenementen plaats kunnen vinden en dat daarmee de vertragingstijd van repressie bepaald wordt.

Onze bevindingen in hoofdstuk 4 geven de suggestie dat MeCP2 geïnduceerde chromatine ontvouwing het chromatine voorbereidt op veranderingen in genactiviteit en daarmee als het ware een switch in genactiviteit faciliteert.

Het causale verband tussen de moleculaire interacties die ten grondslag liggen van eiwitkinetiek, veranderingen van chromatinestructuur en transcriptieactiviteit is een belangrijke uitdaging in het onderzoeksveld en biochemisch ingewikkeld te ontrafelen. Het gebruik van geconstrueerde celsystemen levert de mogelijkheid om ons te richten op een vooraf gedefinieerde set van moleculaire factoren binnen de context van een levende cel en de mogelijkheid om deze te manipuleren in zowel tijd als in de ruimtelijke dimensies van de celkern. Zo een *cell engeneered* aanpak biedt ons de mogelijk om complexe temporale regulatie op het niveau van een enkel molecuul zowel in een enkele cel, alsook genoomwijd te testen en te demonstreren en vergroot ons begrip van de gecoördineerde stappen van transcriptie *in vivo.* In dit proefschrift is het ontwerp en de constructie beschreven van een dergelijke celsysteem die in het genoom worden geïntegreerd door middel van homologe recombinatie. Tegenwoordig biedt het CRISPR/Cas9 *moleculair bioenegeneering* systeem veel mogelijkheden om genomische aanpassingen te genereren en om moleculaire interacties van transcriptie regulatie te volgen van endogene genen en in een gemodificeerde epigenetische context. CRISPR/Cas9 engeneering opent een geheel nieuw veld met oneindige veel mogelijkheden om veranderingen in cellen aan te brengen. Een andere recente

vooruitgang in het veld is de biochemische bepaling van genactiviteit regulatie in een enkele cel met de resolutie van de DNA sequentie. Zulke genoomwijde enkele cel analyses bieden de mogelijkheid om een robuust profiel te maken van het aantal transcripten, DNA methylatie en chromatinevouwing, maar geeft geen inzicht in de tijd of de ruimtelijke ordening van deze processen in de celkern. Ondanks de enorme vooruitgangen van deze biochemische 'celpopulatie aanpak', samengevoegd met microscopiedata van enkele levende cellen is het mechanisme van de moleculair verweven processen welke transcriptie reguleren in rijd en ruimte toch nog grotendeels onontgonnen.

Voor dit proefschrift leggen wij de aandacht op MeCP2, een epigentisch regulatie- eiwit, vooral bekend vanwege 2 neurodegeneratieve ziekten veroorzaakt door mutaties in de MeCP2 coderende genregio. We bespreken de verschillende functies die MeCP2 kan uitvoeren, zoals de tweezijdige functie van MeCP2 als zowel transcriptie activator als transcriptie repressor. We concluderen dat het belangrijk is om alle functies van MeCP2 goed in kaart te brengen, inclusief de dynamiek, om tot methodes te komen om MeCP2 gerelateerde ziektes te kunnen onderzoeken en behandelen. In onze studies waar we gebruik maken van reportergenreeksen laten we zien dat MeCP2 in staat is om chromatine structuur te veranderen en de timing van transcriptierepressie te beïnvloeden. Deze data wijzen erop dat MeCP2 functioneert als een 'facilitator' van zowel transcriptie activering als van transcriptie repressie, afhankelijk van de door MeCP2 veroorzaakte gefaciliteerde volgorde van gebeurtenissen. Deze facilitatorfunctie kan een algemeen concept zijn waarmee regulatie-eiwitten transcriptie-patronen vastleggen en behouden

Dankwoord

Dankwoord

Het heeft even geduurd, maar het is zo ver: tijd voor een dankwoord. Zoals bekend is het dankwoord misschien niet het belangrijkste, maar wel het meest gelezen deel van een proefschrift. Dus ik ga ervoor.

Heel veel mensen ben ik dank verschuldigd voor hun ondersteuning, advies, het plezier dat we samen gehad hebben, de soms enorme eyeopeners, op vele terreinen, ook niet-wetenschappelijke. Omdat ik ongetwijfeld iemand zal vergeten, dank ik jullie allen hierbij.

Een aantal mensen wil ik persoonlijk bedanken, en ik begin met Pernette. 10 jaar geleden ben ik als studente in jouw groep terecht gekomen. Ik heb al die jaren met erg veel plezier gewerkt. Je was een geweldige baas, die mij geholpen heeft om te groeien. Je hebt je ingezet om mij te kunnen laten starten met deze promotie en daar ben ik je zeer dankbaar voor. Tijdens mijn promotieonderzoek ben je een onmisbare steun geweest voor mijzelf en mijn ontwikkeling als onderzoeker.

Tijdens mijn promotietraject heb ik maar liefst 2 professoren gehad; Roel en Hans stonden, elk op zijn eigen wijze, allebei klaar om mij te helpen wanneer ik daar om vroeg, gaven mij de ruimte om dit onderzoek te volbrengen en mij van analist tot onderzoeker te ontwikkelen.

In de groep NOG heb ik veel steun ondervonden van de mensen die er werken en werkten, onderzoekstechnisch van Marillis, Paul V, Maike en Paul F. Als ik het allemaal niet meer zag zitten kon ik altijd rekenen op hun hulp om alles weer goed op een rijtje te krijgen. Rechien, jij was mijn steunpilaar op het lab, jij was er 10 jaar geleden om mij als stagiair/analist wegwijs te maken en staat nu aan het eind naast mij, als paranimf.

Maartje, jij hebt aan de wieg gestaan van dit proefschrift. Je was eerst mijn stagebegeleider en het project waar ik jou toen bij heb ondersteund, heb ik zelf mogen afronden en staat nu ook in mijn proefschrift. Ik wil je bedanken voor de leuke tijd, de begeleiding en de samenwerking.

Mannus, dank voor je hulp bij alle berekeningen, het opzetten van macro's en het controleren van mijn werk.

Dit hele proefschrift had natuurlijk nooit tot stand kunnen komen zonder de Universiteit van Amsterdam en NWO, die het onderzoek hebben gefaciliteerd en gefinancierd.

Ik heb uiteraard ook het een en ander gevergd van mijn directe omgeving. Allereerst mijn zus Lies, met wie ik samenwoonde, en die ik soms gek heb gemaakt met mijn gechagrijn en frustraties. Jouw geduld met mij is vrijwel oneindig geweest. Dank aan mijn ouders voor alle adviezen, gevraagd en ongevraagd, en niet te vergeten al het heerlijke eten.

Micha, heel erg bedankt voor de hulp bij het maken van figuren en het uiteindelijke omslagontwerp.

Malka, we waren het soms wel en soms niet eens, ook in de wekelijkse pubquiz, maar vriendinnen waren, zijn en blijven we! Dank voor het vormgeven van dit boekje en vooral voor de vele, vele steun om tot dit resultaat te komen.